1540

MAGNETIC RESONANCE ON AROMATIC ANIONS WITH THREEFOLD SYMMETRY

J. A. M. van BROEKHOVEN

MAGNETIC RESONANCE ON AROMATIC ANIONS WITH THREEFOLD SYMMETRY

Promotor:
PROF.DR. E. de BOER

MAGNETIC RESONANCE ON AROMATIC ANIONS WITH THREEFOLD SYMMETRY

PROEFSCHRIFT

TER VERKRIJGING VAN DE GRAAD VAN
DOCTOR IN DE WISKUNDE EN NATUURWETENSCHAPPEN
AAN DE KATHOLIEKE UNIVERSITEIT TE NIJMEGEN,
OP GEZAG VAN DE RECTOR MAGNIFICUS MR. W.C.L. VAN DER GRINTEN,
HOOGLERAAR IN DE FACULTEIT DER RECHTSGELEERDHEID,
VOLGENS BESLUIT VAN DE SENAAT
IN HET OPENBAAR TE VERDEDIGEN OP VRIJDAG 2 OKTOBER 1970,
DES NAMIDDAGS TE 2 UUR PRECIES

door

JOHANNES ADRIANUS MARIA van BROEKHOVEN
Geboren te Tilburg

Druk: Offsetdrukkerij Faculteit der Wiskunde en Natuurwetenschappen
Nijmegen
1970

Aan mijn ouders
Aan Ini

ACKNOWLEDGEMENT

I am much indepted to Dr. H. van Willigen under whose guidance I started the investigations and to Dr. J.L. Sommerdijk whose cooperation is greatly appreciated.

The help of Dr. F.W. Pijpers, Mr. Th. Vermeegen and Mrs. J. Schwartz has been indispensable for the numerous computer calculations.

I wish to thank Mr. J.C.A.M. Janssen and Mr. H. Coenen for their skillful assistance in the performance of the experiments and Drs. W. Philipsen, H. Langendam, Drs. R.A.F. Deeleman and Drs. H.J.M. Andriessen who have also contributed to the experimental work.

The technical assistance of many departments of the Faculty of Science is gratefully acknowledged.

CONTENTS

CHAPTER I

INTRODUCTION

Aromatic ions with threefold symmetry are of special interest for spectroscopic studies because they have electronic properties that may be quite different from those of ions with a lower symmetry.

According to MO calculations the lowest two π antibonding orbitals of trigonal aromatic hydrocarbons often have the same energy. If this is the case, the unpaired electron in the corresponding mononegative ions will occupy a degenerate set of orbitals. This orbital degeneracy may influence the physical properties of the molecules.

The dianions of molecules with trigonal symmetry may occur in the triplet ground state because usually the correlation energy for this state is smaller than for the corresponding singlet state (Hund's rule). The properties of both the monoanions and the triplet dianions can be studied with various methods, among which magnetic resonance techniques play an important role.

1.1 Mononegative ions

Aromatic negative ions can be prepared by alkali reduction of the corresponding hydrocarbons in ethereal solvents

$$Ar + Me \rightleftarrows Ar^- + Me^+ \ .$$

The aromatic ions Ar^- are paramagnetic, which render them suitable for electron spin resonance (ESR) investigations. The ESR spectra show hyperfine structure due to the interaction of the magnetic moments of the unpaired electron and the protons in the molecule. A solution ESR spectrum is further characterized by its isotropic g value, which may deviate from the free electron g value, and the width of the hyperfine lines.

Some years ago Townsend and Weissman reported unusually broad ESR lines exhibited by hydrocarbon aromatic free radicals which are predicted to have degenerate groundstates because of their high symmetry (e.g. benzene anion) [1]. These authors also observed that these symmetrical radicals are much more difficult to saturate than comparable radicals of lower symmetry. Since then more experimental data have become available which all have confirmed the original observation that orbitally degenerate radicals have unusual linewidths (or more precisely: relaxation times). In all cases studied the unusual linewidth was accompanied by a anomalous g value. It has been suggested that both effects are associated with enhanced spin-orbit coupling [2,3].

In this work the monoanions of triphenylene (Tp) and 1, 3,5-triphenylbenzene (Tpb) both of which are in orbitally degenerate groundstates, have been studied. Whereas the ESR spectra of Tp^- indeed exhibit hyperfine lines with unusually high linewidths and a too large g value, none of the above characteristics have been found in the ESR spectra of Tpb^- in liquid ammonia.

ESR spectra of negative ions dissolved in solvents of low polarity often exhibit an additional splitting that is

temperature dependent. This splitting is caused by the interaction of the unpaired electron with the alkali ions which are assumed to associate with the anions in solvents of low dielectric constant [4]. The variation of the alkali splitting with temperature or solvent has been satisfactorily explained with ion pairing theory.

It was found for Tp^- that ionic association not only introduced an alkali splitting in the ESR spectra, but also caused changes in the electron spin distribution and the electronic g value [5]. Different species present in solution manifested themselves as superpositions of ESR spectra or spectra which were weighed averages of two other ESR spectra. Thermodynamic quantities characterizing the different equilibria have been determined.

With the help of nuclear magnetic resonance (NMR) additional information has been obtained about the sign of some proton hfs constants in the negative ion of Tpb. Electron- and rotational correlation times have been determined from the NMR linewidth.

1.2 Dinegative ions

Many monoanions can be further reduced to dianions

$$Ar^- + Me \rightleftarrows Ar^{=} + Me^+ .$$

Most symmetrical dianions are paramagnetic. This does not imply, however, that they can be studied with ESR, because the lifetime of the spin states may be too short. This shortening is caused by the time dependence of the anisotro-

pic dipolar interaction between the unpaired electrons. This difficulty can be circumvented by measuring the triplet molecules diluted in diamagnetic single crystals, in powders or in a glassy solvent matrix. A single crystal ESR study will give more information than studies from powders or glassy solvents. Unfortunately, attempts to prepare single crystals have failed hitherto. Useful information, however, can also be abstracted from ESR spectra of glassy solutions. In this way the triplet spectra of the dianions of triphenylene ($Tp^{=}$), 1,3,5-triphenylbenzene ($Tpb^{=}$) and 2,4,6-triphenyl-sym-triazine ($Tpt^{=}$) have been studied. The experimental evidence for the triplet groundstates of these dianions is in flagrant contradiction with calculations of Murrell and Hinchliffe who predicted singlet groundstates [6]. Recent calculations by Sommerdijk are in agreement with the experimental data [7,8].

It was found that in solvents of low solvating power the dianions become associated with the alkali ions [9]. The electric field of the cations strongly perturbs the triplet spin distribution in the dianions, leading to a loss of symmetry in the dianions of Tp and Tpt. For the latter ion the spin multiplicity of the groundstate changed from triplet to singlet upon association with cations.

The experimental data have been interpreted in terms of ion pairs (triples) with different geometrical structures. Numerical calculations of the zero-field splitting (ZFS) parameters of various triplet species by Sommerdijk proved to be in excellent agreement with experimental values. Theoretical results obtained for $Tpt^{=}$ were, however, less

satisfactory. A tentative explanation for the discrepancy between theory and experiment will be given.

In chapter II the basic theory underlying magnetic resonance (ESR and NMR) on paramagnetic systems is presented and a survey is given of the quantum mechanical calculation of the zero-field splittings of triplet molecules. Chapter III describes the way in which the samples have been prepared and measured. In the first part of chapter IV ESR and optical studies on Tp^{-} are discussed; the second part deals with ESR and NMR on the monoanion of Tpb. The last chapter is an ESR study of triplet dianions of Tp, Tpb and Tpt. At the end of this chapter some experiments on other trigonal aromatic molecules are discussed.

CHAPTER II

THEORY

2.1 Electron spin resonance of doublet states.

Liquid solution ESR spectra of molecules or ions possessing only one unpaired electron can be interpreted with the following spin hamiltonian:

$$\mathcal{H} = g_e\beta_e H_z S_z - g_N\beta_N H_z \sum_i I_{zi} + \sum_i A_i \bar{S}.\bar{I}_i \qquad (1)$$

g_e is the isotropic g value of the electron
β_e and β_N are the electron and nuclear Bohr magneton
g_N is the nuclear g value
H_z is the external magnetic field
A_i is the isotropic coupling constant of nucleus i.
The summation is over all nuclei i in the molecule that possess a nuclear spin.

The terms describing the nuclear Zeeman interactions can be neglected since they do not affect the positions of the absorption lines in the liquid phase spectrum. The ESR spectra described in this work can be interpreted by first order perturbation theory which means that the off-diagonal elements of the $\mathcal{H}$ matrix can be neglected. If the basic spin functions are constructed by multiplying the electron spin function α or β with all possible nuclear spin functions, then these product spin functions are correct eigenfunctions of the hamiltonian:

$$\mathcal{H} = g_e \beta_e H_z S_z + \sum_i A_i S_z I_{zi} \qquad (2)$$

and their energies are given by

$$E = m_s (g_e \beta_e H_z + \sum_i A_i m_i) \qquad (3)$$

with $m_s = \pm \frac{1}{2}$ and $m_i = I, I-1, I-2, \ldots, -I$.

The allowed ESR transitions are those for which $\Delta m_s = \pm 1$ and $\Delta m_i = 0$ and the corresponding resonance frequency is

$$h\nu = g_e \beta_e H_z + \sum_i A_i m_i \ . \qquad (4)$$

Working at a fixed frequency ($\nu = 9.10^9$) and varying the magnetic field H, resonance will be observed at the following field positions:

$$H = H_o - \frac{\sum_i A_i m_i}{g_e \beta_e} \qquad (5)$$

where H_o is the resonance field of the isolated electron spin:

$$H_o = \frac{h\nu}{g_e \beta_e} \ . \qquad (6)$$

The intensities of the lines described by equation 5 are proportional to the degeneracy of the nuclear spin states m_i. This means for example that the interaction of the odd electron with n equivalent protons (with spin of $\frac{1}{2}$) gives rise to n+1 resonance lines with a binomial intensity distribution.

The coupling constant A_i is proportional to the spin density $\rho(\bar{r}_i)$ at nucleus i [10]:

$$A_i = \frac{8\pi}{3} g_e \beta_e g_N \beta_N \rho(\bar{r}_i) \quad . \tag{7}$$

In aromatic radicals the odd electron occupies a π molecular orbital delocalized over the carbon frame work. As this orbital is composed of $2p_z$ functions, it has a node in the plane of the molecule where the hydrogen atoms are situated which would imply that $\rho(\bar{r}_i)$ is zero both for the carbon and hydrogen atoms. An M.O. description that mixes excited configurations with the ground state of the radical can account for small spin densities at the protons. McConnell has shown that the integrated spin densities ρ_π at adjacent carbons are proportional to the spin densities at the proton nuclei. In good approximation the result can be summarized as follows [11]:

$$a_H = Q.\rho_\pi \tag{8}$$

a_H is the proton hyperfine splitting (hfs) constant expressed in gauss.
Q is a proportionality constant, approximately equal to -25 gauss.
The relation between A and a is given by:

$$A = \gamma_e \hbar a \qquad \text{or} \qquad A = g_e \beta_e a$$

where γ_e is the magnetogyric ratio of the electron.

Measurement of a_H from ESR spectra thus gives information about the unpaired spin distribution in the aromatic radical. The values for ρ_π obtained in this way can be compared with values calculated with M.O. theories.

2.2 ESR of triplet states.

2.2.1 The spin hamiltonian

In the spin hamiltonian which describes the magnetic interactions in molecules possessing two unpaired electrons the electron-electron dipolar interaction is accounted for by the term:

$$\mathcal{H}_D = g_e^2\beta_e^2 \left[\frac{\bar{S}_1.\bar{S}_2}{r_{12}^3} - \frac{3(\bar{S}_1.\bar{r}_{12})(\bar{S}_2.\bar{r}_{12})}{r_{12}^5} \right] \qquad (9)$$

Expressing $\mathcal{H}_D$ in terms of the total spin S and averaging over all positions r_1 and r_2 of the two unpaired electrons the dipolar interaction can be written as:

$$\mathcal{H}_D = \bar{S}.\bar{\bar{D}}.\bar{S} \quad . \qquad (10)$$

In terms of principle molecular axes x, y and z which diagonalize the zero-field tensor $\bar{\bar{D}}$, equation 10 can also be written as:

$$\mathcal{H}_D = - XS_x^2 - YS_y^2 - ZS_z^2 \qquad (11)$$

where $X = \frac{1}{2} g_e^2 \beta_e^2 \langle \psi(1,2) \left| \frac{r_{12}^2 - 3x_{12}^2}{r_{12}^5} \right| \psi(1.2) \rangle$

$\psi(1,2)$ is the triplet wave function; the expressions for Y and Z are analogous.

Because the tensor $\bar{\bar{D}}$ is traceless (X+Y+Z=0) the dipolar interaction can be rewritten in terms of two independent constants D and E. The relation between the two different sets of parameters is given by:

$$X = \frac{1}{3} D - E; \qquad Y = \frac{1}{3} D + E; \qquad Z = -\frac{2}{3} D . \tag{12}$$

Substituting these expressions in equation 11 the spin hamiltonian becomes:

$$\mathcal{H}_D = D(S_z^2 - \frac{1}{3} S^2) + E(S_x^2 - S_y^2) \tag{13}$$

with $D = \frac{3}{4} g_e^2 \beta_e^2 \langle \psi(1,2) \left| \frac{r_{12}^2 - 3z_{12}^2}{r_{12}^5} \right| \psi(1,2) \rangle$

$$E = \frac{3}{4} g_e^2 \beta_e^2 \langle \psi(1,2) \left| \frac{x_{12}^2 - y_{12}^2}{r_{12}^5} \right| \psi(1,2) \rangle .$$

For molecules with axial symmetry the zero-field splitting parameter E vanishes.

2.2.2 Triplet lineshapes

The lineshape of the ESR triplet spectrum can in principle be derived from the spin hamiltonian

$$\mathcal{H} = g_e \beta_e \bar{H}.\bar{S} + \bar{S}.\bar{\bar{D}}.\bar{S} \quad . \tag{14}$$

The Fermi contact interaction and the nuclear Zeeman term have been omitted in this equation because their influence on the triplet lineshape is generally negligible.

It is easy to see that three transitions can be induced in a triplet molecule: two transitions with $\Delta m_s = \pm 1$ and one for which $\Delta m_s = \pm 2$. In all our experiments we have measured triplet molecules in glasses so that the molecules are oriented at random. Because the high field transitions ($\Delta m_s = \pm 1$) are strongly dependent on the orientation of the molecule with respect to the magnetic field, the description of a triplet spectrum in a glass or powder becomes rather involved. An exact treatment of triplet ESR lineshapes can be found in the literature [12]. Still it is possible to give a simple classical picture of the dipolar interaction and derive in this way an ESR lineshape for an axial symmetric case [13].

Suppose the two electrons are at fixed distance $\bar{r}$. The magnetic dipole μ_e of one electron causes a magnetic field at the position of the other electron, its magnitude along the direction of the external field being equal to

$$H_e = \frac{\mu_e}{r^3} (3\cos^2\theta - 1) \tag{15}$$

where θ is the angle between $\bar{r}$ and the external field $\bar{H}$.

Because $\bar{H}_e$ adds to $\bar{H}$, resonance will occur, keeping the resonance frequency constant, at a field:

$$H = H_o - H_e = H_o - \frac{\mu_e}{r^3}(3\cos^2\theta - 1) \qquad (16)$$

where H_o is the resonance field in the absence of dipolar interaction. A continuous absorption can be observed between the two extrema of this function:

$$H_o + \frac{\mu_e}{r^3} \text{ when } \theta = \frac{\pi}{2} \text{ and } H_o - \frac{2\mu_e}{r^3} \text{ for } \theta = 0.$$

For random orientation of the resonant molecules the absorption will increase with θ, since the number of molecules at a given angle θ is proportional to $\sin\theta$ (see figure 1). This is true for one orientation of μ_e; for the opposite orientation absorption is observed between

$$H_o - \frac{\mu_e}{r^3} \text{ when } \theta = \frac{\pi}{2} \text{ and } H_o + \frac{2\mu_e}{r^3} \text{ when } \theta = 0.$$

The sum of the two absorption envelopes is shown in figure 1; the first derivative, shown in figure 2, represents the ESR spectrum of triplets in a glassy medium.

However, this model of two localized spins at fixed positions is too simple for aromatic systems we have measured, in which the unpaired electrons are delocalized over the whole molecule. This situation can be approximated by describing the aromatic molecule as a ring with the unpaired electrons moving rapidly around its circumference separated at constant distance $\bar{r}$ (figure 3).

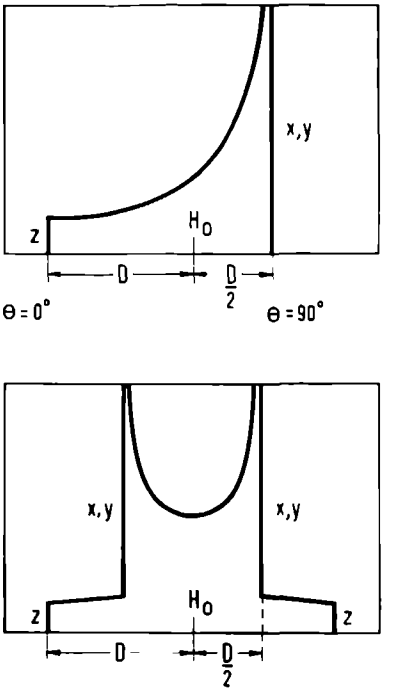

Figure 1
Absorption envelope for one orientation of μ_e (shown above) and for two orientations (shown below).

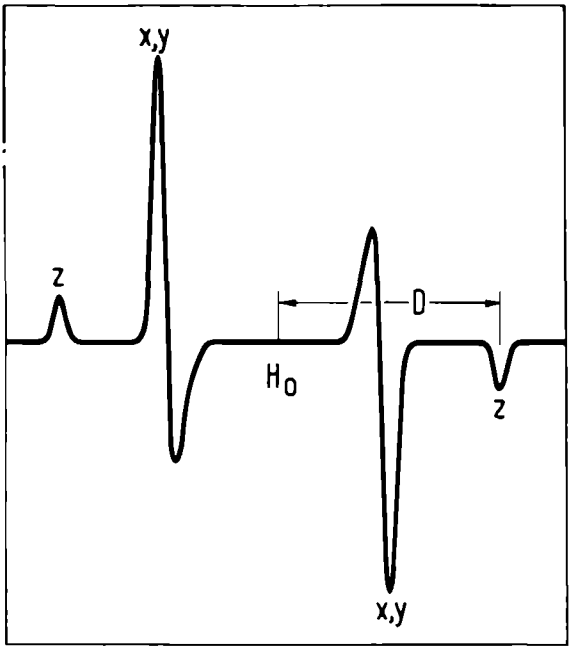

Figure 2
First derivative ESR spectrum of triplet molecules randomly oriented in a glass. ($\Delta m_s = \pm 1$ transitions)

If the magnetic field is perpendicular to the molecular plane, θ is constant ($\frac{\pi}{2}$) and $\bar{H}_e = -\bar{\mu}_e/r^3$. If $\bar{H}$ lies in the plane of the ring all values of θ occur with equal probability and the average internal field H_e is given by:

$$H_e = \frac{\mu_e}{2\pi r^3} \int_0^{2\pi} (3\cos^2\theta - 1)d\theta = \frac{\mu_e}{2r^3} \qquad (17)$$

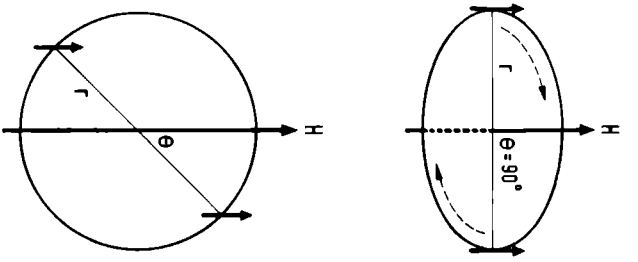

Fig. 3 - Model for an aromatic triplet system; in the picture shown left the external magnetic field is perpendicular to the aromatic plane, in the right figure the field is parallel to the plane.

With the exception of a factor of two in width the absorption will have the same shape as for the first model. Denoting μ_e/r^3 by D (expressed in gauss) the total width of the spectrum will be equal to 2D. Singularities in the absorption curve will occur at fields $H_o \pm D$ and $H_o \pm \frac{1}{2}D$ which correspond with orientations of the molecules for which the magnetic field is perpendicular to the molecular plane and parallel to this plane, respectively. Since in ESR experiments the first derivative of the absorption curve is recorded, the spectrum of random oriented molecules with trigonal symmetry will consist of four peaks located at positions where the absorption changes suddenly (see figure 2). ESR spectra of molecules with lower symmetry will show six peaks, since now there are three orientations for which the absorption changes suddenly; i.e. for $\bar{H}$

along each of the three principle axes of the molecule. The peak denoted by X,Y in figure 2 is then split into two peaks X and Y, the distance between these two peaks being equal to 3E.

2.2.3 Calculation of the zero-field splitting (ZFS) parameters

For the calculation of the ZFS parameters D and E the method of van der Waals and ter Maten has been followed [14]. A brief outline of their method will be presented here.

The triplet wave function for the state with $m_s = +1$ is given by the following Slater determinant:

$$\psi_o = |\phi_1\bar{\phi}_1 \ldots\ldots \phi_m\bar{\phi}_m \; a \; b| \tag{18}$$

where a and b denote π M.O.'s occupied by the unpaired electrons. Because closed shells do not contribute to D and E, ψ_o may also be written as

$$\psi_o = |ab| = 2^{-\frac{1}{2}} \{a(1)b(2) - a(2)b(1)\} \tag{19}$$

where $a = \sum_i a_i\varphi_i$ and $b = \sum_j b_j\varphi_j$.

φ_i and φ_j are $2p_z$ functions of the carbon atoms i and j. The expression for the ZFS parameters becomes:

$$\left(\frac{D}{E}\right) = \langle\psi_o|\frac{\bar{D}}{\bar{E}}|\psi_o\rangle =$$

$$\frac{1}{2}\int\int \left[\sum_i a_i\varphi_i(1)\sum_j b_j\varphi_j(2) - \sum_j b_j\varphi_j(1)\sum_i a_i\varphi_i(2)\right]^2 \left(\frac{\bar{D}}{\bar{E}}\right)d\tau_1 d\tau_2 \tag{20}$$

with $\bar{D} = \frac{3}{4} g_e^2 \beta_e^2 \left| \frac{r_{12}^2 - 3z_{12}^2}{r_{12}^5} \right|$ and $\bar{E} = \frac{3}{4} g_e^2 \beta_e^2 \left| \frac{y_{12}^2 - x_{12}^2}{r_{12}^5} \right|$

if only two center integrals are retained we find:

$$\binom{D}{E} = \sum_{i<j} (a_i b_j - a_j b_i)^2 \binom{D_{ij}}{E_{ij}} \qquad (21)$$

with $\binom{D_{ij}}{E_{ij}} = \int\int \varphi_i^2(1) \left(\frac{\bar{D}}{\bar{E}}\right) \varphi_j^2(2) d\tau_1 d\tau_2$

$$- \int\int \varphi_i(1)\, \varphi_j(2) \left(\frac{\bar{D}}{\bar{E}}\right) \varphi_i(2)\, \varphi_j(1) d\tau_1 d\tau_2 \quad . \qquad (22)$$

The coefficients a and b are obtained from open shell PPP SCF calculations for the triplet groundstate. Values of D_{ij} and E_{ij} are given by van der Waals and ter Maten.

More accurate values for D and E are calculated when one takes into account configuration interaction of ψ_o with doubly excited triplet wavefunctions ψ_i:

$$\psi = N(\psi_o + \sum_i \lambda_i \psi_i) \qquad (23)$$

where $N = (1 + \sum_i \lambda_i^2)^{-\frac{1}{2}}$ and $\lambda = - \frac{H_{oi}}{E_i}$

$$H_{oi} = \langle \psi_o | \mathcal{H} | \psi_i \rangle \qquad E_i = H_{ii} - H_{oo}$$

Writing $\psi_o = |\phi_1 \bar{\phi}_1 \ldots\ldots a\ b|$ and $\psi_i = |\phi_1 \bar{\phi}_1 \ldots\ldots c\ d|$

we find in the zero differential overlap approximation

$$H_{oi} = \sum_{i<j} (a_i b_j - a_j b_i)(c_i d_j - c_j d_i)\gamma_{ij} \qquad (24)$$

where γ_{ij} is the repulsion integral $\int\int \varphi_i^2(1) \frac{e^2}{r_{12}} \varphi_j^2(2) d\tau_1 d\tau_2$. The values of these integrals have been taken from Pariser [15]. Neglecting second order contributions to D and E we can write:

$$D = N^2(D^{oo} + 2 \sum_i \lambda_i D^{oi}) \quad . \qquad (25)$$

The expression for E is analogous.

In this formula $D^{oo} = \langle\psi_o|\bar{D}|\psi_o\rangle$ and $D^{oi} = \langle\psi_o|\bar{D}|\psi_i\rangle$. Applying the zero differential overlap approximation again D^{oi} can be written completely analogous to H_{oi}:

$$D^{oi} = \sum_{i<j} (a_i b_j - a_j b_i)(c_i d_j - c_j d_i) D_{ij} \quad . \qquad (26)$$

With the aid of these expressions the ZFS parameters of the unperturbed triplet dianions are calculated.

In solvents with low solvating power the triplet dianions are associated with counter ions resulting in different ZFS parameters D and E. To account for these effects the same procedure has been followed as has been used by Sommerdijk [7,8]. He accounted for the perturbing influence of the counter ions semi-empirically by using an extension of the method given by Reddoch [16]. The elements of the Hückel matrix are modified as follows:

$$H_{ii} = \alpha + \left[\frac{5.6}{r_{iM_1}} + \frac{5.6}{r_{iM_2}}\right]\beta$$

$$H_{ij} = \beta \left[1 + \frac{2.8}{r_{iM_1}+r_{jM_1}} + \frac{2.8}{r_{iM_2}+r_{jM_2}}\right] \qquad (27)$$

where r_{iM_1} is the distance of the cation M_1 to the carbon atom i (Å units).

In this way modified Hückel MO's are obtained that can be used for the calculation of the SCF MO's. After first order CI has been carried out, the ZFS parameters are calculated according to the method pointed out above.

2.3 NMR of paramagnetic molecules

2.3.1 The fermi contact shift

The presence of an unpaired electron in a molecule can produce drastic changes in the NMR spectrum when compared to the spectra of diamagnetic molecules [17]. Typical for paramagnetic molecules are large shifts and very broad lines. The observed phenomena can in principle be derived from the spin hamiltonian

$$\mathcal{H} = -g_N\beta_N H_z I_z(1-\sigma) + A\bar{I}.\bar{S}(t) + \bar{I}.\bar{\bar{T}}(t).\bar{S}(t) \quad . \qquad (28)$$

The electron Zeeman term has been omitted in this equation since it does not affect the nuclear resonance.
$-g_N\beta_N H_z I_z(1-\sigma)$ represents the nuclear Zeeman energy

$A\bar{I}.\bar{S}(t)$ is the Fermi contact interaction

$\bar{I}.\bar{\bar{T}}(t).\bar{S}(t)$ is the anisotropic dipolar interaction between the nucleus I and the unpaired electron spin.

Only the first two terms determine the position of the NMR resonance lines. The Fermi contact interaction produces a local field at the nucleus that is time dependent because the electron spin relaxes very fast. If the variation of S(t) is characterized by a correlation time τ_e much shorter than $\hbar A^{-1}$, equation 28 can be written as

$$\mathcal{H} = -g_N\beta_N H_z I_z(1-\sigma) + AI_z \langle S_z(t)\rangle \qquad (29)$$

with $\langle S_z(t)\rangle = \dfrac{g_e\beta_e S(S+1)H_z}{3kT}$.

Performing a NMR experiment at constant frequency ω_o and sweeping the magnetic field the resonance condition for a nucleus N in a molecule with one unpaired electron becomes:

$$H_p(1-\sigma_p) + \frac{Ag_e\beta_e H_p}{g_N\beta_N 4kT} = \frac{\omega_o\hbar}{g_N\beta_N} \qquad (30)$$

where H_p is the resonance field.

As the resonance condition of a diamagnetic molecule is given by

$$H_d(1-\sigma_d) = \frac{\omega_o\hbar}{g_N\beta_N} \qquad (31)$$

the Fermi contact shift can be defined as

$$\delta_o^c = H_p(1-\sigma_p) - H_d(1-\sigma_d) \quad . \qquad (32)$$

From equations 30, 31 and 32 follows:

$$\delta_o^c = - \frac{A g_e \beta_e H p}{g_N \beta_N 4kT} \quad . \tag{33}$$

Combining equations 7, 8 and 33 it is clear that the sign and magnitude of the spin density at the nucleus can be inferred directly from the contact shift δ_o^c which is independent of the sign of g_N.

2.3.2 The NMR linewidth

The width of the resonance line will be largely determined by intramolecular interactions. For protons, that have a spin of $\frac{1}{2}$, two time dependent mechanisms are responsible for the NMR linewidth. The first contribution arises from a modulation of the Fermi contact interaction by the time dependence of $\bar{S}$. The other important process is the modulation of the anisotropic dipolar interaction between the magnetic moments of the unpaired electron and the protons, caused both by the rapid tumbling of the molecule in the liquid and the fluctuations of $\bar{S}$ in time. The appropriate time dependent hamiltonian consists of two terms:

$$\mathcal{H}_1(t) = \mathcal{H}_{F.c.}(t) + \mathcal{H}_D(t) \tag{34}$$

with $\mathcal{H}_{F.c.}(t) = A\bar{I}.\bar{S}(t)$ and $\mathcal{H}_D(t) = \bar{I}.\bar{\bar{D}}(t).\bar{S}(t)$

where $D_{ij}(t)$ is given by

$$D_{ij}(t) = \langle \psi \left| \frac{r^2 \delta_{ij} - 3i(t)j(t)}{r^5} \right| \psi \rangle \gamma_e \gamma_N \hbar^2$$

i,j = x, y, z, referring to the laboratory coordinate system.
$\delta_{ij} = 1$ if $i = j$ and $\delta_{ij} = 0$ if $i \neq j$.
ψ is the electronic wave function.

The contribution to the linewidth from the Fermi contact interaction is given by [18]:

$$(T_2^{-1})_{Fc} = \frac{1}{3} \left(\frac{A}{\hbar}\right)^2 S(S+1) \left[\tau_e + \frac{13\tau_e}{1+\omega_e^2\tau_e^2}\right] \qquad (35)$$

where $\omega_e = \gamma_e H$ and τ_e is the electron correlation time.

Solomon [19] has derived an expression for the contribution of $\mathcal{H}_D(t)$ to the linewidth for the case of two point dipoles of spin $\frac{1}{2}$ separated by a distance r:

$$(T_2^{-1})_D = \frac{1}{20} \left(\frac{B}{\hbar}\right)^2 \left[7\tau_c + \frac{13\tau_c}{1+\omega_e^2\tau_c^2}\right] \qquad (36)$$

with $B = \dfrac{\gamma_e\gamma_N\hbar^2}{r^3}$; τ_c is the rotational correlation time.

In the molecule we have measured the situation is essentially different: the unpaired electron is delocalized over the whole molecule and must be described by a molecular orbital. We must therefore adapt formula 34 to our situation and write the dipolar hamiltonian in full length:

$$\begin{aligned}\mathcal{H}_D(t) = \big[& D_{xx}(t)S_xI_x + D_{xy}(t)(S_xI_y + S_yI_x) \\ & + D_{xz}(t)(S_xI_z+S_zI_x) + D_{yy}(t)S_yI_y + D_{yz}(t)(S_yI_z+S_zI_y) \\ & + D_{zz}(t)S_zI_z\big] \quad . \end{aligned} \qquad (37)$$

Writing

$$I_x = \tfrac{1}{2}(I_+ + I_-) \qquad \text{and} \qquad S_x = \tfrac{1}{2}(S_+ + S_-)$$

$$I_y = \frac{1}{2i}(I_+ - I_-) \qquad\qquad S_y = \frac{1}{2i}(S_+ - S_-)$$

it follows that

$$\begin{aligned}\mathcal{H}_D(t) = \Big[&\{I_zS_z - \tfrac{1}{4}(I_+S_- + I_-S_+)\}\, D_{zz}(t) \\ &+ \tfrac{1}{2}(I_+S_z + I_zS_+)\{D_{xz}(t) - iD_{yz}(t)\} + \tfrac{1}{2}(I_-S_z + I_zS_-)\{D_{xz}(t) + iD_{yz}(t)\} \\ &+ \tfrac{1}{4} I_+S_+\{D_{xx}(t) - D_{yy}(t) - 2iD_{xy}(t)\} + \tfrac{1}{4} I_-S_-\{D_{xx}(t) - D_{yy}(t) + 2iD_{xy}(t)\} \Big] .\end{aligned} \tag{38}$$

In deriving this expression $D_{xx} + D_{yy}$ has been replaced by $-D_{zz}$ ($\bar{\bar{D}}$ is a traceless tensor).
If we write:

$$\begin{aligned} D_{zz}(t) &= F_0(t) \\ \frac{1}{4}(D_{xx}(t) - D_{yy}(t) - 2iD_{xy}(t)) &= F_2(t) \\ \frac{1}{2}(D_{xz}(t) - iD_{yz}(t)) &= F_1(t) \end{aligned} \tag{39}$$

we have obtained an equation for $\mathcal{H}_D(t)$ completely equivalent to the expression of Solomon for the point dipole model. He derived that the contribution of $\mathcal{H}_D(t)$ to T_2^{-1} is equal to

$$\frac{1}{T_2} = \frac{1}{4\hbar^2}\Big[\{\tau_c + \frac{\frac{1}{4}\tau_c}{1+(\omega_I-\omega_S)^2\tau_c^2}\}\ \langle F_o^2\rangle$$

$$+\ \{\frac{2\tau_c}{1+\omega_I^2\tau_c^2} + \frac{4\tau_c}{1+\omega_S^2\tau_c^2}\}\langle|F_1|^2\rangle$$

$$+\ \frac{4\tau_c}{1+(\omega_S+\omega_I)^2\tau_c^2}\langle|F_2|^2\rangle\Big] \quad . \qquad (40)$$

This formula is still valid for our case. The ensemble averages $\langle F_o^2\rangle$, $\langle|F_1|^2\rangle$ and $\langle|F_2|^2\rangle$ have been calculated using the following relations for the average value of tensor elements in the laboratory coordinate system [20]:

$$D_{ii}D_{ii} = \frac{2}{15}(D:D)$$

$$D_{ii}D_{jj} = -\frac{1}{15}(D:D)$$

$$D_{ij}D_{ij} = \frac{1}{10}(D:D) \qquad (41)$$

with $(D:D) = \sum_{\alpha,\beta}(D_{\alpha\beta})^2$; i,j refer to the laboratory coordinate system, α,β are principle axes.
For the latter system the following relation holds ($D_{\alpha\beta}$ diagonal):

$$(D:D) = \sum_{\alpha}(D_{\alpha\alpha})^2 = \text{Trace}\,(\bar{\bar{D}}.\bar{\bar{D}}) \quad . \qquad (42)$$

With this information the following relations are derived:

$$\langle F_o^2 \rangle = \langle D_{zz}^2 \rangle = \frac{2}{15} (D:D)$$

$$\langle |F_1|^2 \rangle = \frac{1}{4} \left[\langle D_{zx}^2 \rangle + \langle D_{yz}^2 \rangle \right] = \frac{1}{20} (D:D)$$

$$\langle |F_2|^2 \rangle = \frac{1}{16} \left[\langle D_{xx}^2 \rangle + \langle D_{yy}^2 \rangle - 2\langle D_{xx} D_{yy} \rangle + 4\langle D_{xy}^2 \rangle \right] = \frac{1}{20} (D:D) \quad (43)$$

Substituting these values in equation 40 the expression for the linewidth parameter becomes:

$$T_2^{-1} = \frac{(D:D)}{120\hbar^2} \left[4\tau_c + \frac{\tau_c}{1+(\omega_I-\omega_S)^2\tau_c^2} + \frac{3\tau_c}{1+\omega_I^2\tau_c^2} \right.$$

$$\left. + \frac{6\tau_c}{1+\omega_S^2\tau_c^2} + \frac{6\tau_c}{1+(\omega_I+\omega_S)^2\tau_c^2} \right] . \quad (44)$$

So far only the time dependence of the D tensor has been considered. In the concentrated paramagnetic solutions that have been measured the unpaired electron relaxes very fast and the time dependence of S must also be considered. This means that the autocorrelation functions take the form

$$\langle D_{ij}(t+\tau) D_{ij}(t) \rangle \langle S_j(t+\tau) S_j(t) \rangle = \langle D_{ij}^2 \rangle \exp(-\frac{\tau}{\tau_c}) \langle S_j^2 \rangle \exp(-\frac{\tau}{\tau_e}) \quad (45)$$

where i and j refer to the laboratory coordinate system.

Because $\langle S_j^2 \rangle = \frac{1}{3} S(S+1) = \frac{1}{4}$, the above expression can be written as

$$\frac{1}{4} \langle D_{ij}^2 \rangle \exp(-\frac{\tau}{\tau_d})$$

with

$$\frac{1}{\tau_d} = \frac{1}{\tau_c} + \frac{1}{\tau_e} \quad . \tag{46}$$

Due to this time dependence of S, τ_c in equation 44 must be replaced by τ_d: the dipolar correlation time. Bearing also in mind that $\omega_S >> \omega_I$ and $\omega_I^2 \tau_d^2 << 1$, equation 44 simplifies to

$$(T_2^{-1})_D = \frac{(D:D)}{120\hbar^2} \left[7\tau_d + \frac{13\tau_d}{1+\omega_e^2\tau_d^2} \right] \quad . \tag{47}$$

The elements of the D tensor, that are very similar in form to the tensor elements of the electron-electron dipolar interaction (equation 11), are given by

$$D_{\alpha\beta} = \langle \psi \mid \frac{r^2\delta_{\alpha\beta} - 3\alpha\beta}{r^5} \mid \psi \rangle \gamma_e \gamma_N \hbar^2 \tag{48}$$

α and β are components of $\bar{r}$ (the distance between the unpaired electron and nucleus N) along principle axes; ψ is the wavefunction describing the unpaired electron.

Writing $\psi = \sum_i c_i \varphi_i$ where φ_i are $2p_z$ carbon functions we find:

$$D_{\alpha\beta} = \sum_{i,j} c_i^* c_j \langle \varphi_i \mid \frac{r^2\delta_{\alpha\beta} - 3\alpha\beta}{r^5} \mid \varphi_j \rangle \gamma_e \gamma_N \hbar^2 \quad . \tag{49}$$

If α and β are principle axes we can write:

$$D_{\alpha\alpha} = \sum_{i,j} \rho_{ji} D_{ij} = \mathrm{Tr}(\rho . D) \qquad (50)$$

with

$$D_{ij} = \langle \varphi_j \mid \frac{r^2 - 3\alpha^2}{r^5} \mid \varphi_i \rangle \gamma_e \gamma_N \hbar^2$$

and

$$\rho_{ji} = c_i^{\star} c_j \quad .$$

C H A P T E R III

EXPERIMENTAL PART

3.1 Apparatus

The ESR experiments have been performed on a Varian 4502 X band spectrometer equipped with a variable temperature control and a fieldial. The magnetic field was measured with an AEG gaussmeter and the frequency was monitored with a HP 5245 L frequency counter. Variable temperatures down to 10°K were obtained by passing cold helium gas along the sample. The temperature was measured with a copper-constantan couple, calibrated at liquid helium and liquid nitrogen temperature. NMR experiments have been performed on a Varian DP 60 EL spectrometer employing both high resolution and wide line technique. Optical spectra were recorded on a Cary 14 spectrometer equipped with a Cryoson installation for variable temperatures. Microwave powers were measured with a HP 431 C power meter.

3.2 Preparation of the samples.

The aromatic negative ions were prepared in a standard way on a vacuum line. The solvents tetrahydrofuran (THF), 2-methyltetrahydrofuran (MTHF), 1,2 dimethoxyethane (DME) and diethylether (DEE) were dried over a sodium dispersion in parafin, distilled in vacuo and stored on a Na/K alloy.

The polyethers diglyme, triglyme and tetraglyme were dried on Na or a Na/K alloy and distilled on the vacuum line just before use. A cyclic ether (2,3,11,12-dibenzo-1,4,7,10,13,16-hexaoxacyclo-octadeca-2,11-diene, see figure 5) was synthetized [21] and sublimed before use. Sodium tetraphenylboron was also sublimed in vacuo. 2-D-triphenylene has been synthetized starting from 2-Br-triphenylene:

$$2\text{-Br-Tp} + C_4H_9Li \rightarrow 2\ \text{Li-Tp} \xrightarrow{D_2O} 2\text{-D-Tp} \quad .$$

To a solution of 400 mg 2-Br-Tp [22] (mp 131.5-133.5°C) in 20 ml dry DEE a butyllithium solution was added at 0°C in a nitrogen atmosphere. The solution was stirred for one hour at 0°C and for two hours at room temperature. At 0°C 3 ml D_2O was gradually added while stirring the solution during 15 minutes. The solution was washed, dried and filtered. After evaporating the diethylether the residue (305 mg) was purified on an Al_2O_3 column using petrol ether (bp. 40-60°C) as eluating solvent. The final yield was 130 mg 2-D-Tp (mp 191-195°C). 0.1 Molar solutions of polyglymes in MTHF have been prepared by drying the two components separately (figure 4). The polyether was dried in compartment A over Na, Na-Pb alloy or Na-K alloy on a vacuum line. The dried ether was then distilled into ampoule B, that is attached to A by a ground joint, and was sealed off after distillation. As B was of known weight, the amount of dried polyether could be determined by weighing. B was attached to a storage vessel C which was then connected to a vacuum line and filled with a known amount of dried MTHF. Next C was sealed off from the line, the breakseal between B and C was destroyed and the

two solvents were mixed.

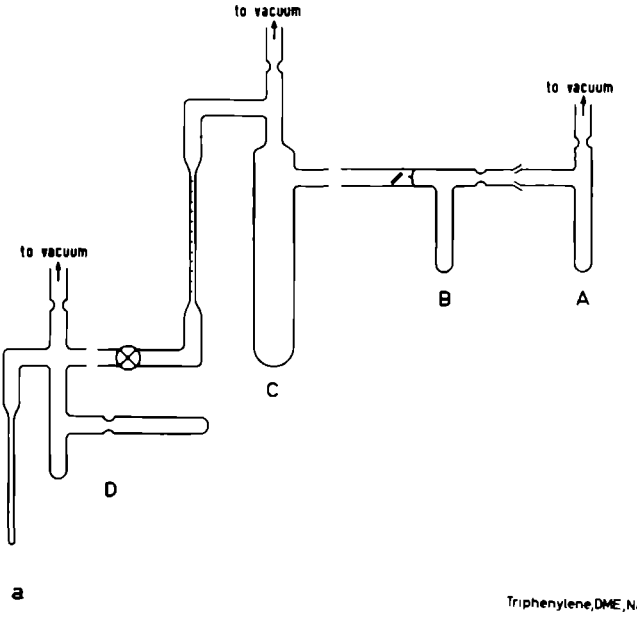

Fig. 4 - Apparatus for titrations with polyether solutions in MTHF.

C also contained a sodium mirror to remove final traces of moisture or oxygen. The storage bottle C is connected to an ESR sample tube by a teflon membrane stop cock.

Fig. 5

cyclic ether (crown ether)

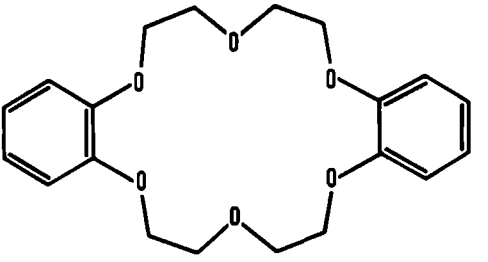

Negative ions of the aromatic compounds that have been studied with ESR are listed in Table 1.

Table 1

The syntheses have been carried out by the author except those that are marked with an asterix

Triphenylene	(Flucka)
2-D-triphenylene	(synthesis)*
2-CH_3-triphenylene	(gift)**
1,3,5-triphenylbenzene	(Flucka)
1,3,5-tris-(2,5-dimethylphenyl)-benzene	(synthesis) [23]
1,3,5-tris-biphenyl(4)-benzene	(synthesis) [23]
hexaphenylbenzene	(synthesis) [24]
2,4,6-triphenyl-sym-triazine	(synthesis) [25]
2,4,6-tri-p-tolyl-sym-triazine	(synthesis) [25]
hexabenzocoronene	(Rütgerswerke)
decacyclene	(Rütgerswerke)
c,i,o-tribenzo-triphenylene	(synthesis)*** [26]

The optically excited triplet states of trinaphthylene and tribenzotriphenylene have been measured in ethanol after irradiation with a high pressure mercury lamp. By passing cold helium gas along the samples they could be cooled down to about -260°C.

* Synthetized by Drs. W. Bassi
** Gift of Dr. P. Cossee
*** Synthetized by Dr. W. Laarhoven

C H A P T E R IV

MONONEGATIVE IONS

4.1 The mononegative ion of triphenylene.

4.1.1 ESR experiments

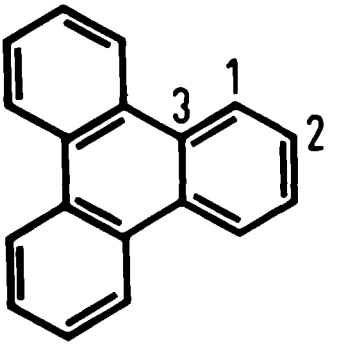

Electrolytical or alkali reduction of triphenylene (Tp) in ethereal solvents gives rise to blue paramagnetic solutions. By ESR measurements on these solutions three types of fluid solution spectra, differing in hyperfine structure, can be observed. The characteristic features of these spectra and the conditions under which they were recorded will be discussed below.

a) Spectrum I

The spectrum that will be discussed first is reproduced in figure 6. Computer simulations showed that the exhibited hyperfine structure can be assigned to a contact interaction between the unpaired electron and two sets of equivalent protons. The coupling constants and linewidth were determined by an iterative computer adaption program. The experimental spectrum was fed to the computer on a tape, together with trial values for the parameters characterizing the ESR spectrum. These values were varied in such a way as to minimize the deviation from the input spectrum. After 10 iterations the following values were found for the coupling constants: a_1 = 1.097 gauss and a_2 = 1.613 gauss. A value of 0.245 gauss was obtained for the derivative linewidth. Analysis of the spectrum obtained from Tp^- deuterated at position 2 proved that the smallest hfs constant must be assigned to position 1.

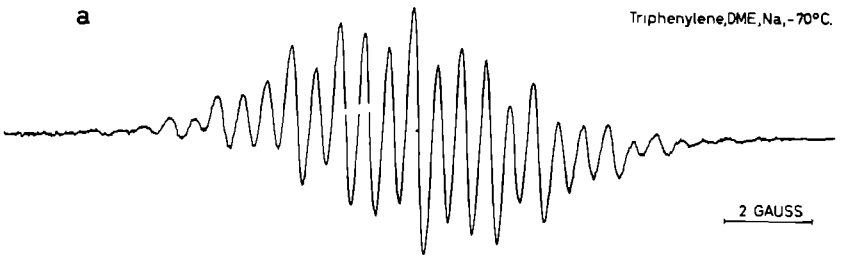

Fig. 6 - ESR spectrum of Tp^- reduced with sodium in DME.

Spectrum I was obtained irrespective of the temperature and reducing agent from Tp^- solutions in very polar solvents like NH_3, hexamethylphosphoramide, acetonitril, polyethyleneglycoldimethylethers and from electrolytically generated radicals. Using Li as reducing agent spectrum I could be produced in THF, 2-MTHF, and DME irrespective of the temperature. However, in DEE as solvent spectrum I could only be obtained at temperatures below $-90^{\circ}C$. Above this temperature spectrum II appeared. A similar change occurred in the spectrum of Tp^- solutions in THF and MTHF when the reductor was either Na, K or Rb, the only difference being that the temperature at which spectrum I changed into spectrum II was higher for THF than for MTHF and increased with decreasing radius of the counter ion. Employing DME as solvent and Na as reducing agent spectrum I remained unaffected by temperature changes; an increase in the temperature from $-90^{\circ}C$ to room temperature on the other hand did affect this spectrum when K or Rb had been used for reduction. The hyperfine splittings in the spectra of this type were not influenced noticeably by solvent and/or counter ion variations.

The g value of this spectrum was measured in 2-MTHF at $-100^{\circ}C$ in a dilute solution. To correct for the field difference between the position of the sample and the proton resonance probe of the gauss meter, also the g value of perylene cation in H_2SO_4 was measured. With the help of the absolute g value of the latter ion, reported in the literature [27] and correcting for the second order shift (-1×10^{-6}) the absolute g value of Tp^- was found to be $2.002839 \pm 7\times10^{-6}$.

b) Spectrum II

Spectrum II which is shown in figure 7 consists of 13 equidistant lines (the weak peaks in the tails cannot be observed in the figure) with an almost binomial intensity distribution. This suggests the presence of 12 nearly equal hyperfine splitting constants. It was found that the relative intensities of the hyperfine components and their linewidths varied slightly with metal ion and solvent. To determine the actual values characterizing the spectrum, the latter was fed to a computer on a magnetic tape. A spectrum adaption program then optimized the coupling constants and linewidth. After 10 iterations the following values were obtained: $a_1 = 1.277$, $a_2 = 1.566$ and δ (linewidth) = 0.459 gauss. The standard error in a spectrum calculated with 12 equivalent coupling constants of 1.425 gauss and a linewidth of 0.673 gauss proved to be higher.

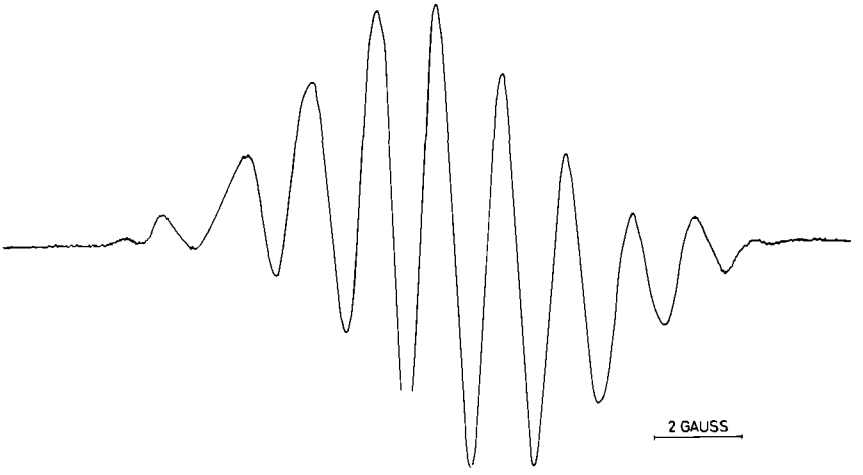

Fig. 7 - ESR spectrum of $Tp^{-}Na^{+}$ in 2-MTHF.

In all cases where spectrum I could only be obtained at low temperatures, spectrum II appeared by increasing the temperature. For instance, a temperature increase from $-120^{\circ}C$ to $-70^{\circ}C$ resulted in a gradual transformation of spectrum I into spectrum II for sodium reduced Tp in MTHF. Similar effects were observed upon temperature increases for K or Rb reduced Tp^- solutions in DME, THF or MTHF and for Tp^- solutions in DEE in the presence of Li^+. It was found that the temperature range in which the gradual transformation of spectrum I into spectrum II took place, could be shifted to lower temperatures by introducing metal ions to the Tp^- solutions. Thus addition of a large amount of sodium tetraphenylboron to a solution of Na reduced Tp in MTHF resulted in a shift to lower temperature of as much as $15^{\circ}C$. Dilution of a Tp^- solution had just the opposite effect: a shift to higher temperatures.

The absolute g value of this spectrum was found to be lower than the g value of spectrum I: $g = 2.00273 \pm 1.10^{-5}$; the second order shift could be neglected. The error in this g value is somewhat larger than the deviation in the g value of spectrum I because of the larger peak to peak distance of the central line.

The spectra observed for sodium reduced MTHF solutions of Tp in the temperature range where spectrum I changes into spectrum II proved to be superpositions of these two spectra, the weight fractions varying with temperature. The spectra were analysed with the help of a computer. A typical example of such a spectrum is shown in figure 8.

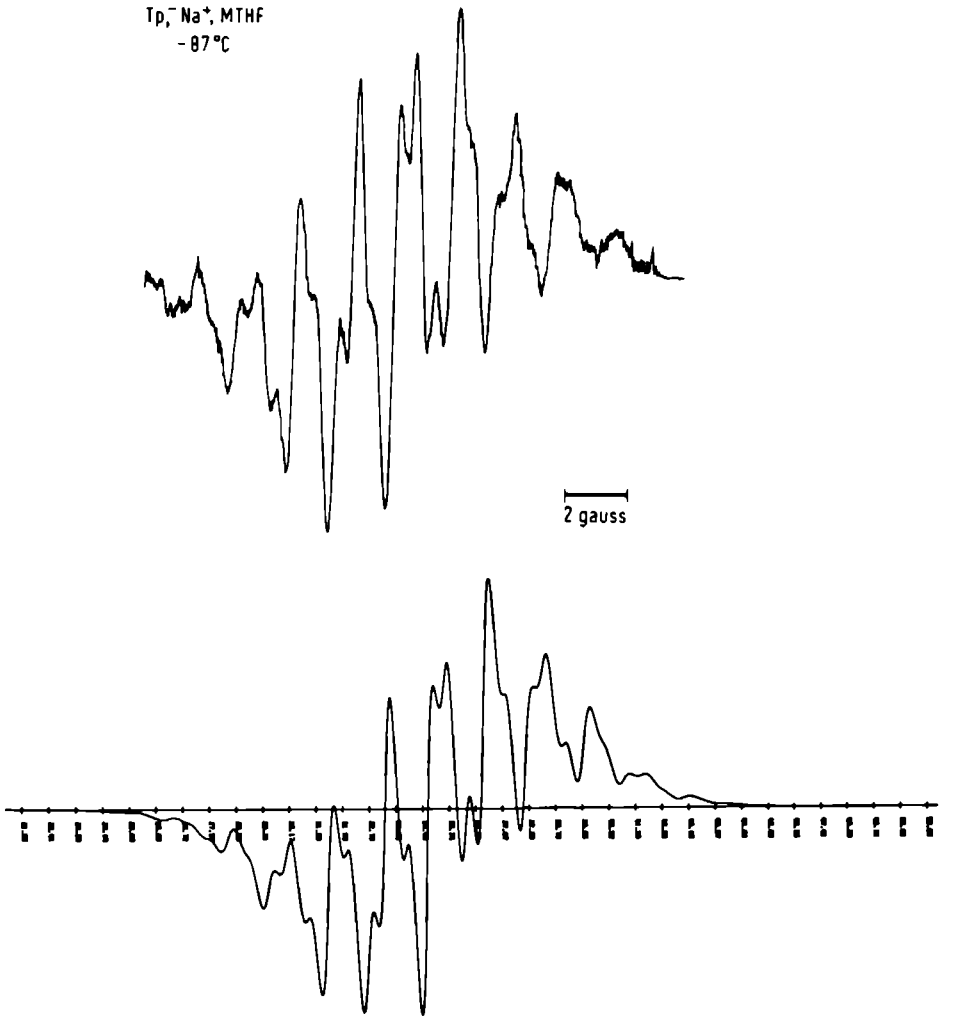

Fig. 8 - Superposition spectrum of T_p^- in MTHF. The asymmetry in the spectrum is due to the g difference between the two components. The computed spectrum is shown below.

Notice again their asymmetrical shape due to the difference in g value. The following input data have been used for the spectrum simulation:

Table 5

Input data for the computer simulation of the spectrum shown in figure 8

Spectrum I	Spectrum II
a_1 = 1.10 gauss	a_1 = 1.28 gauss
a_2 = 1.61 gauss	a_2 = 1.57 gauss
Linewidth = 0.50 gauss	Linewidth = 0.50 gauss
Weight = 80%	Weight = 20%
g value difference between the spectra corresponds to 0.16 gauss.	

c) Spectrum III

Using sodium as reducing agent and MTHF, diethylether (DEE), THP or a MTHF-hexane mixture as solvent, the 13 line spectrum discussed above is affected by further temperature increases. Representative spectra are reproduced in figure 9.

Computer simulations showed that the hyperfine pattern of spectra of type III is that of a 13 line pattern in which each of the components is split once more into four lines of equal intensity. The magnitude of this splitting increases with temperature. The variation of this coupling constant with temperature has been plotted in figure 10.

It was found that spectrum III is also strongly affected by the introduction of additional metal ions to the radical solutions. If a large excess of Na-tetraphenylboron is added to a $Tp^{-}Na^{+}$ solution in MTHF (molar concentration of the

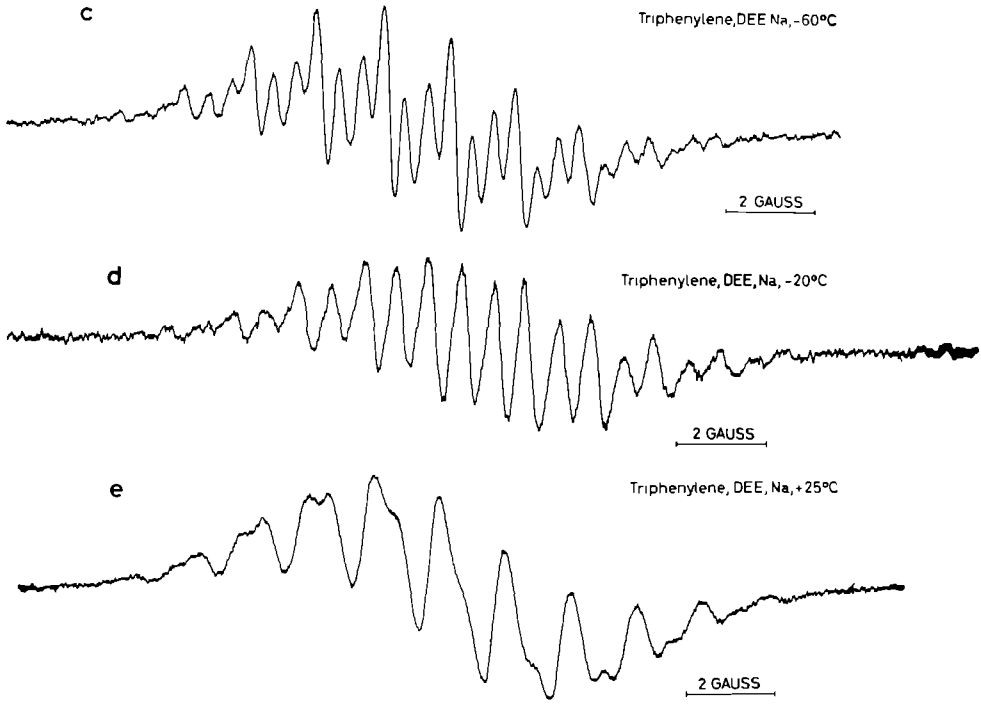

Fig. 9 - ESR spectra of Tp^- in DEE exhibiting different alkali splittings.

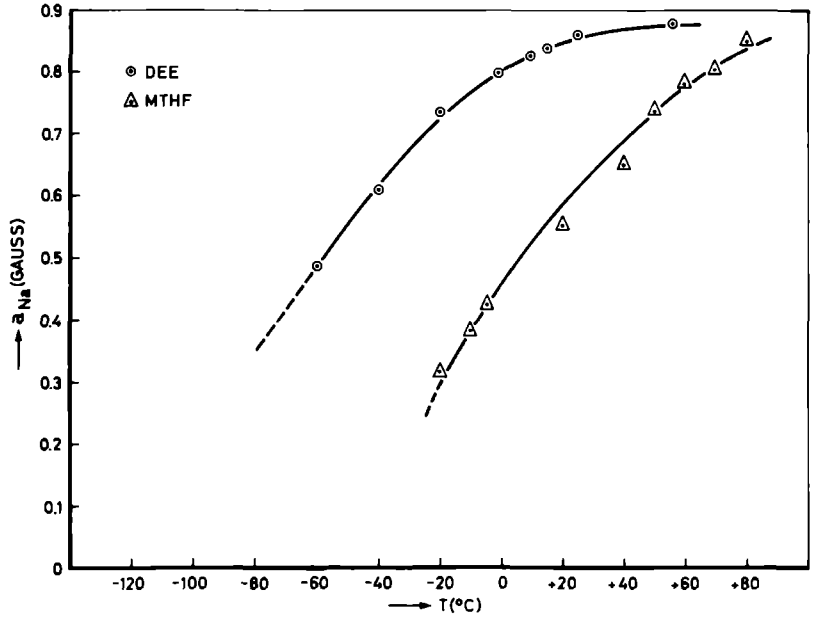

Fig. 10 - Metal ion hyperfine splitting in Tp^-Na^+ dissolved in DEE and MTHF as a function of the temperature.

salt more than 100 × the concentration of Tp^-), temperature increases do not affect spectrum II: the quartet splitting is not observed. However, introduction of smaller quantities of the diamagnetic salt merely broadens the quartet splitting in spectra of type III. Averaging out the sodium hfs completely by a large excess of $NaB(Ph)_4$ and observing the proton lines only, no significant variation in the proton coupling constants could be detected on changing the temperature.

When a polyglycolether was added to Tp^-Na^+ in MTHF at 25°C, spectrum III was gradually converted into spectrum I. Computer analysis showed that the spectra intermediate between spectra I and III were in fact superpositions of these two spectra, while the alkali splitting remained unaffected by the introduction of the polyether. Spectrum II was not observed as an intermediate at this temperature. A typical example of such a superposition spectrum is shown in figure 11 together with the computer simulation. The asymmetry in the spectrum is due to the difference in g values of the two component spectra. The experimental spectrum was recorded at room temperature; the concentrations of Tp^- and (free) tetraglyme were 4.6×10^{-5} and 1.5×10^{-5}, respectively. For the construction of the computer simulated spectrum the following parameters have been used:

Table 2

Computer input data for the simulation of the spectrum shown in figure 11

spectrum I		spectrum III	
6 protons with a	= 1.66 gauss	6 protons with a	= 1.57 gauss
6 protons with a	= 1.10 gauss	6 protons with a	= 1.28 gauss
alkali splitting	= 0.0 gauss	alkali splitting	= 0.50 gauss
linewidth	= 0.50 gauss	linewidth	= 0.46 gauss
weight	= 50%	weight	= 50%
g value	= 2.002839	g value	= 2.002 73

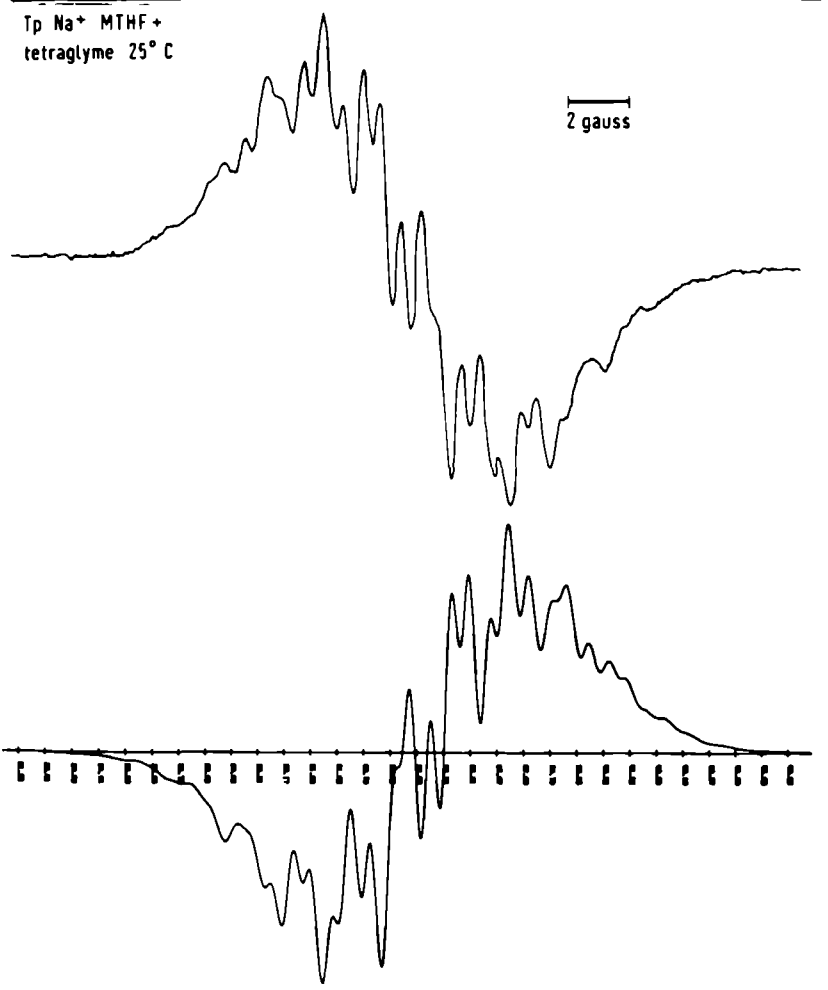

Fig. 11 - $Tp^{-}Na^{+}$ in MTHF. A small amount of tetraglyme has been added. The computer simulation is shown below. Notice the asymmetry in the spectrum.

The difference in g values results in a shift of 0.15 gauss between the two spectra. It was found that the g value of spectrum III did not change measurably with temperature: its value was found to be equal to that of spectrum III.

Finally we like to mention a spectrum recorded from a Na reduced Tp solution in liquid NH_3. After prolonged reduction a spectrum appeared which is shown in figure 12.

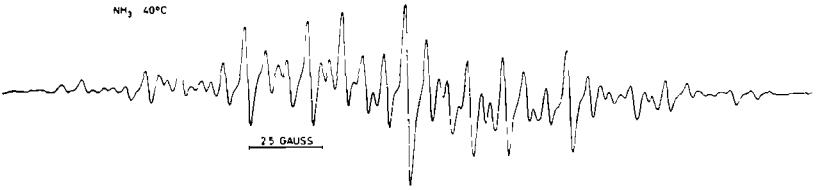

Fig. 12 - Spectrum of hydrogenated Tp^- in liquid ammonia.

The spectrum could be simulated with four sets of two equivalent protons having coupling constants of 5.30, 3.25, 2.10 and 0.70 gauss, respectively.

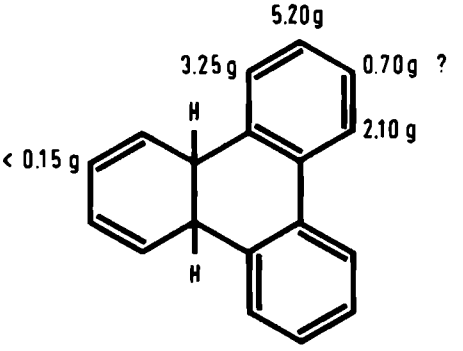

The presence of twofold symmetry and the absence of a quintuplet splitting (which would be caused by four equivalent aliphatic protons) strongly suggests that two carbon atoms in the central ring of Tp^- are hydrogenated. The coupling constants of 5.30, 2.10 and 0.70 gauss may then be attributed to the biphenyl-like part of the molecule (the coupling constants of the biphenyl anion are 5.30, 2.62 and 0.39 gauss). The diene fragment may have hfs constants smaller than the linewidth due to its low electron affinity.

4.1.2 Optical experiments

Optical measurements in the visible region have been carried out on $Tp^{-}Na^{+}$ dissolved in MTHF and MTHF-tetraglyme mixtures.

The optical study has some advantages over the ESR experiments because absolute concentrations can be determined more accurately once the molar extinction coefficients are known. Besides higher concentrations of radicals (10^{-4}-10^{-2} molar) can be studied than with ESR (10^{-4}-10^{-6} molar) because at radical concentrations higher than 10^{-4} molar the ESR lines start to broaden and finally collapse to a single line due to electron exchange reactions.

In pure MTHF the optical spectrum of sodium reduced Tp^{-} remained unchanged from the highest temperatures measured (about + 50°C) to approximately -70°C. This spectrum, denoted by 1 in figure 13, had distinct peaks at 5550, 6650 and 7300 Å with molar extinction coefficients of 6750, 6340 and 6750, respectively. To lower temperatures the spectrum began to change very rapidly till about -100°C: below this temperature, where MTHF is still a liquid, the spectrum did not change any more. This spectrum is denoted by 2 in figure 13. The long wavelength peaks show a bathochromic shift when compared to corresponding peaks in the first spectrum; one peak is shifted from 6650 to 6900 Å and the second one from 7300 to 7650 Å. The molar extinction coefficients are 7074 and 6848, respectively.

The spectra in the intermediate range proved to be superpositions of these two spectra, completely analogous to the ESR results. These superposition spectra were analysed with

a computer adaption program; the spectra to be analysed and the component spectra were fed to the computer on a magnetic tape. Computer analysis (an example is shown in figure 13)

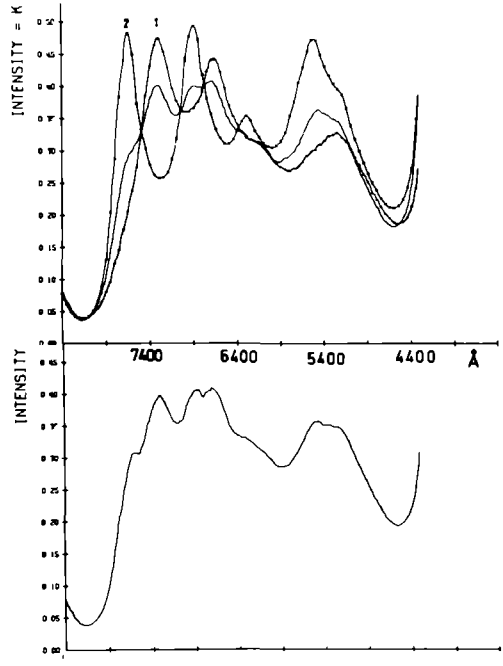

Fig. 13 - Three optical spectra of $Tp^{-}Na^{+}$ in MTHF are shown above; spectra 1, 2 and 3 have been recorded at -71°C, -87°C and -114°C, respectively. A computer calculation (shown below) demonstrated that spectrum 3 was composed by 64.2% of spectrum 1 and by 35.8% of spectrum 2. Notice the presence of several isosbestic points in the upper figure.

showed that the weight fractions of the component spectra did not depend on the total radical concentration in the investigated concentration range (10^{-2} - 10^{-4} molar).

MTHF solutions of $Tp^{-}Na^{+}$ containing an equivalent amount of tetraglyme have also been studied optically. The same kind of superposition spectra were recorded at various radical concentrations in a temperature range from -40°C to +30°C. The complete analysis of these spectra has not yet been carried out so that here no thermodynamic quantities can be given of the latter equilibrium.

The above mentioned experiments have been carried out in evacuated quartz cells with optical path lenghts of 6, 1, 0.1, 0.02 and 0.01 cm, respectively. It proved always necessary to rinse the evacuated sample tubes with radical solutions (which were removed later) in order to obtain reliable results.

4.1.3 Discussion of the ESR results

a) Spectrum I

It has been well established that the conditions favourable for a complete dissociation of radical anion-metal cation pairs are (a) high solvent polarity; (b) low temperature; (c) small ionic radius of the metal. Thus the conditions under which the spectrum depicted in figure 6 was recorded strongly suggests, that it must be assigned to the free* Tp^- ion. The fact that this spectrum is also obtained from electrolytically reduced Tp solutions where the bulky cations are not expected to affect the free radical spectrum, confirms this conclusion. The observation, that the hfs constants obtained from these spectra do not vary with metal ion or solvent changes, is also in agreement with this assignment.

The mononegative ion of Tp is in an orbitally degenerate groundstate like the mononegative ion of benzene and according to the theorem of Jahn and Teller [28] will tend to distort into one or several more stable configurations of lower symmetry with nondegenerate electronic groundstates.

* By "free" we mean that the ESR experiments reveal no counter ion influence. This does not exclude the possibility that conductance measurements might nevertheless prove that in some cases anions and cations are still associated [33]. In fact we have found some cases where spectrum I has to be ascribed to a solvent separated ion pair (see below).

Theoretical calculations have shown that the energy gain as a result of a geometrical distortion of the molecule is small compared to the zero point energy of the normal vibrations [29,30]. The motions of the nuclei and the electrons are then closely coupled and the anion which has been shown to exist in a degenerate vibronic state [31,32] interconverts rapidly between the various distorted configurations. The spin distribution over the anion, therefore, will be a statistical average over the distributions in these configurations and will retain trigonal symmetry [31,32]. The finding that the spectrum of the free anion consists of hyperfine components due to two sets of six equivalent protons is in agreement with such a dynamic Jahn-Teller instability.

The spin distribution in Tp^- has been calculated under the assumption that the ion stays in its symmetrical configuration and that the unpaired electron spends half of its time in the two degenerate first antibonding orbitals. The calculations employed the Hückel method both with the resonance integral β set equal and with resonance integrals adjusted to the bond order variations in Tp^-. The variation of β with the C_i-C_j bond length was assumed to be exponential [34]:

$$\beta_{ij} = C.\beta_o \exp(-r_{ij}/0.3727) \qquad (51)$$

with C = 42.5 and β_o equal to the resonance integral in the symmetrical equilibrium configuration of benzene. The bond lengths r_{ij} in Tp^- were determined by using the Coulson-Golebiewsky bond order-bond length relationship [35]:

$$r_{ij} = 1.517 - 0.18p_{ij} \qquad (52)$$

where p_{ij} is the bond order. The results of the calculations are tabulated in table 3 together with the experimental spin densities derived with the well known McConnell relation [11]

$$a_n = Q.\rho_n \qquad (53)$$

a_n is the hfs constant of the proton adjacent to carbon atom n, ρ_n is the spin density on that carbon atom, and Q is a constant: its value, -27 gauss, was set equal to

$$Q = \frac{\Sigma a_n \text{ (measured)}}{\Sigma \rho_n \text{ (calculated)}}$$

Table 3

Experimental and theoretical spin densities in Tp^-

position	experimental	Hückel	Modified Hückel	SCF	SCF+CI
1	0.041	0.056	0.050	0.050	0.050
2	0.061	0.056	0.055	0.055	0.055
3	(0.065)	0.056	0.062	0.061	0.061

The Hückel calculation with equal resonance integrals gives equal spin densities at all carbon atoms whereas the second Hückel calculation predicts the larger spin density at position 2. The latter is in agreement with experimental re-

sults obtained on 2-D-triphenylene anion. Also included in the table are the spin densities obtained with a P.P.P. open shell SCF calculation. In order to get reliable results with this iterative method, the computer program that calculated the Hartree-Fock matrix F was modified. When using the following formulae

$$F_{rr} = \theta_{rr} + \tfrac{1}{2} P_{rr}\gamma_{rr} + \sum_{u \neq r} P_{uu}\gamma_{ru}$$
$$F_{rs} = \theta_{rs} - \tfrac{1}{2} P_{rs}\gamma_{rs} \qquad (54)$$

where θ is the Hückel matrix, γ_{ij} is a repulsion integral and P_{rs} is the bond order defined as

$$P_{rs} = \sum_{j} \lambda_j \, c_{rj} c_{sj} \qquad (55)$$

the occupation number λ_j of the j-th MO was given the value of $\frac{1}{2}$ for the first two antibonding orbitals of Tp^-.

In general electrons are distributed equally over two or more MO's as long as the energy difference between these orbitals does not exceed 10^{-4} eV. In this way orbital degeneracy is preserved during every iteration. The spin densities obtained in this way are identical to those derived with the second Hückel calculation. Interaction with singly excited configurations (CI) does not alter these values either. The agreement with experimental values is fairly good.

The spectrum of the radical ion of Tp deuterated at position 2 (solvent MTHF, metal ion Na^+, temperature $-110^{\circ}C$) could be simulated using unchanged hfs constants for the

set of 5 equivalent protons and the set of 6 equivalent protons (1.10 and 1.61 gauss) and a deuterium coupling constant of 0.25 gauss (= $1.61 \times \gamma_D/\gamma_H$). Thus deuterium substitution apparently does not lead to measurable changes in the spin density distribution over the radical, contrary to the isotope effect on the spin density in the benzene anion [36,37].

The g value as has been measured in MTHF at -100°C appears to deviate substantially from Stone's plot (see figure 22) [56]. A large deviation from the free electron value was found:

$$\Delta g = 52.0 \pm 0.7 \times 10^{-5} \quad .$$

Using the numerical expression for Δg given by Segal e.a. [27]

$$\Delta g = (27.6 \pm 0.8 - (17.2 \pm 2.0)\lambda).10^{-5} \qquad (56)$$

one finds, inserting the value of the Hückel coefficient λ (-0.684):

$$\Delta g = (39.4 \pm 1.7)10^{-5} \quad .$$

This discrepancy with theory may be related with the orbital degeneracy of the monoanion [2,3] and is probably also a factor in the anomalous high linewidth observed in the spectrum of the free ion (the derivative linewidth is equal to 0.25 gauss, whereas normal linewidths in ESR spectra of hydrocarbon radicals are 0.05 gauss or less). Saturation

studies of Tp^- by Freed e.a. [3] have shown that the electron relaxation times T_1 and T_2 are very short (T_1 = 2.4×10^{-7} sec and T_2 = 1.8×10^{-7} sec at -80°C) as has also been found for other radicals of high symmetry.

An enhanced spin-orbit interaction in these radicals probably affects both the g value and the relaxation times. In figure 22 Stone's plot is shown: it can be seen in the figure that degenerate radicals may strongly deviate from the line.

b) Spectrum II

The spectra of the type shown in figure 7 were obtained under conditions more favourable for ion pair formation [38,39]. It was furthermore emphasized above that the hyperfine components and the linewidths in these spectra depended on the kind of metal ion present in solution. It seems obvious, therefore, that the 13 line spectra must be assigned to some kind of ion pair. The most convincing proof for this assignment is furnished by the pronounced effect that addition of extra metal ions has on the low temperature limit of spectrum II. This effect can be explained if the following equilibrium is assumed:

$$Tp^-//Na^+ \rightleftarrows Tp^- + Na^+$$

which will be shifted to the left by addition of excess Na^+. Computer simulations showed that the change of spectrum I into spectrum II upon temperature increases is not primarily caused by the occurrence of an alkali splitting and/or linewidth increases in the spectrum of the free ion. Al-

though a metal ion splitting might contribute slightly to the spectrum, the calculations showed that the transformation of the hyperfine pattern of figure 7 must be attributed primarily to changes in the Tp^- proton hfs splitting constants. To obtain an optimal fit with the experimental spectrum, the coupling constant of 1.61 gauss was lowered to 1.57 gauss and the second coupling constant of 1.10 gauss was raised to 1.28 gauss.

The data suggest that the ion pair formation causes a significant perturbation of the electron spin distribution over the ion, the magnitude of the perturbation varying from one metal ion to the other. This perturbation is also clearly manifested by the rather large difference in the g values of the two spectra: $\Delta g = 1.1 \times 10^{-5}$, corresponding to a magnetic field shift of 0.17 gauss. It is tempting to associate the large changes in these electronic properties with the orbital degeneracy of the radical ion.

In order to account for the change in the spin densities upon ion pairing, Hückel and SCF calculations were carried out on Tp^- taking into account the perturbing influence of the cation. Treating the solvating cation as a unit point charge and using Reddoch's approximation [16], Hückel and SCF spin densities have been calculated for the perturbed anion with different positions of the cation. The cation was placed 2 and 3 Å above a non central ring and in a third calculation 2 Å above the central ring of the anion . Pictures of the models are shown in figure 14. The same kind of model has been used to calculate ZFS parameters of the dianion of Tp [7,8]. Placing the cation 3 Å above the center of a non central ring, the degeneracy of the

lowest two antibonding orbitals was lifted by 0.081 eV in a Hückel calculation and by 0.016 eV in a SCF calculation. On lowering this distance to 2 Å this energy difference became 0.253 eV for a Hückel and 0.011(!) Å for a SCF calculation. It is interesting to note that the wavefunction with the lower energy in the first calculation (ions 3 Å apart) has the higher energy in the second calculation (2 Å). This means that for some cation-aromatic plane distance between 2 and 3 Å , there will be again (accidental) degeneracy.

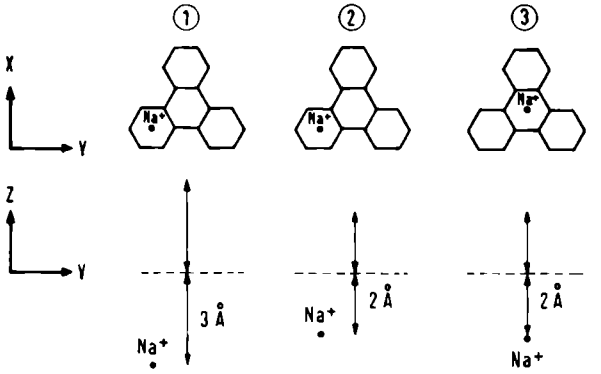

Fig. 14 - Models for the $Tp^{-}Na^{+}$ ion pair.

For the calculation of the spin densities in the perturbed anion a Boltzmann factor has to be taken into account to weigh the populations in the lowest two antibonding levels. In the Hückel calculation the degeneracy is lifted so much that the Boltzmann factor becomes equal to 1 for the lower orbital. Because this factor is less than unity

for the SCF calculations, the SCF spin densities were calculated at 200 and 300°K, as the spectra have been observed in this temperature range. Since the experimental spectra still reflected trigonal symmetry, it was assumed that the counter ion is rapidly jumping from one non-central ring to the other on the average preserving trigonal symmetry. The calculated spin densities averaged over the equivalent positions are shown in table 4. Also shown in this table are Hückel and SCF calculations on Tp^- perturbed by a counter ion placed 2 Å above the center of the central ring.

Table 4

Experimental and calculated spin densities of Tp^- and Tp^-Na^+ ion pair

Na^+ 3 Å above a non central ring				
	Hückel	SCF (300°K)	SCF (200°K)	Exp. value
ρ_1	0.086	0.051	0.050	0.047
ρ_2	0.042	0.055	0.056	0.058
ρ_3	0.038	0.059	0.060	0.061
Na^+ 2 Å above a non central ring				
	Hückel	SCF (300°K)	SCF (200°K)	Experiment
ρ_1	0.101	0.050	0.052	0.047
ρ_2	0.036	0.056	0.056	0.058
ρ_3	0.029	0.060	0.058	0.061
Na^+ 2 Å above the central ring				
	Hückel	SCF		Experiment
ρ_1	0.050	0.049		0.047
ρ_2	0.058	0.058		0.058
ρ_3	0.059	0.059		0.061
Na^+ at distance ∞				
	Hückel	SCF		Experiment
ρ_1	0.056	0.050		0.041
ρ_2	0.056	0.055		0.060
ρ_3	0.056	0.061		0.065

It is immediately evident from the table that the Hückel theory cannot be used when the degeneracy is lifted. It is also clear that the SCF spin densities hardly change in the non centric models. A good fit with experimental values is found for the SCF calculation on model 3. The close correspondence with the experimental values, however, is misleading. This becomes evident if one looks at the spin densities of the unperturbed anion. If anything sensible at all can be said about table 4 it will be about the trend the spin densities follow upon cationic polarization. Then model 3 proves to be unsatisfactory: it predicts a decrease of ρ_1 ($\Delta\rho_1 = -0.001$) and an increase of ρ_2 ($\Delta\rho_2 = +0.003$) fully in contradiction with the change of the experimental values: $\Delta\rho_1 = +0.006$ and $\Delta\rho_2 = -0.002$. On the other hand it remains unclear why an asymmetrical perturbation would have such little effect on the spin distribution. A continuous change of the coupling constants with temperature has not been observed either. A further argument for the models 1 and 2 is the big difference in charge density between the central ring and the outer rings, their values (using SCF theory) being 0.142 and 0.333, respectively, in the free ion. Obviously Coulombic attraction would favour the non-centric position of the cation.

To analyse the dissociation reaction of the ion pairs in pure MTHF the total radical concentration was measured using a MTHF solution of DPPH of known concentration as a standard. The concentration could be determined by double integration of both ESR spectra. The total radical concentration was kept as low as possible to ensure a large degree

of dissociation at the lowest temperatures measured (-120°C). The ESR spectra could be analysed from -120°C (100% "free" (unperturbed) ions) up to -68°C (60% "free" ions). In this temperature range the g shift between the two spectra decreased from 0.2 gauss at -120°C to about 0.12 gauss at -68°C due to an increase of the exchange rate between the two species with increasing temperature. At still higher temperatures the spectra could not be analysed any more because of coalescence.

The optical experiments in §4.1.2 demonstrated that this equilibrium becomes independent of the total radical concentration in concentrated solutions. This fact indicates that more than two species are involved in the dissociation reaction and obviously the complete reaction scheme cannot be derived from the ESR experiments alone. The final analysis will therefore be given at the end of this chapter when the optical results are discussed.

Though exchange contributions to the linewidth and a decrease of the g shift between the two spectra at increasing temperature have been observed, no exchange rate analysis has been made because of the uncertainties in the parameters involved. Still a rough estimate of these rates can be calculated from the observation that the difference in g value between the two spectra starts to average out in the investigated temperature range. Under these circumstances the lifetime of the species must fulfill the following condition:

$$\tau \approx \Delta g^{-1} \quad (\Delta g \text{ expressed in radians per sec.}) \quad . \quad (57)$$

From the observed g shift it is found that the lifetime of the ion pairs and free ions must be about 10^{-6} sec. in the investigated temperature range. As the concentration of free (dissociated) ions is approximately 10^{-6} molar (see below), the association rate constant has a magnitude of about 10^{12} liter.mol^{-1}.sec^{-1}. pointing to a diffusion controlled reaction. In THF the same equilibrium can be studied between -20°C and +20°C, but here the g difference between the spectra is nearly completely averaged out: the lifetime of the species has become too short.

c) Spectrum III

Spectra of the third type were obtained only from sodium reduced Tp in DEE, MTHF, THP or MTHF-hexane mixtures. This kind of spectra of which those in figure 9 are representatives, exhibit a further splitting of the 13 lines found in spectrum II into four lines with equal intensity. This splitting, the magnitude of which varied rapidly with increasing temperature can be assigned to the interaction with the Na^+ ion. This assignment is confirmed by the pronounced effect of introduction of additional sodium ions to the radical solutions. One may expect that these additional ions will exchange rapidly with the associated metal ions, which will destroy the metal ion hfs provided that a sufficiently large excess of Na^+ is present. This has indeed been observed. For example, the 13 line spectrum produced by Tp^-Na^+ in MTHF did not change upon temperature increases to +60°C if a large excess of Na^+ was present. On the other hand, if the sodium concentration was diminished so that the

rate of exchange became of the order of magnitude of the inverse of the sodium hfs constant, the exchange reaction merely gave rise to a broadening of the hyperfine lines.

The significant changes in the metal ion coupling constant with temperature are qualitatively similar to the counter ion splitting variations in the ESR spectra of anthracene$^-$Na$^+$. Hirota and Kreilick [40] attributed these variations to changes in the equilibrium constant of the following reaction

$$\underset{(A)}{Ar^-Me^+} \underset{k_2}{\overset{k_1}{\rightleftarrows}} \underset{(B)}{Ar^-//Me^+}$$

where $Ar^-//Me^+$ and Ar^-Me^+ are two different ion pairs, designated as solvent separated or loose ion pair and contact or tight ion pair, respectively. These authors pointed out that for large k_1 and k_2 (rapid exchange) the experimentally found metal splitting at a particular temperature is a statistical average of the hfs constants in the different ion pairs given by the relation

$$a_{Me} = \frac{a_A + K.a_B}{1 + K} \qquad (58)$$

where a_A and a_B are the metal hfs constants in the ion pairs A and B, respectively, and K is the equilibrium constant of the reaction. The exchange reaction will, furthermore, contribute to the linewidth; the contribution to the different metal ion hyperfine components for rapid exchange reactions (k_1, $k_2 > \gamma_e^{-1} \times a_{Me}^{-1}$) is given by [41]

$$(T_2^{-1})_{exchange} = P_A^2 P_B^2 (\gamma M_z^{Na} a_A - \gamma M_z^{Na} a_B)^2 \tau_A (1+K) \qquad (59)$$

where P_A and P_B denote the probabilities of finding ion pair A or B, respectively, γ is the magnetogyric ratio, M_z^{Na} is the metal ion magnetic quantum number ($\pm 3/2$, $\pm 1/2$) labelling the hyperfine component and τ_A is the lifetime of species A. One expects, therefore,that the hyperfine components with $M_z = \pm 3/2$ will be more broadened than the $M_z = \pm\frac{1}{2}$ components as a result of the exchange reaction. This was indeed observed in the spectrum of sodium reduced Tp dissolved in DEE and recorded at $-100^{\circ}C$ (figure 15). This spectrum could be reproduced with a computer calculation which employed two different linewidths for the sodium hyperfine lines (0.2 gauss for $M_z = \pm 3/2$ and 0.4 gauss for $M_z = \pm\frac{1}{2}$). A calculation based on this linewidth variation and equations 58 and 59 demonstrated that at $-100^{\circ}C$ τ_A and τ_B are greater than the inverse of the maximum sodium splitting ($\simeq 0.4\times10^{-6}$ sec).

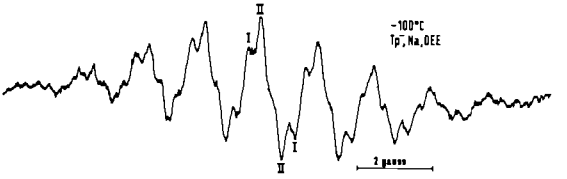

Fig. 15 - $Tp^{-}Na^{+}$ in DEE at $-100^{\circ}C$. The alkali hfs has been marked by I ($\pm 3/2$ components) and II ($\pm\frac{1}{2}$ components).

The fast exchange limit condition, therefore, is not fulfilled so that an adequate reproduction of the spectrum shown in figure 15 can be obtained only by using the complete lineshape formula [42]. No such variation in linewidth was observed at higher temperatures, where a perfect fit between the calculated and experimental spectra could be obtained by using only one linewidth parameter. This suggests that the fast exchange case applies; using equation 58 and 59 and setting $\tau_A < 10^{-7}$ sec, in accordance with fast exchange, one calculates for the derivative linewidth increase at -60°C a value of less than 0.01 gauss, which will be unobservable in the spectra. The drastic decrease of τ_A upon a temperature increase from -100 to -60°C is attributed to the sudden decrease in viscosity of DEE in this temperature range.

Equation 58 can be employed to derive values for the thermodynamic quantities governing the ion pair equilibrium [46]. From the graph of a_{Na} versus the temperature (see figure 10) the limiting values of a_A and a_B can be shown to be 0 and 0.9 gauss, respectively. Using these values and the experimentally found metal splittings at various temperatures, a plot of log K versus T^{-1} was obtained (figure 16).

It is evident that all points fall reasonably on a straight line, which suggests that the proposed reaction mechanism is correct. Moreover, the values for ΔH and ΔS obtained from a least square line fit (-5.3 Kcal and -19.4 e.u., respectively, when the solvent is MTHF and -5.1 Kcal and -23.2 e.u., respectively, when the solvent is DEE) are of the same order of magnitude as the values found by Hirota and Kreilick. Probably similar types of ion pairs are in-

volved in both studies.

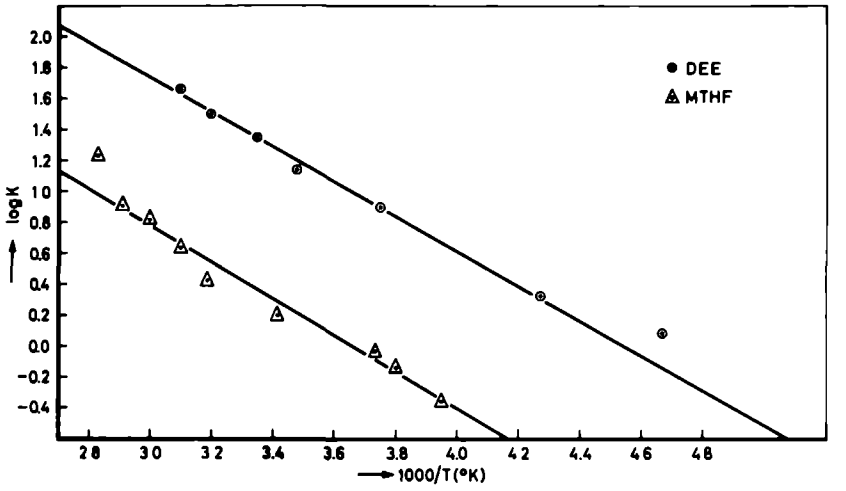

Fig. 16 - Log K versus T^{-1} for the ion pair equilibrium ir DEE and MTHF, respectively.

It was found that traces of a more polar solvent like DME shifted the equilibrium considerably to the side of the solvent separated ion pair A, while addition of a less polar solvent did not affect the equilibrium at all. When, however, a polyether like tetraglyme was added to a sodium reduced Tp solution in MTHF at constant temperature (25°C) a new species appeared the spectrum of which closely resembled the spectrum of the free ion (type I), only its linewidth was larger: 0.5 gauss. This spectrum was superimposed on the spectrum with the alkali splitting (see figure 11) and its intensity increased with increasing polyether concentration. At the same time spectrum III decreased in intensity but

the alkali splitting remained the same. In order to formulate an equilibrium equation for this reaction, some important experimental data must be considered. It was immediately evident from experiment that one ion pair was solvated by approximately one tetraglyme molecule. This could be seen by comparing the amount of polyether added with the decrease in concentration of species III. Furthermore, the composition of the superposition spectra changed drastically upon dilution; a change of 30%-40% in the weight fractions of the component spectra could easily be obtained by diluting the solution. On dilution the weight fraction of spectrum III increased, while spectrum I decreased by the same amount. These data rule out the possibility of the following equilibrium equation

$$Tp^-Na^+ + TEGD \rightleftarrows Tp^- + Na^+_{solvated}$$

TEGD = tetraethylene glycol dimethylether

because this equilibrium would be concentration independent which is in contradiction with experiment. The possibility of this equilibrium must be mentioned, however, because spectra of type I have been ascribed to the free ion of Tp^-.

Apparently some other equilibrium must be invoked to explain the experimental facts. It proved that the following equilibrium equation could explain both qualitatively and quantitatively the observed phenomena:

$$Tp^-Na^+ + n\ TEGD \rightleftarrows Tp^-/Tg/Na^+ \qquad \text{with } n \approx 1 \quad . \quad (60)$$

For simplicity we have written here Tp^-Na^+ instead of the

rapid equilibrium reaction

$$Tp^-//Na^+ \rightleftarrows Tp^-Na^+ \quad .$$

This does not alter the arguments, however, because it was found that addition of tetraglyme does not influence this equilibrium. Besides, if the variable alkali splitting had to be assigned to a static ion pair which changes its structure gradually with temperature [43](an explanation that cannot be absolutely excluded), equilibrium 60 would describe the actual situation. $Tp^-/Tg/Na$ represents an ion pair separated by tetraglyme molecules. Writing

$$K = \frac{[Tp^-/Tg/Na^+]}{[Tp^-Na^+][TEGD]^n}$$

one finds

$$\log \frac{[Tp^-/Tg/Na^+]}{[Tp^-Na^+]} = n \log [TEGD] + \log K \quad . \qquad (61)$$

A plot of the first term against log [TEGD] should give a straight line with slope n and intercept log K. A graph of this equation is shown in figure 17. From a least square line fit the following data were derived

$$n = 1.01 \pm 0.07$$
$$K = (5.7 \pm 0.2)\times 10^4 \ M^{-1} \ (\text{at } 25^\circ C) \ .$$

A similar value for the solvation number of sodium was also found by other authors [44-47]. The equilibrium constants

they found, however, were much smaller ($\approx 10^2$). The difference in the K values may be attributed to the larger charge delocalisation in Tp^- as compared to smaller ions like the anions of biphenyl or naphthalene. The Coulombic forces holding the ion pairs together will be smaller for the larger anions, which makes it easier to convert them into solvent separated ion pairs.

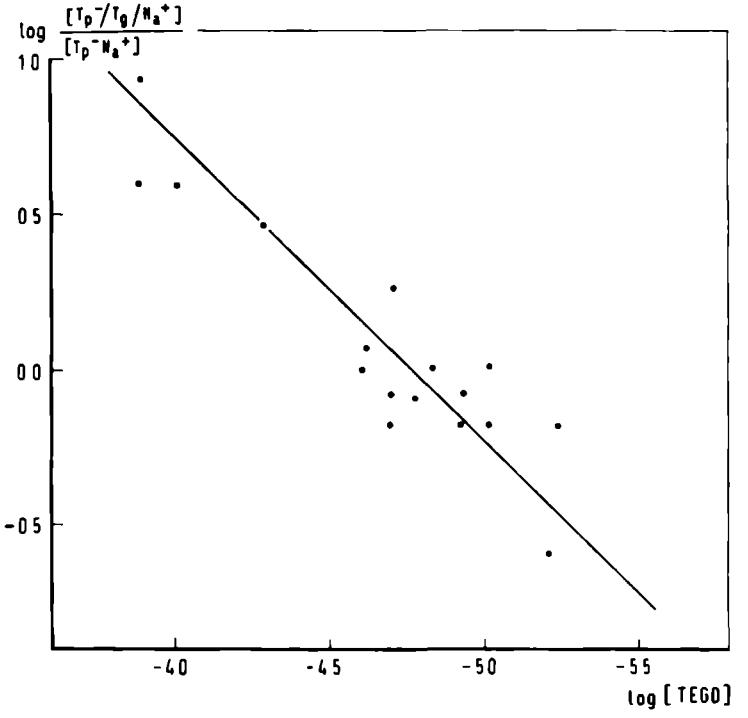

Fig. 17 - Plot of log $[Tp^-//Na^+]/[Tp^-Na^+]$ versus log [TEGD] for the tetraglyme titration of Tp^-Na^+ in MTHF.

4.1.4 Discussion of the optical measurements

a) Optical spectra at low temperatures.

The optical superposition spectra of Tp^- in MTHF have been observed in the same temperature range as the ESR superposition spectra. Apparently the high temperature optical spectrum (denoted by 1 in figure 13) originates from the same species as the 13 line spectrum (spectrum of type II) measured with ESR. This ESR spectrum has been ascribed to a solvent separated ion pair $Tp^-//Na^+$. Since the optical superposition spectra proved to be independent of the total radical concentration (from 10^{-2} to 10^{-4} molar) the low temperature spectrum (denoted by 2 in figure 13) cannot be ascribed to the unperturbed free Tp^- ion. Instead of this we suggest an equilibrium between two solvated ion pairs of different geometrical structure, symbolically written as

$$Tp^-//Na^+ \underset{K_1}{\rightleftarrows} Tp^-/S/Na^+$$

where $Tp^-/S/Na^+$ represents a very loosely bound solvated ion pair. The experimental data have been rationalized in terms of these two species. A plot of Ln K_1 versus the reciprocal of the temperature is shown in figure 18. From a least square line fit to the experimental points the solvation enthalpy and entropy have been determined:

$$\Delta H = -9.3 \pm 0.2 \text{ Kcal/mol}$$
$$\Delta S = -48 \pm 2 \text{ e.u./mol} .$$

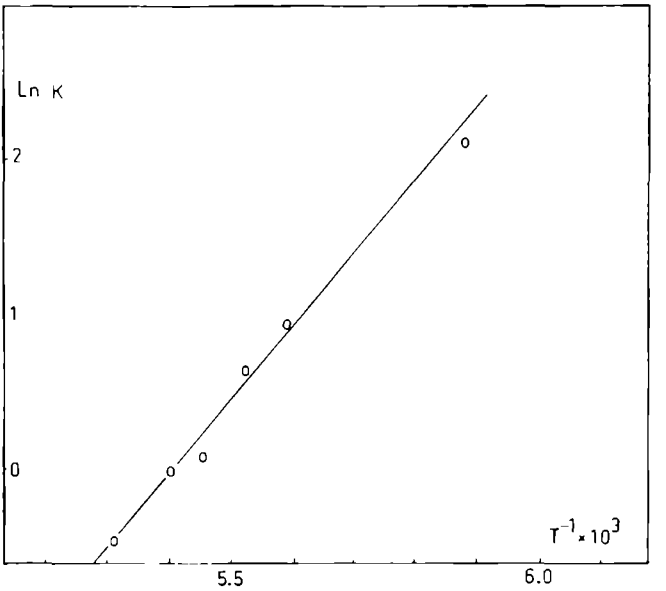

Fig. 18 - Plot of Ln K_1 for the ion pair equilibrium measured in MTHF as a function of the temperature.

b) ESR experiments at low temperatures.

The ESR experiments have been performed under identical conditions as the optical experiments, except that the total radical concentration was much lower ($\approx 3 \times 10^{-6}$ molar). It has been demonstrated in 4.4.1 that the ESR superposition spectra could be strongly influenced by addition of extra metal ions or variations in the total radical conentration. In view of these observations and the phenomena occurring in the optical spectra, the following reaction scheme is proposed for the interpretation of the ESR spectra at low temperatures:

$$\begin{array}{ccccc} Tp^-//Na^+ \ (A) & \overset{K_1}{\rightleftharpoons} & Tp^-/S/Na^+ \ (B) & & (62) \\ \quad \overset{K_2}{\searrow\!\!\nearrow} & & \quad \overset{K_3}{\searrow\!\!\nearrow} & & \\ & Tp^- \ (C) + Na^+ & & & \end{array}$$

The ESR spectra could be explained as superpositions of two independent spectra, viz. spectrum II and spectrum I. The former has been assigned to species A (13 line spectrum), so the latter has to be assigned to species B and C. This implies that B and C have indistinguishable ESR spectra. From the combined ESR and optical data the different K values in equation 62 can be determined:

a) the ration $\frac{[B]}{[A]} = K_1$ is known from the optical spectra, taken at high concentrations ($[C] \approx 0$).

b) the ratio $\frac{[B]+[C]}{[A]}$ is equal to the ratio of the two components in the ESR spectra measured at low concentrations.

c) $[A] + [B] + [C]$ is equal to the total radical concentration.

From these data it was found that in the investigated temperature range (-70°C to -100°C) the concentration of C was practically constant (1.7×10^{-6} molar). As a consequence the overall dissociation constant K_d, defined as

$$\frac{[Tp^-][Na^+]}{[Tp^-//Na^+] + [Tp^-/S/Na^+]} \quad \text{or} \quad \frac{[C]^2}{[A] + [B]}$$

$(K_d^{-1} = K_2^{-1} + K_3^{-1})$

is independent of the temperature.

Therefore

$$\frac{d \, Ln \, K_d}{d \, T} = \frac{\Delta H_d}{RT^2} = 0 \qquad (63)$$

so that the dissociation enthalpy is zero in the investigated temperature range. It is interesting to know that conductance studies of Szwarc e.a. [33,48] on $Tp^{-}Na^{+}$ in THF also indicated a zero enthalpy difference for the ion pair(s) dissociation at low temperatures.

c) Optical and ESR spectra at high temperatures.

The optical studies show that the species which might be present in the temperature range between +50°C and -70°C are indistinguishable as far as their optical properties are concerned. However, with ESR two types of spectra have been observed: type III with a measurable sodium splitting and type II with no detectable sodium coupling constant (13 line spectrum). Apparently the interaction with the alkali nucleus has no noticeable effect on the optical spectra. The latter fact needs some comment.

It has been found with ESR that the appearance of the sodium splitting was not accompanied by a measurable change of the g value or the proton hfs constants (spin densities). This must imply that there is no correlation between the change of the sodium splitting and the perturbation by the cation. This can probably be explained by assuming that, when the alkali splitting increases, the distance from the sodium ion to the aromatic plane will hardly change. A movement of the cation parallel to the aromatic plane may account for this. Such a movement will change the alkali splitting, since this depends criticilly on the overlap of the MO containing the odd electron and the alkali wavefunctions, whereas the perturbation will remain more or

less the same because the distance between the cation and the aromatic plane is constant.

When the cation becomes completely surrounded by solvent molecules its effective radius increases and its electrostatic perturbation upon the anion will decrease. For Tp^- this manifests itself in observable changes in the proton hfs constants (spin densities), the g value and the electronic transitions. Apparently complete dissociation is accompanied by minor changes in the already weak perturbation, so that the ESR and optical spectra from loosely bound ion pairs ($Tp^-/S/Na^+$) and free ions are indistinguisable.

4.2 The mononegative ion of 1,3,5-triphenylbenzene.

4.2.1 ESR measurements.

a) Hyperfine splitting constants and g value.

Reduction of 1,3,5-triphenylbenzene (Tpb) in ethereal solvents resulted in a green-brown paramagnetic solution which exhibited ESR hyperfine structure characteristic for an organic doublet radical.

Initial attempts in 2-MTHF yielded ESR spectra with rather broad lines (300 milligauss) which could not be analysed. Eventually the linewidth could be reduced to 0.2 gauss by carefully choosing the experimental conditions:

a) concentration of Tpb^- much larger than that of unreduced Tpb or Tpb dianion in order to reduce electron transfer reactions.
b) very dilute monoradical solution (10^{-5} molar Tpb^- in MTHF).

c) temperature range -80 to -90°C; at higher temperature rapid broadening (a reversible process) occurred which eventually destroyed all hyperfine structure.

The spectrum recorded under these circumstances is shown in figure 19.

Much better results, however, could be obtained when more polar solvents were used like DME or NH_3. A sodium reduced solution of Tpb^- in NH_3 showed a remarkable decrease in linewidth when compared to a MTHF solution. The spectrum which is shown in figure 20 is completely resolved and has been analysed in terms of four different proton h.f.s. constants.

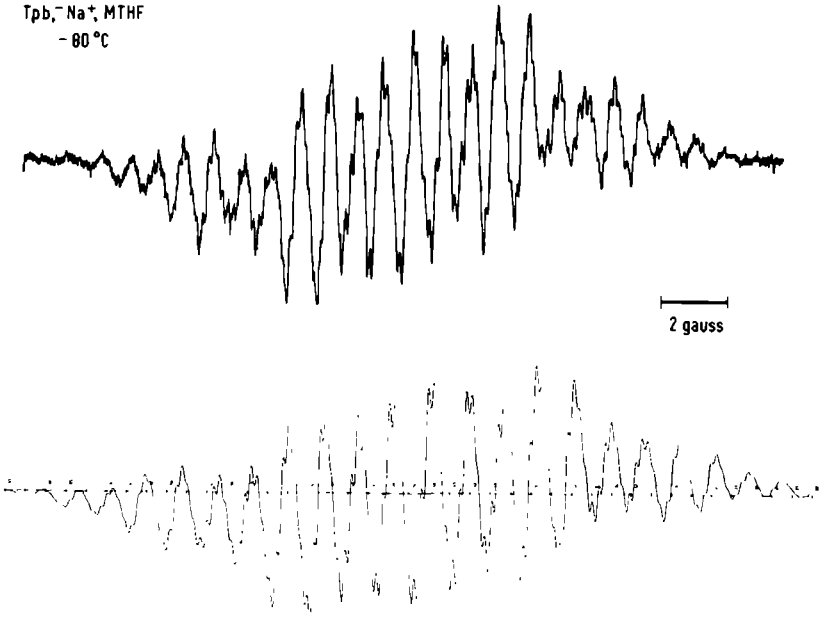

Fig. 19 - ESR spectrum of Tpb^-Na^+ in MTHF. The computer simulation is shown below.

A perfect match of a computer simulated spectrum could be constructed when the following values were used as input parameters:
two sets of six equivalent protons with coupling constants of 0.155 and 0.930 gauss, respectively; two sets of three equivalent protons with coupling constants of 1.55 and 3.58 gauss, respectively; derivative linewidth equal to 0.060 gauss.

It will be noticed, that accidentally all coupling constants are a multiple of the smallest value (0.155 gauss):

$$a_8 = 6 \times a_9, \quad a_{10} = 10 \times a_9 \text{ and } a_2 = 23 \times a_9$$

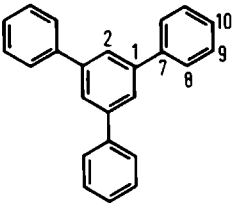

This fortuitous fact is responsible for the complete resolution of the ESR spectrum. With the help of these known h.f.s. constants, the spectra recorded in DME and MTHF could also be simulated using larger input linewidths: $\delta = 0.120$ gauss for Tpb^- in DME and $\delta = 0.200$ gauss for Tpb^- in MTHF.

Prolonged reduction of Tpb^- in DME or MTHF yielded red-brown paramagnetic solutions containing triplet dianions of

Tpb (see chapter 5.2). The NH_3 solutions showed decomposition upon further reduction; the dianion is probably hydrogenated in this solvent.

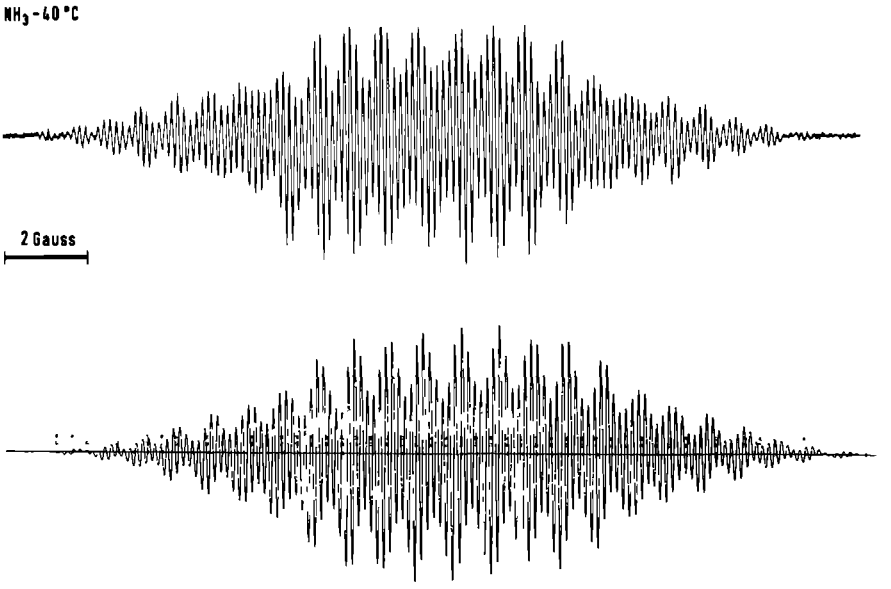

Fig. 20 - ESR spectrum of $Tpb^{-}Na^{+}$ in liquid NH_3 at -40°C. The lower spectrum is simulated.

The g value of Tpb^{-} has been measured in liquid NH_3. To correct for the magnetic field difference inside and outside the cavity, the g value of the negative ion of anthracene in NH_3 was measured as a reference. The absolute g value of the latter ion has been reported in the literature [27]. The absolute g value of Tpb^{-} measured in this way ($g = 2.002725 \pm 4.10^{-6}$) had still to be corrected for the second

order shift [27]. This shift was calculated from the experimental coupling constants and amounted to $\Delta g = -2.5\times10^{-6}$. The absolute g value of Tpb^- becomes 2.002722 ± 4.10^{-6}.

b) Relaxation times T_1 and T_2.

Continuous saturation experiments have been performed on Tpb^- in NH_3, DME and MTHF to determine the magnitude of the relaxation times T_1 and T_2. The experiments are based on formula 64 which can easily be derived starting from Bloch's equations:

$$\delta^2 = 4/3(\gamma^2 T_2^2)^{-1} + 4/3\ H_1^2\ T_1/T_2 \qquad (64)$$

δ = derivative linewidth (in gauss)
H_1 = circularly polarized field at the sample
γ = gyromagnetic ratio of the electron
T_2 = linewidth parameter
T_1 = spin-lattice relaxation time.

Thus from a linear plot of δ^2 as a function of H_1^2, $T_1T_2^{-1}$ can be derived from the slope of the line and T_2 from the intercept. $2H_1$, the amplitude of the r.f. magnetic field at the center of the cavity is connected to the microwave power incident on the cavity (P_{inc}) by formula 65 [49]

$$H_1^2 = \frac{8Q_L}{\nu_c V_c}\frac{4a^2}{(4a^2+c^2)}(1\pm|\Gamma|^2)P_{inc} \qquad (65)$$

Q_L = the loaded Q of the cavity with the sample in place
ν_c = resonance frequency of the cavity
V_c = volume of the cavity
a and c are the length of the small and broad faces of the cavity: c/2a = 1.00
$|\Gamma|^2 = P_{refl.}/P_{inc.}$, where $P_{refl.}$ is the power reflected by the cavity.

In practice $|\Gamma|^2$ was neglected in equation 65 because the reflected power was kept negligible small in all experiments by the use of very thin ESR sample tubes (i.d. 1-2 mm). The samples were measured in a rectangular cavity operating in the TE_{102} mode provided with a quartz dewar insert parallel to the broad faces of the cavity. Because line samples rather than point samples were used, H_1^2 was not constant over the length of the sample inside the cavity and the values of H_1 determined by equation 65 had to be corrected for the sinusoidal pattern along the sample. Because the experimental conditions were identical to that described by Freed e.a. [2] his correction factor has been taken over:

$$H_1^2(\text{average}) = (0.76 \pm 0.09)\, H_1^2(\text{measured}) \quad .$$

As $|\Gamma|^2$ was approximately zero the expression for the loaded Q [50] simplifies to

$$Q_L = \frac{\nu_c}{\Delta\nu} \tag{66}$$

ν = resonance frequency of the cavity
$\Delta\nu$ = the width in frequency units of the resonator dip measured at half height.

Inserting numerical values in equation 65 one finds

$$H_1^2 = 3.86\times10^{-4} Q_L P_{inc.} \tag{67}$$

where $P_{inc.}$ is expressed in Watts and Q_L was 4320, 4500 and 4460 for the MTHF, DME and NH_3 sample, respectively.

The linewidth of the ESR spectrum of Tpb^- in the different solvents as a function of the microwave power could not be measured directly due to large overlap of the hyper-

fine lines. Therefore the experimental spectra were compared with computer simulations that had different input linewidth. In the computer calculations the linewidth was varied from 0.050 to 0.50 gauss with 10 milligauss intervals.

Figure 21 shows a graph of δ^2 versus $P_{inc.}$ for Tpb^- measured in liquid NH_3. Similar plots have been constructed for MTHF and DME solutions.

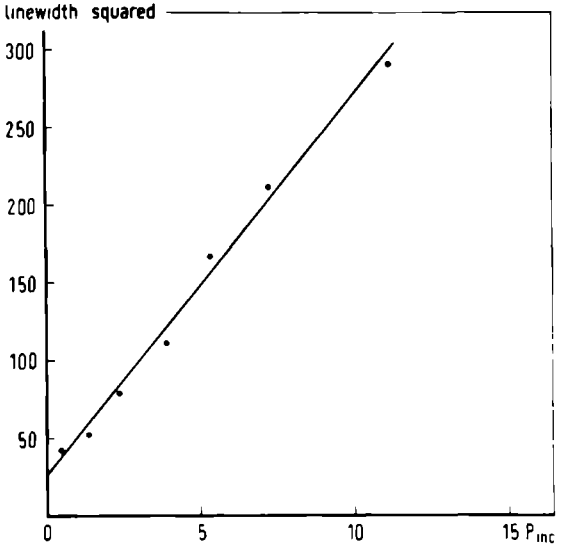

Fig. 21 - Plot of the linewidth squared against microwave power for Tpb^-Na^+ in NH_3. The drawn line is a least square fit to the experimental points.

The values of T_1 and T_2 obtained in this way are shown in table 6. Whereas in the above described procedure the ratio T_1/T_2 is determined, the product T_1T_2 can be derived from a plot of the amplitude of the ESR signal as a function of the microwave power. As the intensity of the ESR signal is proportional to $d(\chi''H_1)/d(\omega-\omega_o)$, this ex-

pression must be evaluated at the peaks of the hyperfine lines (where $d^2(\chi''H_1)/d(\omega-\omega_o)^2 = 0$) and then maximized with respect to H_1:

$$\frac{d}{dH_1} \left[\frac{d(\chi''H_1)}{d(\omega-\omega_o)} \right]_{max} = 0 \quad . \tag{68}$$

Table 6

Relaxation times of Tpb^-Na^+ in different solvents

	$T_1 \times 10^6$ sec	$T_2 \times 10^6$ sec
MTHF -79^oC	0.78 ± 0.23	0.32 ± 0.01
DME -77^oC	0.47 ± 0.14	0.65 ± 0.02
NH_3 -51^oC	1.9 ± 0.5	1.3 ± 0.1

From the condition in equation 68 follows $T_1T_2 = (2\gamma^2H_1^2)^{-1}$. If T_2 is calculated from the linewidth at low power, an estimate of T_1 can be obtained. Table 7 shows the values of the microwave field that produced maximum ESR signals together with the relaxation times calculated by this method.

Table 7

Relaxation times of sodium reduced Tpb in different solvents.

solvent	P_{inc}(Watts)	H_1^2(gauss^2)	$T_1 \times 10^6$	$T_2 \times 10^6$
MTHF	19×10^{-3}	24×10^{-3}	0.27±0.06	0.32±0.01
DME	10×10^{-3}	13×10^{-3}	0.21±0.06	0.65±0.02
NH_3	1.3×10^{-3}	1.7×10^{-3}	0.70±0.26	1.3 ±0.1

It must be stressed that this method is much less reliable than the first one. The reason is the large overlap of hyperfine lines which makes it practically impossible to determine the amplitude of an individual ESR line. The overall amplitude of a group of lines was used to determine the saturation field and this resulted in too low values for T_1.

It may be concluded, also from relaxation studies reported in the literature, that the applicability of the method of continuous saturation is very limited. The method becomes more reliable when no other dielectrica but a very small sample (a point sample) are placed inside the resonance cavity.

Pulse or spin echo experiments would give more accurate results, but these methods have only been applied for rather concentrated solutions and then electron exchange and electron transfer processes become dominant relaxation mechanisms that obscure the information one wants to obtain about intramolecular processes.

4.2.2 NMR measurements.

To determine the sign of the proton hfs constants in Tpb^-, the NMR spectrum of this ion has been recorded. The different protons in the paramagnetic ion give resonance signals at quite different magnetic fields; the different shifts they experience (Fermi contact shifts) are due to the magnetic interaction of the unpaired electron spin with the proton spin. The coupling constants can be derived from the Fermi contact shift using equation 33.

The contact shift δ_c is measured with respect to the resonance signal of the solvent, eliminating in this way

the contribution to the shift from the paramagnetic susceptibility of the solution. If a solution is not completely reduced, the measured contact shift is only a fraction f_p of the maximum obtainable shift δ_c, where f_p is the fraction of aromatic molecules that have been reduced.

In principle the degree of reduction can be derived from the shift of the solvent. Theoretically an one molar paramagnetic solution produces a solvent shift of 157 Hz at room temperature [51]. In a typical experiment 1.5 gram Tpb was added to 5 ml DME; only a small fraction dissolved at room temperature. After prolonged reduction with Na all Tpb was dissolved and the volume of the solution had expanded to about 5.5 ml, which would result in a 0.9 molar solution if all Tpb were reduced. It was checked with ESR that no dianions were present at this stage of the reduction. The observed solvent shift was 107 Hz, indicating only 74% reduction to the monoanion.

Applying at this stage a "wide line" technique [52] three proton lines could be observed (figure 22), two of which were reasonably well resolved. These two lines were characterized by the following parameters:

	meta protons	ortho protons
contact shift	-600 Hz	+3930 Hz
derivative linewidth	37 Hz	870 Hz

If the coupling constants are calculated from the observed contact shifts combined with the degree of reduction (74%) one finds

a ortho = -1.17 gauss (ESR: 0.930 gauss)
a meta = +0.179 gauss (ESR: 0.155 gauss).

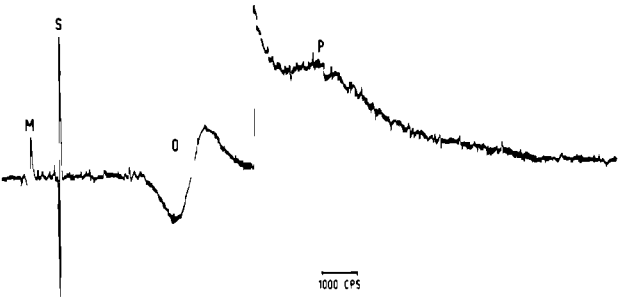

Fig. 22 - Proton spectrum of $Tpb^{-}Na^{+}$ in DME at 30°C, concentration 0.9 molar. M = meta protons, S = solvent, O = ortho protons and P stands for para protons.

It has been found, however, that the observed solvent shift is generally lower than the theoretical value [76]. If it is assumed that the coupling constants measured with NMR should not noticeable deviate from the ESR values, the degree of reduction can be calculated from the measured contact shifts:

$$f_p = \frac{\delta_c}{\delta_c^o} \qquad (69)$$

where δ_c^o is the contact shift calculated from ESR coupling constants and δ_c is the observed contact shift.

From this follows that the degree of reduction is about 0.91 instead of 0.74, which means that the observed solvent shift is 21 Hz lower than the theoretical value. This downfield shift of the solvent is probably due to a contact interaction with the paramagnetic Tpb^{-} ions.

Because the contact shifts of the aromatic protons have been measured with respect to the shifted solvent peak, a correction of +21 Hz must be made for the contact shift of the low field proton line (meta protons) and -21 Hz for the high field line (ortho protons). The ratio of the two contact shifts determined in this way still deviates somewhat from the ratio of the two ESR coupling constants:

$$\frac{\delta_c(\text{ortho})}{\delta_c(\text{meta})} = 6.3 \qquad \frac{a(\text{ortho})}{a(\text{meta})} = 6.0 \text{ (ESR)} \quad .$$

From the corrected contact shifts the coupling constants are calculated: $a_8(\text{ortho}) = -0.954$ gauss and $a_9(\text{meta}) = +0.151$ gauss. These values will be used for the calculation of the electron and dipolar correlation times.

4.2.3 Discussion.

a) Spin densities.

According to a Hückel MO calculation the first two antibonding π orbitals of Tpb are degenerate, the next energy level being 0.58 eV higher. Therefore, the spin density distribution in Tpb^- has to be calculated in a way analogous to that described for Tp^-. The experimental spin densities were derived from the ESR and NMR coupling constants with McConnell's relation

$$a = Q.\rho \quad . \tag{70}$$

A value of Q of -27 gauss is calculated by setting Q equal to $\Sigma a_i/\Sigma\rho_i$, where a_i is the negative coupling constant

and ρ_i the positive spin density on the carbon atoms 2, 8 and 10, derived from an open shell SCF calculation with configuration interaction. Calculated and experimental spin densities are shown in table 8.

Table 8

Theoretical and experimental spin densities in Tpb^-.

Carbon atom	Hückel	SCF	SCF + CI	ESR	NMR
1	0.052	0.038	0.047		
2	0.118	0.103	0.150	0.135	
7	0.037	0.058	0.038		
8	0.032	0.026	0.032	0.035	0.036
9	0.006	0.011	-0.008	0.006	-0.006
10	0.051	0.059	0.050	0.058	

It is seen that an open shell SCF calculation with inclusion of CI predicts spin densities that have correct sign and magnitude. MO calculations which do not take into account interactions with excited configurations, never can predict negative spin density at aromatic carbon atoms. In fact, the experimental values have been assigned to particular carbon atoms based on the close correspondence with calculated values.

b) g Value and relaxation times.

In view of the orbital degeneracy of Tpb^- it was expected that the g value of Tpb^- would deviate from Stone's empirical relation

$$\Delta g = b + \lambda c \qquad \text{(see equation 56)} \quad . \qquad (71)$$

Large deviations from this expression have been found for orbitally degenerate ions like the cations of symmetric benzene derivatives [53] the anion of benzene [27], coronene [27], triphenylene, cyclooctatetraene [27] and the trinegative ion of trinaphthylene [54]. In figure 23 which gives a picture of Stone's plot, the degenerate radicals are denoted by circles.

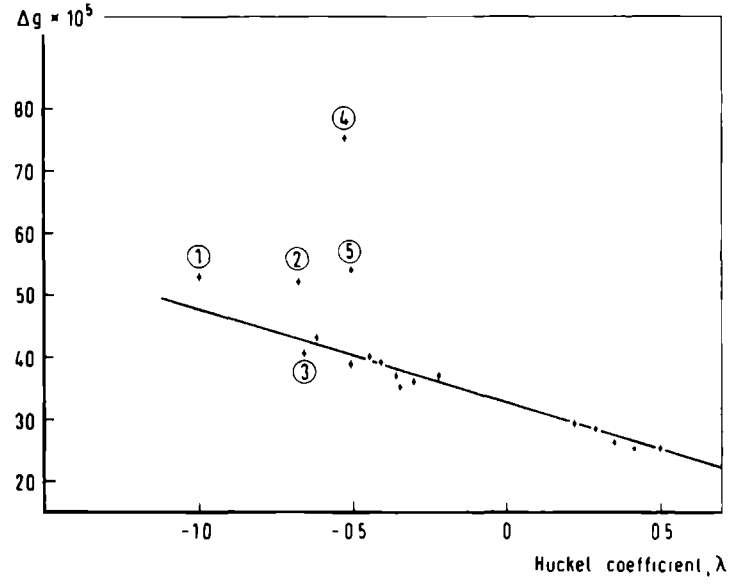

Fig. 23 - Stone's plot. (1) = benzene$^-$, (2) = triphenylene$^-$, (3) = Tpb$^-$, (4) = coronene$^-$ and (5) = trinaphthylene^{3-}.

Knowing the Hückel coefficient λ (λ = -0.66), Δg for Tpb$^-$ can be calculated from formula 56:

$$\Delta g = (39.0 \pm 1).10^{-5} \quad .$$

From the experimental g value follows:

$$\Delta g = 2.002722 \pm 4.10^{-6} - 2.002322$$
$$= (40.0 \pm 0.4).10^{-5} \quad .$$

The deviation from Stone's plot is within the limits of error and is an order of magnitude smaller than deviations found for other degenerate radicals.

A second characteristic feature of degenerate radicals is their relatively large linewidth, varying from 250 to 700 mgauss for various radicals [3]. It was also observed already a long time ago that these molecules were difficult to saturate with ESR as a consequence of their short spin-lattice relaxation times [1]. Relaxation times reported in the literature of benzene$^-$ [2,55], hexatrifluoromethyl-benzene$^-$ [53], triphenylene$^-$ [3] and the tropenyl radical [2] are all of the order of 10^{-7} second, whereas T_1 and T_2 are about 10^{-6} second for non-degenerate radicals. The values that have been found for Tpb$^-$ in ammonia are also of the order of 10^{-6} sec. and have no resemblance with values for degenerate radicals.

At this moment there is no conclusive evidence for the mechanism that causes the enhanced spin-lattice relaxation in orbitally degenerate aromatic radicals. The larger g values of these radicals indicate that spin-orbit interaction may be responsible for the short relaxation times [3]. It still remains an open question why this mechanism is quenched in the mononegative ion of Tpb, that has a g value and relaxation times comparable to those of non-degenerate radicals. It might be due to an out of plane bending of the phenyl rings, which would lift the degeneracy. The degeneracy cannot be lifted very much, however, since the

dianion has a triplet ground state.

The enhanced linewidth of Tpb^- in MTHF or DME is also hard to explain. It was first thought that the broadening of the ESR lines was caused by a small alkali splitting or a little change of the proton h.f.s. constants. It has been stated before that the complete resolution of the spectrum in liquid NH_3 was not only caused by the small linewidth but also by the accidental relationship between the coupling constants. Small changes of the latter in other solvents would, therefore, immediately lead to apparent line broadening. The relaxation study has ruled out these mechanisms, because they could have no effect upon the saturation behaviour. The shortening of T_1 in MTHF when compared to NH_3 indicates that rapid time dependent processes are responsible for the line broadening. Rapid exchange reactions of the cations might cause a time dependent modulation of the spin density distribution in the anion, which may also influence T_1 if the process occurs at very high frequencies. Wether association with counter ions actually takes place in the less polar solvents MTHF and DME has to be established by conductance measurements.

c) NMR Linewidth.

There are two major contributions to the NMR proton linewidth of paramagnetic molecules [18]. The first one results from a modulation of the Fermi contact interaction and the second from the electron nuclear anisotropic dipolar interaction. For the case that

$$\omega_e^2\tau_d^2 >> 1 \text{ and } \omega_e^2\tau_e^2 >> 1$$

equations 35 and 47 reduce to

$$T_2^{-1} = (T_2^{-1})_{Fc} + (T_2^{-1})_D$$

$$= \frac{1}{4}\left(\frac{A}{\hbar}\right)^2 \tau_e + \frac{7}{20}\left(\frac{B}{\hbar}\right)^2 \tau_d \qquad B = \frac{1}{6}(D:D) \qquad (72)$$

Because two proton NMR lines have been observed, the two unknowns τ_e and τ_d can be calculated if B is known. For the numerical calculation of B at four different proton positions use was made of a computer program written by Canters [52] who followed the method of McConnell and Strathdee [57]. It was assumed that the C-H distances were 1.08 Å and all C-C lengths were equal to 1.39 Å. The spin densities on the carbon atoms with adjacent protons, viz. ρ_2, ρ_8, ρ_9 and ρ_{10}, were obtained from ESR coupling constants. The other two, ρ_1 and ρ_7, were calculated with a SCF + CI procedure. With the parameters listed in table 9 the correlation times τ_e and τ_d could be calculated.

Table 9

Parameters used to calculate correlation times for Tpb^-.

Proton	a (gauss)	$(\frac{A}{\hbar})^2 .10^{-12}$ $(rad.sec^{-1})^2$	$(\frac{B}{\hbar})^2 .10^{-12}$ $(rad.sec^{-1})^2$	T_2^{-1} (sec^{-1})
8	0.952	281	24.7	4700
9	0.151	7.06	10.1	170

The values reported for T_2^{-1} have been corrected for inter-

molecular broadening. This effect (8 Hz) could be measured from the broadening of the solvent peaks. For τ_e, τ_d and τ_c the following values were found, respectively: 6.5, 1.6 and 2.1×10^{-11} sec. They are of the same order of magnitude as those obtained for other aromatic ions. With the known values of τ_e and τ_d the linewidths of protons 2 and 10 can be predicted (table 10).

Table 10

Parameters used to calculate the linewidths of protons 2 and 10.

Proton	a (ESR) (gauss)	$(\frac{A}{\hbar})^2 .10^{-12}$ $(rad.sec^{-1})^2$	$(\frac{B}{\hbar})^2 .10^{-12}$ $(rad.sec^{-1})^2$	T_2^{-1} (sec^{-1})
2	3.58	3947	280	6.6×10^4
10	1.55	744	67.5	1.3×10^4

If protons 2 and 10 could be observed with NMR they would be characterized by contact shifts of 15.300 and 6570 Hz and derivative linewidths of 14700 and 2230 Hz, respectively. There will be a good chance to observe these lines when the protons are replaced by deuterium atoms. The contact shifts remain the same but the linewidths will be reduced approximately by a factor $\gamma_H^2/\gamma_D^2 = 43$.

Perhaps also the spin density distribution in the dianion of Tpb could be obtained from deuterium resonance of deuterated Tpb.

C H A P T E R V

TRIPLET DIANIONS

5.1 The dianion of triphenylene

5.1.1 Experimental results

Prolonged reduction of Tp^- solutions in 2-MTHF or polyethers with K or Rb resulted in a colour change of the solution from blue to black. Coupled with this colour change was a decrease of the Tp^- concentration and an increase in concentration of a species with triplet character as was evident from rigid matrix ESR spectra. These spectra, taken as a function of the reduction showed a decreasing monoradical intensity and the simultaneous appearance of a half field ($\Delta_M = 2$) resonance signal [58-60] and full field ($\Delta_M = 1$) resonances characteristic for triplet species randomly oriented in a glass [61,12].

Two fundamentally different classes of triplet spectra were found. A representative of the first class is shown in figure 24.

This spectrum was observed when MTHF was used as solvent and K as reducing agent. Computer simulations [62] of the experimental spectrum demonstrated that the lineshape in figure 24 is determined by zero-field splitting (ZFS) parameters D and E of 492 and 96 gauss, respectively. Hence this triplet spectrum must be assigned to triplet species which have lost trigonal spin density distribution.

The second class of spectra, on the other hand, is

characterized by a signal lineshape originating from triplet species possessing trigonal symmetry [12,61] so that the ZFS parameter E vanishes. These triplet spectra (figure 25D) with vanishing E were obtained in pure polyethyleneglycol-ethers by reduction with K or Rb and also in mixtures of MTHF and these polyethers. The D value of this spectrum is 304 gauss and is independent of the metal ion present and also independent of the solvent.

Addition of successive amounts of polyether to a MTHF solution causes drastic changes in the spectra recorded. This has been illustrated in figure 25. Figure 25A shows the triplet spectrum in pure MTHF, figure 25B when a very small amount of diglyme is added to the solution.

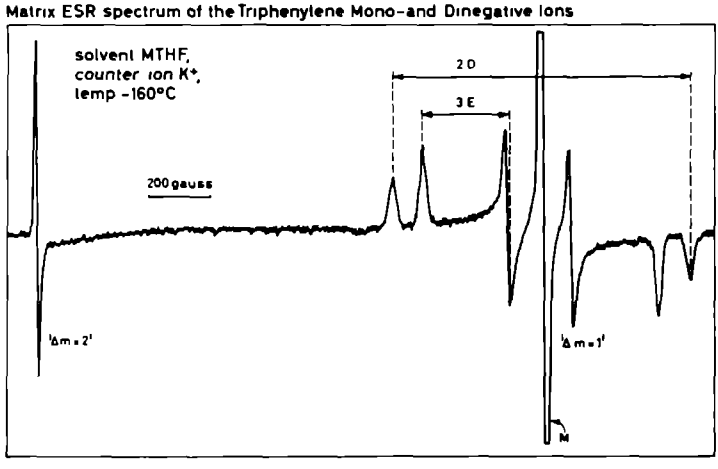

Fig. 24 - High and low field resonances of $Tp^{=}$ in a glassy matrix of MTHF at -160°C. The resonance line denoted by "M" is due to the mononegative ion Tp^{-}.

It is evident that the addition of diglyme causes new peaks (indicated by II), whereas the intensity of the triplet peaks (denoted by I) observed in pure MTHF is diminished. The new triplet species also gives rise to spectra characterized by two ZFS parameters D = 414 gauss and E = 79 gauss. This type of spectra will further be referred to as non-axial spectra. When more polyether is added (figure 25C) triplet species I vanishes completely, triplet species II gains somewhat in intensity, while a third triplet spectrum arises due to species possessing a trigonal spin distribution (indicated in the figure by III). The D value is 304 gauss. Addition of more polyether leads to the disappearance of species II, while triplet spectrum III remains with enhanced intensity (figure 25D). When the full field spectra consisted of two triplet species (e.g. figure 25C,D) two partially resolved half-field peaks were observed. The dipolar interaction parameters D and E of the non axial spectra vary with counter ions and upon introduction of small amounts of DME or THF. Using polyethers containing more oxygen atoms than diglyme (e.g. triglyme or tetraglyme) it was found that the amounts of polyether needed to generate diverse triplet species were much lower than in the case of diglyme. Table 11 gives a survey of experiments carried out with Tp. Inspection of the table shows that there are essentially three types of triplet species each with ZFS parameters within a narrow defined range. Considering the three types of triplet species observed for K, Tp we find the following values:

D_1 = 492-461 gauss E_1 = 96-90 gauss
D_2 = 414-381 gauss E_2 = 79-60 gauss
D_3 = 305 gauss E_3 = 0 gauss .

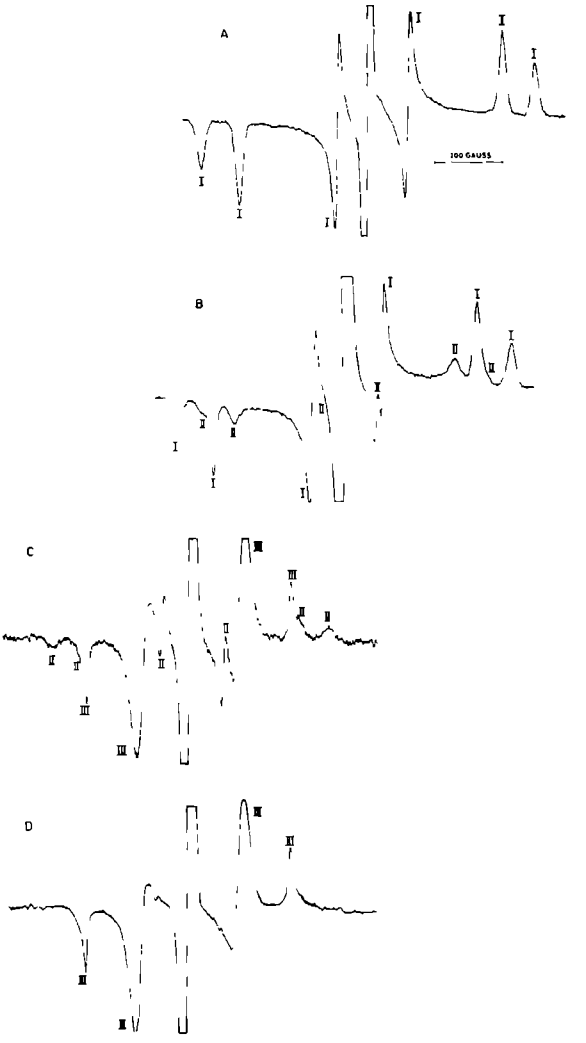

Fig. 25 - Triplet spectra of $Tp^{=}$ randomly oriented in a rigid matrix. Reducing agent K, temperature -160°C. The central peak is due to Tp^{-}. a) In pure MTHF b) after introduction of a trace of diglyme c) after addition of more diglyme d) final spectrum (MTHF: diglyme = 5:1).

Table 11

Zero-field splittings of $Tp^{=}$. The accuracy of the reported values is about 2 gauss

Counter ion	Solvent	D(gauss)	E(gauss)
K	MTHF	492	96
K	MTHF/DME (2:1)	466	90
K	MTHF/THF (2:1)	480	92
K	MTHF/MCH (2:1)	492	96
K	MTHF/diglyme mixtures	492	96
		414	79
		305	0
K	MTHF/triglyme	492-461	96-92
	mixtures	402	75
		305	0
K	MTHF/tetraglyme	492-471	96-92
	mixtures	395	75
		305	0
K	diglyme	381	60
		304	0
Rb	MTHF/DME (2:1)	442	89
RB	diglyme	351	50
		304	0

The corresponding values for Rb, Tp are about 20 to 30 gauss lower except for the lowest D value, which is within the limits of error equal to the value of 305 gauss.

It was found that the continuous decrease of the D value of K, Tp in MTHF upon addition of THF or DME is of the same order of magnitude (20-30 gauss) as the effect of introduction of traces of triglyme or tetraglyme to a MTHF reduced solution of Tp. The additions resulted in a monotonous decrease of the D value from 492 to 461 gauss for triglyme and from 492 to 471 gauss for tetraglyme. Introduction of the

non polar solvent methylcyclohexane (MCH) to K, Tp in MTHF, however, did not have a noticeable effect on the D and E values.

The lineshape of the triplet spectra was invariant under temperature variations between -150°C and -260°C and the intensity of the triplet signal varied in a linear way with the reciprocal of the temperature (see figure 26)

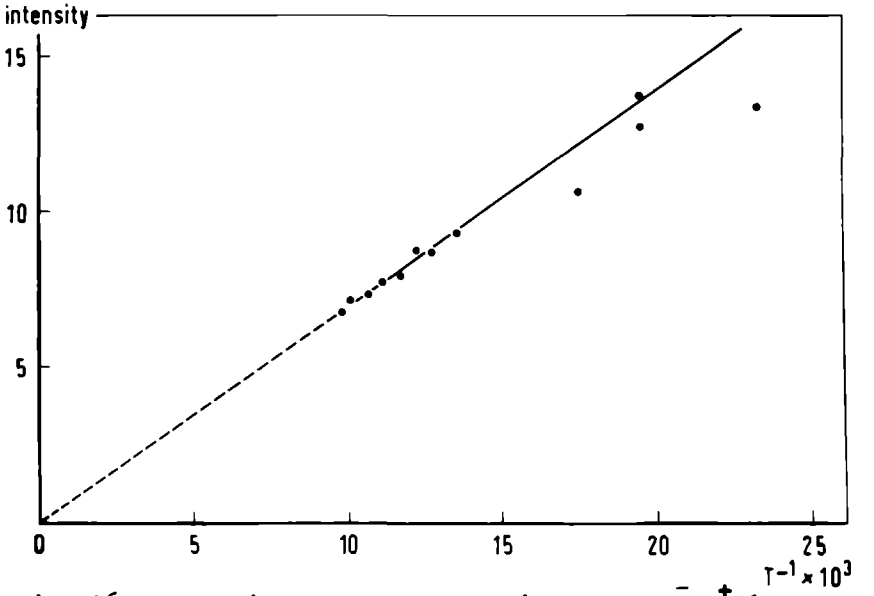

Fig. 26 - Intensity of the $\Delta_M = 2$ signal of $Tp^- 2K^+$ in MTHF as a function of the temperature.

The reversebility of the reduction of Tp^- to the triplet species was checked by adding neutral Tp to completely reduced solutions of Tp. Such additions resulted in a restoration of the blue colour of the solutions and in an increase of the monoradical peak intensity to practically twice the maximum signal intensity, produced by the original Tp^- so-

lutions. Quenching of the completely reduced solutions with air and subsequent analysis of the organic material with vapor phase chromatography showed that it contained only traces of decomposition products besides undecomposed Tp.

Evidence of the decomposition of small amounts of Tp upon prolonged treatment with K or Rb was also furnished by the appearance of a weak fluid solution hyperfine spectrum different from the Tp^- spectra discussed before.

The matrix spectra of completely reduced 2-methyl-triphenylene in MTHF were also recorded. The spectra showed that these radical solutions contained triplet species as well, with ZFS parameters very similar (D=486 gauss, E=92 gauss) to those found for the parent compound. Addition of polar solvents like polyethers to a triplet MTHF solution of Tp resulted in a decrease of the overall triplet concentration, accompanied by a simultaneous increase of the doublet concentration. This decrease in concentration of the triplet species was not caused by decomposition of reduced Tp due to impurities which might be present in the polyethers because no decrease in signal intensities could be observed when these polyethers were added to solutions containing only mononegative ions. Moreover the decrease in triplet concentration was also dependent on the alkali metal used for reduction.

No triplet species have been obtained with Li, Na or Cs as reducing agent.

5.1.2 Discussion.

The experimental results reported above prove beyond reasonable doubt that reduction of Tp^- with K or Rb leads

to the formation of dinegative ions. Since these dianions generate ESR spectra, the intensity of which follows Curie's law, it is clear that the dianion has a triplet groundstate. This is not surprising: the two lowest antibonding orbitals belong to a degenerate representation E" (see Hückel scheme in figure 27) and according to Hund's rule one may expect that the state with the lowest energy will have the highest spin multiplicity.

The matrix spectrum produced by $Tp^{=}$ solutions in polyethers and MTHF-polyether mixtures (figure 25D) which is characteristic for triplet molecules with trigonal symmetry [12,61], therefore, evokes no special questions. The triplet spectrum obtained from $Tp^{=}$ dissolved in MTHF on the other hand (figure 24) is very remarkable since it must be assigned to triplet species which have no trigonal spin distribution.

It is believed that the perturbing influence of the counter ions is the main reason for the loss of trigonal symmetry of the spin density distribution in the dianion. It is reasonable to suppose that the dianions are associated with counter ions in pure MTHF at $-160^{\circ}C$. Hoijtink e.a. [63] have provided data which indicate that other dinegative aromatic ions are associated with their counter ions under those conditions. Furthermore we have seen that the mononegative ions of Tp in MTHF form ion pairs at $-100^{\circ}C$ when present in moderate concentrations ($\approx 10^{-4}$ molar). The counter ions may be even more strongly associated with dinegative ions due to enhanced Coulombic attraction. Hence the spectra obtained from $Tp^{=}$ in pure MTHF are attributed to a non trigonal ion pair (triple). Several experimental

data substantiate this conclusion. Table 11 shows that a counter ion change from K to Rb as well as the introduction of small amounts of the more polar solvents DME or THF do affect the D and E values derived from the matrix spectrum in MTHF. Such effects can only occur if the spin distribution in the anions is perturbed by the cations, which means that ion pairs $Tp^{=}Me^{+}$ or ion triples $Tp^{=}2Me^{+}$ are present.

The solvent effect shows that the counter ion perturbation is modified by the introduction of more polar solvents. This must be ascribed to changes in ion pair geometry, probably as a result of specific solvation of the small positive ions by the more polar solvent molecules.

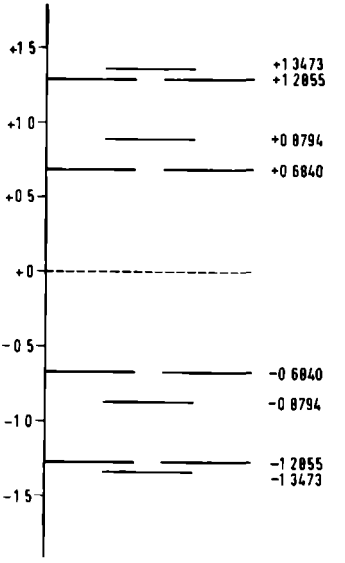

Fig. 27 - Hückel MO scheme of Tp (only the central portion is shown). Energy in eV (right) or β units (left).

The fact that the D and E values are not affected by the introduction of a solvent (MCH) with less solvating power than MTHF confirms the latter conclusion. The existence of triplet ion pairs (triples) with differing geometrical structures was unambiguously established by experiments in which small amounts of polyglymes, solvents with high solvating power, were added to $Tp^{=}$ in MTHF (see figure 25). The matrix ESR spectra consist of superpositions of signals generated by two non trigonal triplet species both at full field and at half field. If we assign the spectrum with the larger D value (492 gauss) to an ion triple $Tp^{=}2K^{+}$ and the spectrum with the lower D value (400 gauss) to an ion pair $Tp^{=}K^{+}$, than this would imply that removal of a counter ion from the triplet molecule will lower the D value by about 100 gauss. If the removal of the second K^{+} ion will produce the same decrease of the ZFS parameter, one may expect a D value of about 300 gauss for the free dinegative ion of Tp. The matrix spectrum which is observed on addition of larger amounts of polyethers and which is characteristic for triplet molecules with trigonal symmetry (D = 305 gauss, E = 0 gauss) is therefore attributed to the free dinegative ion. By "free" we mean here that no perturbing influence of the cations can be measured any more. This does not necessarily imply that the ion triples $Tp^{=}2Me^{+}$ are completely dissociated. As has been mentioned before, addition of tetraglyme to MTHF solutions containing the mononegative ions of Tp, results in the formation of solvent separated ion pairs $Tp^{-}/Tg/Na^{+}$. In these ion pairs the perturbation of the cations on the spin distribution of Tp^{-} is also absent: the spectrum is characterized by the same coupling constants

as the free monoanion. Conclusive evidence about the dissociation of $Tp^{=}2Me^{+}$ can therefore only be obtained by conductance studies. If the cations would still be associated with the anions, they can only be very loosely bound, since the ZFS parameter D (305 gauss) is practically independent of the counter ion present (Rb^{+} or K^{+}) or the constitution of the solvent (di- tri- or tetraglyme or polyglyme-MTHF mixtures).

Introduction of very small amounts of tri- or tetraglyme to MTHF solutions containing $Tp^{=}2K^{+}$ results in more subtle changes which can also be observed when DME or THF is added to these solutions (see table 11): A quasi continuous decrease of the ZFS parameters occurs (D = 492-460 gauss, E = 96-90 gauss). Since this decrease is accompanied by linebroadening, it indicates that probably several triplet species are present, differing slightly in their ZFS parameters. In the case of $Tpb^{=}2K^{+}$ the different triplet species have indeed been observed (see below). Probably the first polyether molecules only peripherically solvate the associates $Tp^{=}2Me^{+}$ without changing their structure too much and only the following ether molecules can completely solvate the cations, one after another. The decrease of the overall triplet concentration on addition of polyethers which was not caused by decomposition of $Tp^{=}$ has been ascribed to the following reaction

$$Tp^{=}2Me^{+} + nPEGD \rightleftarrows Tp^{-}//Me^{+} + Me \quad .$$

This reaction can explain both the increase in the Tp^{-} concentration and the precipitation of metal.

De Groot e.a. [64,65] made plausible that the apparent loss of trigonal symmetry of phosphorescent benzene in its lowest $^3B_{1u}$ state might be due to an indirect Jahn-Teller instability through coupling with the nearby $^3E_{1u}$ state which lies about 1 eV higher. Such an indirect Jahn-Teller instability might also operate in the Tp dianions. If electron correlation is taken into account the lowest state of $Tp^=$ (group D_{3h}) is $^3A_2'$, an orbitally nondegenerate state. The first excited triplet state belongs to the representation $^3E'$ and is formed by promoting an electron out of the lowest antibonding E" orbitals into the second non degenerate A_1'' antibonding orbital (figure 27). The excitation energy was calculated by Sommerdijk who found a value of 2.6 eV [7]. If the symmetry is lowered from D_3h to for instance C_2v the representations $^3A_2'$ and $^3E'$ of the trigonal structure transform into $^3B_1$ and $^3A_1 + {}^3B_1$, respectively and configuration interaction between the original $^3A_2'$ and $^3E'$ states may occur. As a result the most favourable conformation of $Tp^=$ will not possess trigonal symmetry and the spin-distribution will be non-trigonal.

The spectrum of the free dianions, nevertheless, proved that the triplet species had retained trigonal symmetry. It has been pointed out in § 4.1.2 in which the geometrical instability of Tp^- was discussed, that the energy difference between the various distorted and symmetrical conformations of Tp^- is less than the zero point energy of the normal vibrations. This causes a rapid interconversion between all possible configurations so that as far as ESR is concerned, the trigonal symmetry is retained. In view of the rather large excitation energy to the first excited triplet state

(2.6 eV) the same dynamic effect is likely to occur also in the free Tp dianions, so that the matrix spectrum is that of a triplet species with trigonal symmetry.

The loss of trigonal symmetry of the ion pairs (triples) of $Tp^{=}$ with alkali metal ions has been accounted for in a quantitative way by Sommerdijk who calculated the ZFS parameters of the dianion of $Tp^{=}$ [7,8] following the method of van der Waals and ter Maten. The change in the ZFS parameters was accounted for by assuming that the counter ions are located above and below the center of the same non central aromatic ring. Table 12 shows a comparison of his calculations with our experimental results.

Table 12

Calculated and experimental ZFS parameters of $Tp^{=}$. The distance of the cations to the aromatic plane is given in parentheses

	D(gauss) calculated	E(gauss) calculated	D(gauss) experimental	E(gauss) experimental
$Tp^{=}2Me^{+}$ (3 Å)	450	30	492-442	96-89
(2 Å)	500	50		
$Tp^{=}Me^{+}$ (3 Å)	390	20	414-351	80-50
(2 Å)	420	40		
$Tp^{=}$ (∞)	330	0	305	0

The correspondence of calculated and experimental D values is rather good whereas only the order of magnitude of the E values is obtained. Sommerdijk also found that in

spite of the non symmetrical perturbation of the counter ions the triplet state of $Tp^{=}2K^{+}$ is more stable than the singlet state by at least 0.312 eV, which is in agreement with experiment. In view of all these data it can be concluded that the asymmetry in the spin distribution of the dianions is caused by the electrostatic perturbation of the cations. Since two independent quantities, the zero-field splittings and the spin multiplicity of the ground state are predicted correctly by the theory, the conclusion seems justified that the ion pair and ion triple models give a reliable picture of the actual situation.

5.2 The dianion of 1,3,5-triphenylbenzene.

5.2.1 ESR experiments.

Prolonged reduction of 1,3,5-triphenylbenzene (Tpb) in MTHF with alkali metals resulted in the formation of triplet dianions which could be detected with ESR in a glassy matrix [9]. It was found that the parameter D characterizing the triplet spectrum of this dianion was a function of solvent and counter ion (table 13). The same characteristic features as have been found for $Tp^{=}$ can also be observed in the case of $Tpb^{=}$. Successive introduction of small amounts of polyethers to MTHF reduced solutions of Tpb yield in principle three different triplet species, differing largely in their zero-field splittings. It is also evident from table 13 that the smallest ZFS that can be observed for $Tpb^{=}$ (355 gauss) is practically independent of solvent and/or counter ion. This was also found for $Tp^{=}$. The most marked difference with $Tp^{=}$ is the absence of a measurable

E value in the spectra of $Tpb^{=}$. However, in one case ($Tpb^{=}$ $2Na^{+}$ in MTHF) a very small E value (5-10 gauss) was observed at very low temperature: 10°K. This ZFS became unobservably small already at 20°K.

Table 13

ZFS parameters of $Tpb^{=}$

Counter ion	Solvent	D(gauss)
Li	MTHF	473 347
Li	MTHF/tetraglyme- mixtures	473 347
Na	MTHF	523
Na	MTHF/DME	523 432 355
Na	MTHF/diglyme	523 440 361
Na	MTHF/triglyme	523 440 355
Na	MTHF/tetraglyme	523 435 360
K	MTHF	498, 488
K	MTHF/DME	498-458
K	MTHF/diglyme	498, 488 405
K	diglyme	354
K	MTHF/triglyme	498-455 405 354
K	MTHF/tetraglyme	498, 488, 463 408 354
Rb	MTHF	478
Rb	MTHF/triglyme	478 400

Since Tpb can be reduced to its dianion by more alkali metals than Tp, the counter ion effect on the ZFS parameters could be studied more accurately for $Tpb^{=}$.

In table 13 $Tpb^{=}2Li^{+}$ is somewhat exceptional when compared to the salts of the other alkali metals. Reduction of Tpb with Li in MTHF produced two triplet spectra superimposed on each other with D values of 473 and 347 gauss, the spectrum with the smaller D value being predominantly present. When tetraglyme was added to this solution the species with D value of 473 gauss was completely converted into the triplet dianion with D equal to 347 gauss. Unlike in the case of the other alkali salts no spectrum with intermediate D value was observed. On the other hand, the spectrum with the lowest D value (350 gauss) could not be obtained when small amounts of diglyme were added to MTHF solutions of $Tpb^{=}2K^{+}$. The spectrum could however be measured in pure diglyme. For $Tpb^{=}2Rb^{+}$ this spectrum could not even be produced when using triglyme as a solvating agent.

Addition of very small amounts of triglyme or tetraglyme to MTHF solutions of $Tpb^{=}2K^{+}$ caused a very slight decrease of the largest D value, as has also been found for $Tp^{=}2K^{+}$. Only when tetraglyme was added to $Tpb^{=}2K^{+}$ it became clear that this variation of the D value was in fact a discontinuous process: here three triplet species were observed differing only slightly in their D values (498, 488, and 463 gauss, respectively). They are designated as 1, 2 and 3 in figure 28a.

Introduction of polyethers to MTHF solutions of $Tpb^{=}$ generally resulted in a decrease of the triplet concentration with simultaneous increase of the doublet concentration.

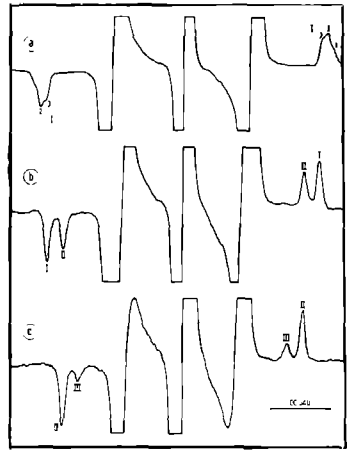

Fig. 28 - Triplet spectra of $Tpb^{=}$ at different MTHF/tetraglyme ratios.

The magnitude of the change in concentration depended on the counter ion and the kind of polyether used. It was found that the concentration of $Tpb^{=}2K^{+}$ changed hardly upon introduction of tetraglyme. We therefore "titrated" completely reduced solutions of Tpb, containing about 90% dianions, with a 0.1 molar solution of tetraglyme in MTHF using an

apparatus similar to that depicted in figure 4. Figure 29 shows a graph of the relative concentrations of the three triplet species (denoted by I, II, III) as a function of the tetraglyme-$Tpb^{=}$ ratio (Solvation of the mononegative ions was neglected).

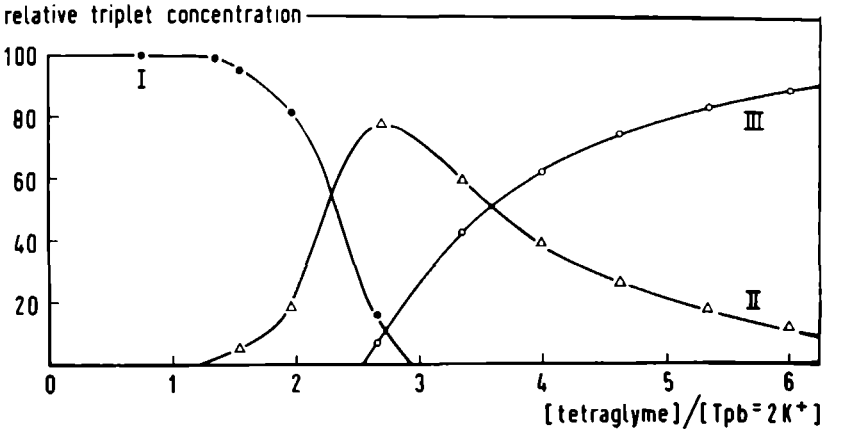

Fig. 29 - Titration curve showing the solvation of $Tpb^{=}2K^{+}$ by tetraglyme.

Comparison with computer simulations showed that the relative triplet concentrations could be accurately determined by considering the product of the amplitude A of the '$\Delta m_s=1$' signal at field positions $H_o \pm D$ (see figure 3) and the ZFS parameter D. Relative concentrations of triplets determined by the product A.D deviated about 3% from computer simulations of superposition spectra.

Representative triplet spectra measured at concentration ratios tetraglyme/$Tpb^{=}$ of about 1, 2 and 3 are shown in figure 28. The weight fractions and the shape of the spec-

tra remained unchanged when the solutions were cooled down to 20°K. The signal intensities of the triplet spectra varied linear with T^{-1} over the whole temperature range.

5.2.2 Discussion.

The dianions of $Tp^{=}$ and $Tpb^{=}$ have several features in common. The most important correspondence is again the presence of three different classes of triplet species. Here also the presence of ion pairs and ion triples is evident from the strong variation in the zero-field splittings. Since Tpb could be reduced to its dianion by more alkali metals than Tp, more can be said about the solvent and counter ion effect on the D values. The spectra with the lowest D value (350 gauss) must be ascribed to dianions that are not perturbed by cations and can be described as free ions or as very loosely bound ion pairs (triples). A distinction between these two possible structures cannot be inferred from ESR experiments alone. The D values of the second class of triplet molecules increase with decreasing ionic radius of the counter ion; for Li, Na, K and Rb the corresponding D values are 473, 440, 405 and 400 gauss, respectively. These triplet spectra are ascribed to ion pairs $Tpb^{=}Me^{+}$. The D values of the third class also increase with decreasing ionic radius of the cations, the D values being 523, 498 and 478 gauss for Na, K and Rb respectively. The spectra are ascribed to ion triples $Tpb^{=}2Me^{+}$. The corresponding spectrum of $Tpb^{=}2Li^{+}$ was never observed: in most solvents the Li salts are completely dissociated (solvated).

From the experiments two general features become evident:

a) The larger the ionic radius of the metal ion, the greater the amount of polyether necessary to generate successive triplet species like $Tpb^{=}Me^{+}$ and non-associated $Tpb^{=}$.

b) Polyethers with more coordination sites available solvate more rapidly: DME < diglyme < triglyme < tetraglyme.

These features have also been observed when mononegative ions are solvated [66]. The stronger solvation of the smaller ions is caused by the enhanced electrostatic interaction between the cations and the solvent molecules. The larger ions have a more diffuse charge distribution, which weakens the charge-dipole interaction. Polyethers with many coordination sites (oxygen atoms) available can form suitable solvent cages for the cations so that one large polyether molecule can completely solvate a metal ion.

Striking differences in solvation of $Tpb^{=}2Na^{+}$ and $Tpb^{=}2K^{+}$ by polyglymes can be observed: $Tpb^{=}2Na^{+}$ can be completely solvated to give free ions even when DME is used as a solvating agent. In the case of $Tpb^{=}2K^{+}$ this can only be effected by tri- or tetraglyme, with diglyme only one K^{+} ion can be removed and with DME the ion triple is only peripherically solvated (The D value decreases from 498 continuously to 458 gauss). $Tpb^{=}2Rb^{+}$ cannot be completely solvated even by triglyme whereas $Tpb^{=}2Li^{+}$ is practically fully dissociated in solvents with low solvating power like 2-MTHF or THP. Addition of glymes to $Tpb^{=}2Me^{+}$ in MTHF causes in many cases a decrease of the total triplet concentration which is ascribed to the following reaction:

$$Tpb^{=}2Me^{+} + n\ PEGD \overset{\leftarrow}{\rightarrow} Tpb^{-}//Me^{+} + Me$$

PEGD = polyethylene glycol dimethylether.

Precipitation of alkali metals could actually be observed in these cases.

Because also the mononegative ions which are always present in the solutions of $Tpb^{=}$ will be solvated by the polyether molecules, it was practically impossible to determine accurate solvation numbers for the reactions

$$Tpb^{=}2Me^{+} + nPEGD \overset{\rightarrow}{\leftarrow} Tpb^{=}Me^{+} + (Me^{+})_{solv.}$$

$$Tpb^{=}Me^{+} + n'PEGD \overset{\rightarrow}{\leftarrow} Tpb^{=} + (Me^{+})_{solv.}$$

Only for the potassium salt something more can be said about the solvation by tetraglyme. Inspection of figure 29 shows that the first two tetraglyme molecules hardly influence the concentration of the ion triple $Tpb^{=}2K^{+}$, denoted in the figure by class I. This class, however, consists of three different triplet species with slightly different D values (498, 488 and 463 gauss). Their relative concentrations vary with increasing polyether concentration, the species with the smallest D value being predominantly present when two glyme molecules have been added for every ion triple. It is believed that these two glyme molecules solvate the ion triple complex on the outside without changing the ion pair structure abruptly. The next ether molecule converts species I for 80% into species II which has a much lower D value (408 gauss) and when four ether molecules are available about 70% of the dianions is completely dissociated. Though the perti-

nent equilibrium constants are not known, it may be concluded that complete removal (solvation) of a potassium ion probably involves two tetraglyme molecules.

In contrast to the dianion of Tp, $Tpb^{=}$ retains trigonal symmetry when associated with metal ions. To explain this, we have suggested [9] that the cations must be located on the threefold axis or must be rapidly jumping around the molecule from one phenyl ring to the other, on the average preserving trigonal symmetry. The latter possibility has been ruled out by calculations of Sommerdijk [7]. Using the same ion triple model as for $Tp^{=}2Me^{+}$ he calculated a singlet groundstate for $Tpb^{=}$ when the cations are located above and below the center of one of the outer phenyl rings. Considering an other model, where the cations are located on the threefold axis of $Tpb^{=}$, the same author was able to account in a quantitative way for the observed ZFS parameters of $Tpb^{=}2Me^{+}$ and $Tpb^{=}Me^{+}$. Table 14 gives a comparison of the calculations with the experimental values.

Table 14

Calculated and experimental ZFS parameters of $Tpb^{=}$. The cation-aromatic plane distance is given in parentheses

	D calculated	D experimental
$Tpb^{=}$	310 gauss (∞)	350 gauss
$Tpb^{=}Me^{+}$	360 gauss (3 Å)	405 gauss ($Me^{+} = K^{+}$)
	400 gauss (2 Å)	440 gauss ($Me^{+} = Na^{+}$)
$Tpb^{=}2Me^{+}$	430 gauss (3 Å)	478 gauss ($Me^{+} = Rb^{+}$)
	460 gauss (2.5 Å)	498 gauss ($Me^{+} = K^{+}$)
	490 gauss (2 Å)	523 gauss ($Me^{+} = Na^{+}$)

The calculated D values are about 40 gauss systematically too low. The change in D value for the different triplet species is fairly well accounted for, together with the effect of changing the cationic radius. The calculated and experimental decrease of the D value when one counter ion is removed from $Tpb^{=}2Me^{+}$ is in good agreement: approximately 100 gauss. Removal of the second cation produces a decrease of 90 gauss (Na^{+}) and 55 gauss (K^{+}) which is also in good agreement with calculated values. The change in the D values with different cations, 30-40 gauss, is accounted for by changing the cation-aromatic plane distance by 0.5 to 1 Å, while the ionic radii of Na^{+}, K^{+} and Rb^{+} are 0.98, 1.33 and 1.48 Å, respectively.

MO calculations [7] showed that the central phenyl ring of $Tpb^{=}$ has a larger charge density than the outer rings. It is not surprising then that the cations are located on positions with favourable Coulombic interaction.

At very low temperature ($10^{o}K$) the spectrum of $Tpb^{=}2Na^{+}$ exhibited a non-vanishing E value of a few gauss. It is not quite clear what kind of mechanism may cause this splitting. It might be due to an out of plane bending of the phenyl rings or a small displacement of the sodium ions from the trigonal axis.

5.3 Dianions of 2,4,6-triphenyl-sym-triazine and 2,4,6-tri-p-tolyl-sym-triazine.

5.3.1 ESR Experiments

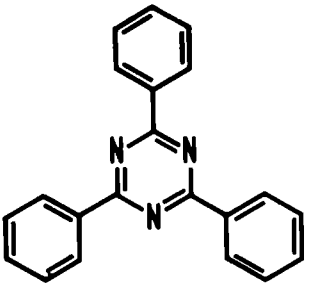

Triphenyltriazine (Tpt) and tritolyltriazine (Ttt) can also be reduced to dinegative ions by alkali metals. On prolonged reduction the green solutions of the mononegative ions turn blue: the colour of the dianions. The reduction must be carried out in a dry ice-aceton bath at -80°C. At room temperature the blue solutions change irreversibly to reddish-purple. This colour persists when the solution is exposed to air and must be due to a decomposition product. In pure MTHF a triplet ESR spectrum can only be obtained when sodium is used as reducing agent and even then the triplet concentration is rather low. With the other alkali metals the reduction in MTHF is accompanied by decomposition or precipitation. The triplet spectra obtained with Na as reducing agent are characterized by two ZFS parameters: D = 680 gauss and E = 25 gauss (figure 30).

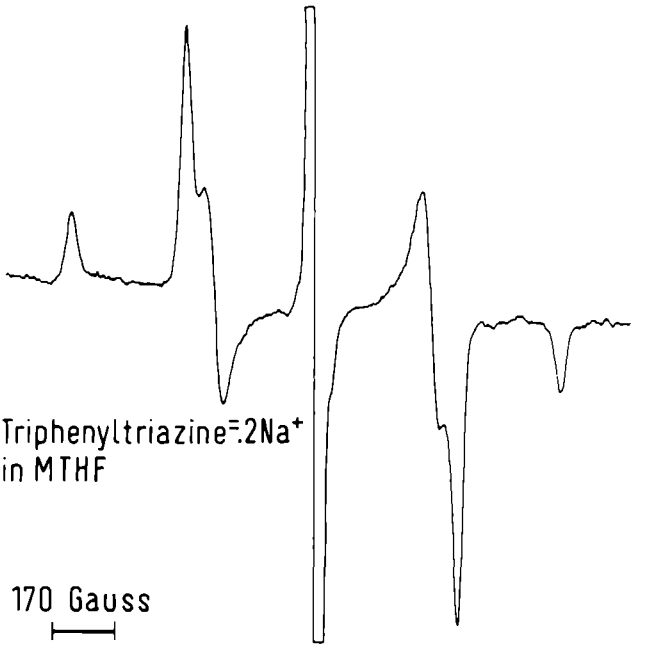

Fig. 30 - Triplet spectrum of triphenyltriazine$^{=}$. The central line is due to the monoanion.

By lowering the temperature from -160°C to -260°C the E value increases by a few gauss. This was observed both for Tpt$^{=}$2Na^{+} and Ttt$^{=}$2Na^{+} in MTHF. In table 15 a survey is given of the experiments carried out on Tpt$^{=}$ and Ttt$^{=}$.

The reason for investigating the methyl substituted compound (Ttt) was the better solubility of its dianion in MTHF. It can be seen from the table that addition of tetraglyme to Ttt$^{=}$2Na^{+} in MTHF will yield three triplet spectra with different zero-field splittings. The E value of the second spectrum (D = 650 gauss) could not be determined due to overlap with the other triplet spectra. The axial spectra (i.e. spectra generated by molecules with axial symmetry) could be observed

Table 15

ZFS parameters of triphenyltriazine and tritolyltriazine dianions

counter ion		solvent	D (gauss)	E (gauss)
$Tpt^{=}$	Li	Diglyme	600	0
	Na	MTHF	680	25
	Na	diglyme	616	0
	K	MTHF + tetraglyme	613	0
	K	diglyme	600	0
	Rb	diglyme	611	0
$Ttt^{=}$	Li	diglyme	600	0
	Na	MTHF	680	25
	Na	MTHF + DME (2:1)	680	25
			650	?
	Na	diglyme	625	0
	Na	MTHF + tetraglyme	680	25
			650	?
			625	0
	K	diglyme	606	0
	Rb	diglyme	609	0

with Li, Na, K and Rb as reducing agent in pure diglyme or in a mixture of MTHF and polyethers (figure 31).

It can be seen that the axial spectra are still somewhat dependent on the counterion and solvent, the D value varying from 600 to 625 gauss. Addition of a crown ether (2,3,11,12-dibenzo-1,4,7,10,13,16-hexaoxacyclo-octadeca-2,11-diene) to Na reduced Tpt in MTHF also gave triplet spectra characterized by a D value of 600 gauss. Unfortunately an ether with extremely high chelating power, a diaza-polyoxa-bicyclic ether [67] (gift of Prof. J.M. Lehn) gave a

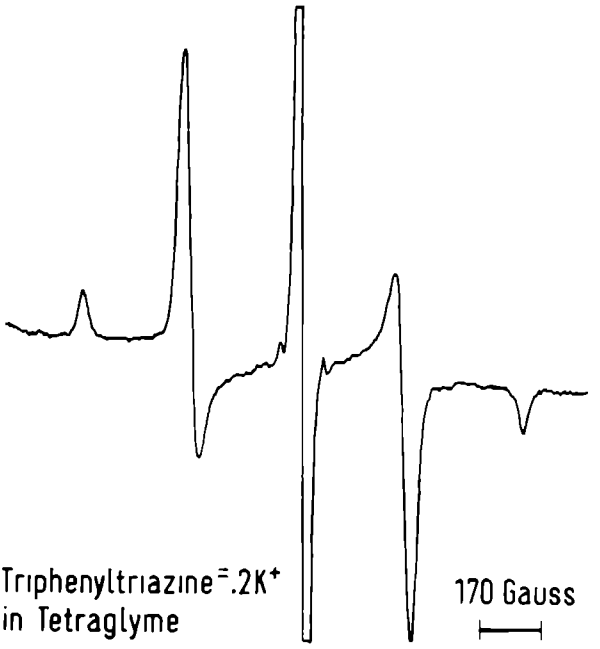

Fig. 31 - Triplet spectrum of Tpt dianion. The central line is due to the mononegative ion.

paramagnetic precipitate when added to dianions of Tpt.

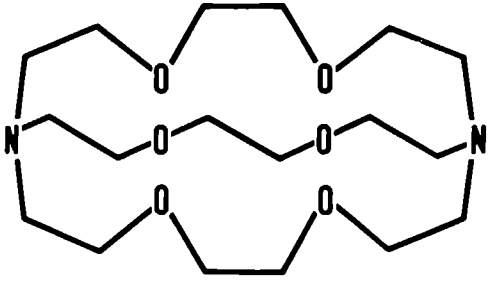

bicyclic ether

The signal intensities of the axial triplet spectra varied in a linear way with the reciprocal temperature. The intensity of the non-axial spectra, however, showed a marked decrease when the temperature was lowered from -160°C to -250°C. This

was observed both for $Tpt^{=}2Na^{+}$ and $Ttt^{=}2Na^{+}$ in MTHF. At the same time the signal intensities of the corresponding mononegative ions varied in a normal way as T^{-1}.

5.3.2 Discussion

a) The groundstate of triphenyltriazine.

Though the dianion of triphenyltriazine is isoelectronic with that of triphenylbenzene it behaves quite differently. In the first place the solubility in less polar solvents like MTHF is poor: only with Na^{+} as counter ion triplet signals could be detected, the triplet species being very unstable at room temperature. A second difference with $Tpb^{=}$ is the much larger value of D and the non-vanishing E value of $Tpt^{=}$ in MTHF. Addition of tetraglyme restored the threefold symmetry as has also been found for the triplet dianions of coronene [68] and triphenylene. The axial triplet spectra of $Tpt^{=}$ and $Ttt^{=}$ (figure 31) are generated by groundstate triplet molecules because the triplet signal intensity follows Curie's law of the magnetic susceptibility. The intensity of the non-axial spectra, however, varied in a way characteristic for thermally excited triplets. The strong deviation from Curie's law can be seen from figure 32. This means that the dianions producing these spectra have a singlet groundstate with a nearby triplet state that can be thermally populated.

First a qualitative picture will be given of how such a situation may arise. Hückel and SCF calculations of $Tpt^{=}$ (that will be discussed below) show that the lowest two antibonding orbitals transform according to the representation E'' of the symmetry group $D_{3}h$. The two additional electrons

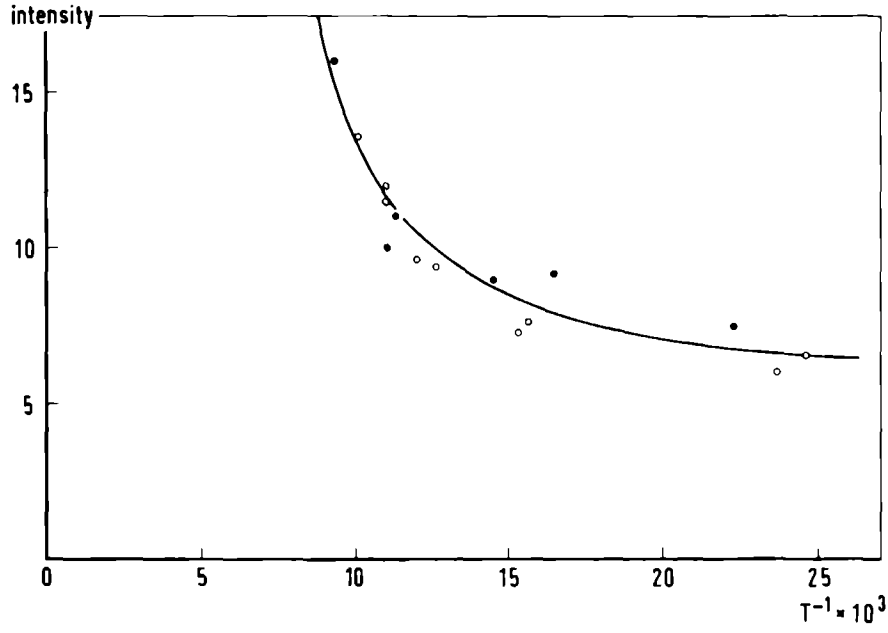

Fig. 32 - Intensity of the $\Delta m = 2$ signal of $Tpt^{=}$(o) and $Ttt^{=}$(●) measured in MTHF as a function of the temperature.

in these MO's give rise to three terms: $^3A_2'$, $^1E'$ and $^1A_1'$ (figure 33). According to Hund's rule the $^3A_2'$ term will have the lowest energy. The perturbing influence of the counter ions may alter this situation. As we have observed a non-axial triplet spectrum the counter ions are not located on the threefold axis of $Tpt^{=}$. As a consequence the symmetry will be lowered from D_3h to C_2v or lower. Taking configuration interaction into account, both the interactions between the triplet terms ($^3B_1$) and the singlet terms ($^1A_1$) must be envisaged. The interactions between the $^1A_1$ terms will be stronger than between the $^3B_1$ terms, which lie further apart.

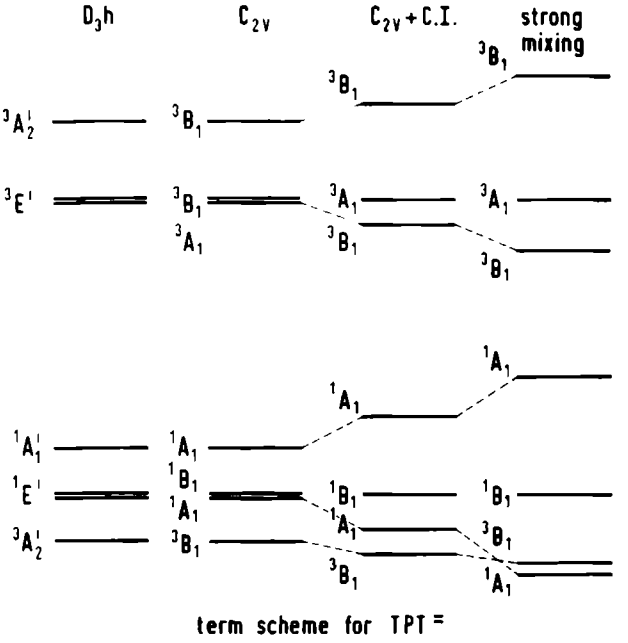

Fig. 33 - Qualitative term scheme for $Tp^{=}$, $Tpb^{=}$ and $Tpt^{=}$.

The strength of the non-symmetrical perturbation determines whether the groundstate will be a $^3B_1$ or a $^1A_1$ state. The first case applies to the dianion of Tp in MTHF, while obviously the groundstate of $Tpt^{=}$ in MTHF is a $^1A_1$. In both cases the triplet molecules (groundstate or thermally excited) give rise to spectra characterized by a non-vanishing E value, as they should, since the $^3B_1$ term will produce a non-axial spin distribution.

The magnetic susceptibility due to thermally excited triplet states will be determined both by the Boltzmann distribution within the Zeeman levels and between the orbital states $^1A_1$ and $^3B_1$ (see figure 34).

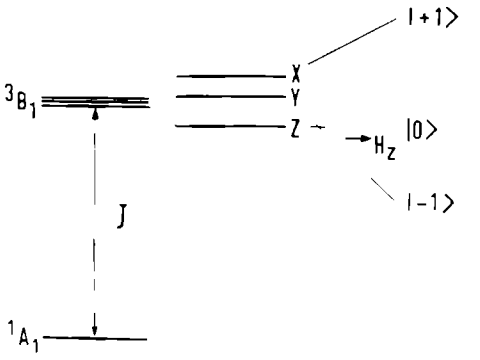

Fig. 34 - Lowest orbital states of $Tpt^{=}(Ttt^{=})$. X, Y and Z are zero-field energies of the $^3B_1$ state. The Zeeman levels are denoted by $|+1\rangle$, $|0\rangle$ and $|-1\rangle$.

The temperature dependence of the magnetic susceptibility can be calculated using van Vleck's formula [69]:

$$\chi_i = \sum_{n,m} \frac{\left[(E^{(1)}_{n,m})^2 - 2E^{(2)}_{n,m}\right]\exp(-E^o_n/kT)}{\exp(-E^o_n/kT)} \quad . \qquad (73)$$

The index i refers to three orthogonal directions in the molecule x, y, z

$$E^{(1)}_{n,m} = \beta\langle\psi_{n,m}|L_i + 2S_i|\psi_{n,m}\rangle \qquad (74)$$

$$E^{(2)}_{n,m} = \sum_{n\neq n',m} \frac{\beta\langle\psi_{n,m}|L_i + 2S_i|\psi_{n',m}\rangle^2}{E_n - E_{n'}} \qquad (75)$$

N = Avogadro's number
β = the Bohr magneton
E_n^o are energy levels in zero magnetic field and
$\psi_{n,m}$ are the corresponding eigenfunctions: the singlet function $^1A_1$ and three triplet functions of the $^3B_1$ state
L_i and S_i are orbital- and spin angular momentum operators.

Some simplifications can be made in the calculation of the susceptibility: contributions to χ_i from terms containing L_i can be neglected because the orbital angular momentum is largely quenched in aromatic radicals. States with higher energy than the $^3B_1$ state do not contribute much to χ_i either. It is further easy to see that the second order terms $E^{(2)}_{n,m}$ vanish.

When calculating χ_z i.e. the susceptibility perpendicular to the molecular plane, we can use the zero order spin functions of the $^3B_1$ state:

$$\begin{aligned} T_x &= 2^{-\frac{1}{2}} \,|\beta\beta - \alpha\alpha\rangle \\ T_y &= 2^{-\frac{1}{2}}\, i\,|\beta\beta + \alpha\alpha\rangle \\ T_z &= 2^{-\frac{1}{2}} \,|\alpha\beta + \beta\alpha\rangle \quad . \end{aligned} \tag{76}$$

Taking $E(^1A_1)$ arbitrarily equal to zero and $E(^3B_1) - E(^1A_1)$ equal to J, we find for E_n^o:

$$\begin{aligned} E_0^0 &= 0 & E_2^0 &= J + X \\ E_1^0 &= J + Z & E_3^0 &= J + Y \end{aligned} \tag{77}$$

and for the first order terms $\beta\langle\psi_{n,m}|2S_z|\psi_{n,m}\rangle$

$$\begin{aligned} E^{(1)}_{0,0} &= 0 & E^{(1)}_{1,1} &= 0 \\ E^{(1)}_{1,0} &= -2\beta & E^{(1)}_{1,2} &= 2\beta \quad . \end{aligned} \tag{78}$$

If we assume for the moment that the singlet-triplet separation J is much larger than the ZFS parameters X, Y, Z we may neglect the latter quantities. Substituting the appropriate terms in equation 73 we find

$$\chi_z = \frac{N\ 2g^2\beta^2/kt.\exp(-J/kT)}{1+3\exp(-J/kt)} \quad . \tag{79}$$

Similar experssions can be derived for χ_x and χ_y so that the isotropic susceptibility is given by

$$\chi = \frac{1}{T(1+1/3\ \exp(J/kT)} \tag{80}$$

where $\frac{2g^2\beta^2N}{3k}$ has been replaced by 1.
With formula 80 the singlet-triplet separation of $Tpt^{=}2Na^{+}$ can now be calculated since the ESR signal intensity I is proportional to the magnetic susceptibility χ. Calculating J by taking various intensity ratios

$$\frac{I_i}{I_j} = \frac{T_j(3+\exp(J/kT_j))}{T_i(3+\exp(J/kT_i))} \tag{81}$$

it was found that J varied with temperature, decreasing from 150 cm^{-1} at 100°K to 100 cm^{-1} at 30°K. Because J is much larger than the ZFS parameters ($\tilde{\sim}$ 0.05 cm^{-1}) the above made assumption (J>>X, Y, Z) proves to be valid. Besides J is also much larger than the microwave quant (0.3 cm^{-1}).

b) Calculation of the zero-field splitting parameters D and E and the singlet-triplet separation J.

In principle it must be possible to calculate J, X, Y and Z (or J, D and E) with the help of MO theory. To perform Hückel and SCF calculations on Tpt$^{=}$ we have to know how to account for the hetero atoms in the central ring. In the Hückel approximation the parameters α_x and β_{cx} (x being the hetero atom) are usually taken as [70]

$$\alpha_x = \alpha_c + k\,\beta_{cc} \qquad (82)$$
$$\beta_{cx} = h\,\beta_{cc}$$

where h and k are empirical parameters. Streitwieser suggested for the case of a nitrogen atom contributing one electron to the π system the following values [70]

$$\alpha_N = \alpha_C + 0.5\beta_{CC} \qquad (83)$$
$$\beta_{CN} = \beta_{CC} \quad .$$

In the Goeppert-Mayer and Sklar approximation [71]

$$\alpha_N = \alpha_C - (W_N - W_C) \qquad (84)$$

where $W_N - W_C$ is a measure of the difference in attraction for an electron of a nitrogen core as compared to a carbon core. The value of $W_N - W_C$ and that of β_{CN} is taken from Anno [72]

$$\alpha_N = \alpha_C - 2.460 \text{ eV} \qquad (85)$$
$$\beta_{CN} = -2.576 \text{ eV} \quad .$$

With these two sets of different parameters Hückel and SCF calculations have been performed on $Tpt^{=}$. The energy scheme of the π electronic levels is nearly the same as for $Tpb^{=}$ [7]. The ZFS parameters have been calculated with the semi-empirical method of van der Waals and ter Maten which was also used by Sommerdijk to calculate the ZFS of $Tp^{=}$ and $Tpb^{=}$ [7,8]. The results are given in table 16 together with experimental values obtained in diglyme (D = 600 gauss, E = 0).

Table 16

Calculated and experimental ZFS parameters of $Tpt^{=}$

Parameters	Method	D(gauss)	E(gauss)
$\alpha_N = \alpha_C + 0.5\beta_{CC}$	Hückel	520	0
$\beta_{CN} = \beta_{CC}$	SCF+CI	330	0
$\alpha_N = \alpha_C - 2.46$ eV	Hückel	490	0
$\beta_{CN} = -2.576$ eV	SCF+CI	290	0
experiment		600	0

As the fourth calculation is certainly the most reliable, one is forced to conclude that there is a large discrepancy with experiment. Similar large deviations from experimental values were found by Glasbeek [68] who calculated the ZFS parameters of coronene dianion. He suggested that the dianions would still be associated with the alkali ions even in polar solvents. It may be possible that we have a similar situation

here for $Tpt^{=}$ because the spectra obtained in polyethers still show some dependence on solvent and counter ion.

To study this situation theoretically a calculation has been performed for $Tpt^{=}2Me^{+}$ with the counter ions on the trigonal axis (because E must be zero) at 2 Å distance from the aromatic plane. The following parameters for the nitrogen have been used:

$$\alpha_N = \alpha_C - 2.46 \text{ eV} \qquad (86)$$
$$\beta_{CN} = -2.576 \text{ eV} \quad .$$

The perturbation of the counter ions was accounted for by using an extension of the method of Reddoch [16]. With Hückel orbitals it followed that D = 520 gauss; with SCF orbitals, taking configuration interaction into account, a lower value was obtained: D = 490 gauss. This is much closer to the experimental value than values obtained from the same type of calculations on the free dianion. In order to account for a non-vanishing E value (25 gauss) that has been measured in MTHF a calculation was performed where the counter ions were located at 2 Å above and below the same nitrogen atom. With the same values for α_N and β_{CN} it was found after SCF+CI calculations: D = 440 gauss, E = 40 gauss.

Probably the model is not correct since the D value is lowered from 490 to 440 gauss, whereas the experimental value increased from 600 to 680 gauss. Furthermore, the groundstate is calculated to be still a triplet state, the energy gap with the lowest singlet state being 0.17 eV (1370 cm^{-1}). To check whether the discrepancy between theory and experiment would be solely due to the presence of hetero atoms in the

molecule, the ZFS parameter D of the optically excited triplet state of Tpt was calculated following the same procedure as before. In this case the correspondence with the experimental value was remarkably good:

D (calculated) = 1270 gauss
D (experimental) = 1320 gauss.

It is believed, therefore, that the theory is essentially reliable and that the discrepancy with experiment has an other origin. It may be suggested that the counter ions associated with the triplet molecules will push the phenyl ring(s) a little bit out of plane. This would certainly lower the singlet state more than the triplet state and would also increase the D value.

5.4 Experiments on other trigonal molecules

After the results, described above, had been obtained, it was tempting to extend the investigation to other trigonal aromatic molecules. Table 1 in chapter III gives a list of the molecules that have been studied. Triplet spectra were only observed in a few cases:

1,3,5-tris-α(or β)-naphthylbenzene$^{=}$	D = 70 gauss
1,3,5-tris-biphenylbenzene$^{=}$	D = 150 gauss
hexabenzocoronene$^{=}$	D = 300 gauss

No counter ion or solvent effect could be observed for these ions because the spectra were only poorly resolved or had a very low signal to noise ratio.

The dianion of decacyclene also gave poorly resolved spectra but here some more data could be obtained showing slight variations in the D value (see Table 17).

Table 17

ZFS parameters of decacyclene dianion

Counter ion	Solvent	D(gauss)
Li	MTHF	240
Na	MTHF	240
K	MTHF	260
K	MTHF+DME (2:1)	215
K	MTHF+ diglyme	245
K	DEE	271, 231
Rb	MTHF	273
Cs	MTHF	246

The experiments on tribenzo-(c,i,o)triphenylene (1) deserve some special attention.

According to ESR experiments on the mono- and dinegative ions of trinaphthylene (2) the electronic groundstate of the monoanion of (2) is orbitally nondegenerate and the dianion is in a singlet groundstate [54]. These results are in agreement with SCF calculations of the anions of (2), which show that the lowest antibonding level is not degenerate in contrast with most other aromatic molecules and ions with trigonal symmetry.

The same type of calculations on an isomeric molecule (1) showed that the lowest antibonding orbitals are degenerate. One might expect, therefore, its dianion to have a triplet groundstate. Since this molecule had not been des-

cribed in the literature, it had to be synthesized [26].

Contrary to our expectations, prolonged reduction of (1) with K or Na in MTHF yielded practically diamagnetic solutions. No triplet spectrum could be observed. Addition of (1) to these solutions restored the spectrum of the mononegative ion with more than twice its original intensity; the green colour of the dianion changed into the red colour of the monoanion. In addition to this the ESR spectrum of the optically excited triplet state of (1) has been measured from -170°C to -220°C (figure 35).

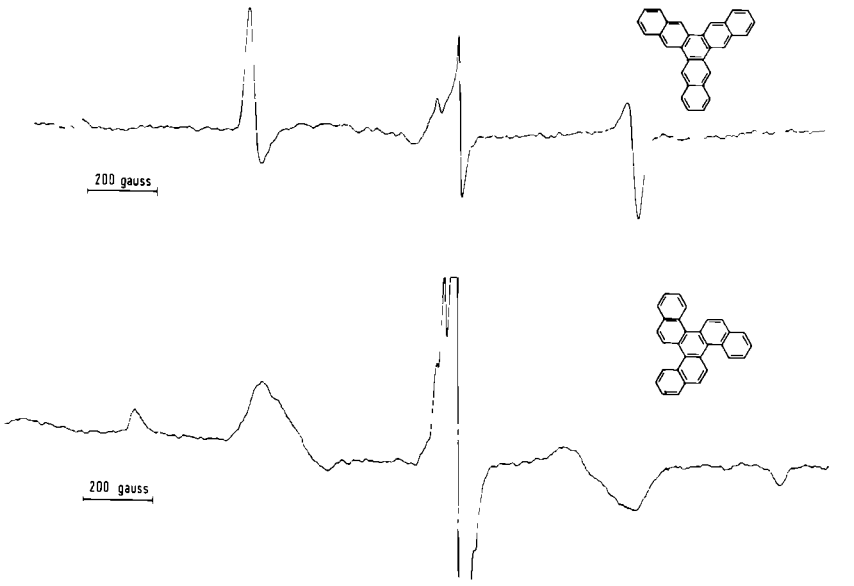

Fig. 35 - Optical triplet spectrum of trinaphthylene (upper) and tribenzotriphenylene (lower). The peaks in the center are partly due to irradiated solvent molecules.

This spectrum which did not change with temperature showed rather broad lines, similar to the triplet spectra of ions with trigonal symmetry studied by van der Waals e.a. [74]. The explanation these authors presented may equally apply for our case. The spectrum may then be interpreted in terms of an assembly of molecules with different geometrical structures and consequently different ZFS parameters D and E. If we attribute the additional linewidth of the spectrum of (1) to variations in D and E, then the D value varies from 893 to 907 gauss and the E value from 0 to 30 gauss.

From the above mentioned experiments one may conclude that the dianion is in a singlet groundstate, in contradiction to expectations based on SCF calculations. This discrepancy, never observed before for similar trigonal aromatic systems [9,75], may originate here from nonplanarity of (1). Taking the system planar, the distance between the nearest protons is 0.6 Å only. Steric factors, therefore, may lower the symmetry of the molecule and may be responsible for the singlet groundstate of the dianion and the non-vanishing E values of the optical triplet. These deviations from planarity are not revealed by the NMR spectrum [26]; the peaks in this spectrum are quite sharp. This is not in contradiction with the ESR results because the interconversion between various nonplanar structures may be rapid compared to the characteristic NMR time scale, but slow with respect to the time scale in ESR. From the maximum E value observed the interconversion rates are estimated to be slower than 9.10^{8} sec^{-1}.

REFERENCES

[1] M.G. Townsend and S.I. Weissman, J. Chem. Phys. 32, 309, 1960.

[2] R.G. Kooser, W.V. Volland and J.H. Freed, J. Chem. Phys. 50, 5243, 1969.

[3] M.R. Das, B. Wagner and J.H. Freed, J. Chem. Phys. 1970.

[4] M. Szwarc, "Carbanions, Living Polymers and Electron Transfer Processes", Interscience Publishers, 1968, Chap. 5.

[5] H. van Willigen, J.A.M. van Broekhoven and E. de Boer, Mol. Phys. 6, 533-548, 1967.

[6] J.N. Murrell and A. Hinchliffe, Mol. Phys. 11, 101, 1966.

[7] J.L. Sommerdijk, J.A.M. van Broekhoven, H. van Willigen and E. de Boer, J. Chem. Phys. 5, 2006, 1969.

[8] J.L. Sommerdijk and E. de Boer, J. Chem. Phys. 11, 4771, 1969.

[9] J.A.M. van Broekhoven, H. van Willigen and E. de Boer, Mol. Phys. 15, 101, 1968.

[10] E. Fermi, Z. Phys. 60, 320, 1930.

[11] H.M. McConnell, J. Chem. Phys. 24, 764, 1956.

[12] E. Wasserman, L.C. Snyder and W.A. Yager, J. Chem. Phys. 41, 1763, 1964.

[13] R. Breslow, H.W. Chang, R. Hill and E. Wasserman, J. Am. Chem. Soc. 89, 1112, 1967.

[14] J.R. van der Waals and G. ter Maten, Mol. Phys. 8, 301, 1964.

[15] R. Pariser, J. Chem. Phys. 24, 250, 1956.

[16] A.H. Reddoch, Actes Colloq. Intern. No 164, "Structure Hyperfine Magnetique Atomes Molecules", Paris, 1966, 419, 1967.

[17] E. de Boer and H. van Willigen, "Progress in NMR Spectroscopy", J.W. Emsley, J. Feeney and L.H. Sutcliffe, eds., Pergamon Press, Vol. 2, Chap. 3.

[18] N. Bloembergen, J. Chem. Phys. 27, 572, 1957.

[19] I. Solomon, Phys. Rev. 99, 559, 1955.

[20] A. Carrington and A.D. McLachlan, Introduction to Magnetic Resonance, New York, Harper and Row, 1967, appendix I.

[21] C.J. Pedersen, J. Am. Chem. Soc. 89, 7017, 1967.

[22] C.C. Barker, R.G. Emmerson and J.D. Periam, J. Chem. Soc., 4482, 1955.

[23] H.O. Wirth, W. Kern and E. Schmitz, Die Makromol. Chemie, 68, 69, 1963.

[24] A. Blomquist and P. Maitlis, J. Am. Chem. Soc. 84, 2333, 1962.

[25] A.H. Cook and D.G. Jones, J. Chem. Soc. 278, 1941.

[26] W. Laarhoven and J.A.M. van Broekhoven, Tetrahedron Letters 1, 73, 1970.

[27] B. Segal, M. Kaplan and G. Fraenkel, J. Chem. Phys. 12, 4191, 1965.

[28] H.A. Jahn and E. Teller, Proc. R. Soc. A 161, 220, 1937.

[29] C.A. Coulson, A. Golebiewski, Mol. Phys. 5, 71, 1962.

[30] L.C. Snyder, J. Chem. Phys. 66, 2299, 1962.

[31] W.D. Hobey and A.D. McLachlan, J. Chem. Phys. 33, 1965, 1960.

[32] H.M. McConnell and A.D. McLachlan, J. Chem. Phys. 34, 1, 1961.

[33] P. Chang, R.V. Slates and M. Szwarc, J. Phys. Chem. 70, 3180, 1966.

[34] L. Salem, The Molecular Orbital Theory of Conjugated Systems, W.A. Benjamin Inc., 1966.

[35] C.A. Coulson and A. Golebiewski, Proc. Phys. Soc. 78, 1310, 1961.

[36] R.G. Lawyer, J.R. Bolton, G.K. Fraenkel and T.H. Brown, J. Am. Chem. Soc. 86, 520, 1964.

[37] M. Karplus, R.G. Lawyer and G.K. Fraenkel, J. Am. Chem. Soc. 87, 5260, 1965.

[38] N.M. Atherton and S.I. Weissman, J. Am. Chem. Soc. 83, 1330, 1961.

[39] K.M. Buschow, J. Dieleman and G.J. Hoijtink, J. Chem. Phys., 42, 1993, 1965.

[40] N. Hirota and R. Kreilick, J. Am. Chem. Soc. 88, 614, 1966.

[41] A. Carrington and A.D. McLachlan, Introduction to Magnetic Resonance, New York: Harper and Row, 1967, Chap. 12.

[42] J.A. Pople, W.G. Schneider and H.J. Bernstein, High Resolution Magnetic Resonance, New York: McGraw Hill Book Co, Inc., p. 222, 1959.

[43] G.W. Canters, E. de Boer, B.M.P. Hendriks and H. van Willigen, Chem. Phys. Letters, 1, 627, 1968.

[44] R.V. Slates and M. Szwarc, J. Am. Chem. Soc. 89, 6043, 1967.

[45] J. Chan and J. Smid, J. Am. Chem. Soc. 89, 4547, 1967.

[46] M. Shinohara, J. Smid and M. Szwarc, J. Am. Chem. Soc. 90, 2175, 1968.

[47] K. Höfelman, J. Jagur-Grodzinski and M. Szwarc, J. Am. Chem. Soc. 91, 4645, 1969.

[48] R.V. Slates and M. Szwarc, J. Phys. Chem. 69, 4124, 1965.

[49] J.W.H. Schreurs, Thesis, Amsterdam, 1962.

[50] E.L. Ginzton, Microwave Measurements, McGraw Hill, New York, 1957.

[51] E. de Boer and C. MacLean, Mol. Phys. 9, 191, 1965.

[52] G.W. Canters, Thesis, Amsterdam,1969.

[53] M.T. Jones, J. Chem. Phys. 42, 4054, 1965.

[54] J. Sommerdijk, H. van Willigen, E. de Boer and F.W. Pijpers, Z. Phys. Chem. 63, 183, 1969.

[55] P. Wormington, Thesis, Minnesota, 1969.

[56] A.J. Stone, Mol. Phys. 6, 509, 1963, ibid. 7, 311, 1964.

[57] H.M. McConnell and J. Strathdee, Mol. Phys. 2, 129, 1959.

[58] J.H. van der Waals and M.D. de Groot, Mol. Phys. 2, 333, 1959.

[59] J.H. van der Waals and M.D. de Groot, Mol. Phys. 3, 1960, 1960.

[60] Ph. Kottis and R. Lefebvre, J. Chem. Phys. 39, 393, 1963.

[61] Ph. Kottis and R. Lefebvre, J. Chem. Phys. 41, 379, 1964.

[62] H. van Willigen and S.I. Weissman, Mol. Phys. 11, 175, 1966.

[63] J.D.W. van Voorst and G.J. Hoijtink, J. Chem. Phys. 45, 1852, 1966.

[64] M.S. de Groot and J.H. van der Waals, Mol. Phys. 6, 545, 1963.

[65] M.S. de Groot, J.A.M. Hesselman and J.H. van der Waals, Mol. Phys. 10, 91, 1965.

[66] A.I.S. Shatenshtein and E.S. Petrov, Russian Chem. Rev., Vol. 36, No 2, 100-110.

[67] B. Dietrich, J.M. Lehn and J.P. Sauvage, Tetrahedron Letters, 34, 2885, 1969.

[68] M. Glasbeek, Thesis, Amsterdam, 1969.

[69] J.H. van Vleck, "Electric and Magnetic Susceptibilities", Oxford University Press, Oxford and New York, 1932.

[70] A. Streitwieser, MO theory for Organic Chemists, John Wiley and Sons, New York, 1967.

[71] M. Goeppert-Mayer and A.L. Sklar, J. Chem. Phys. 6, 645, 1938.

[72] T. Anno and A. Sado, J. Chem. Phys. 29, 1168, 1958.

[73] J.S. Brinen, J.G. Koren and W.G. Hodgson, J. Chem. Phys. 8, 3095, 1966.

[74] J.H. van der Waals, M.S. de Groot and J.A.M. Hesselman, Mol. Phys. 10, 241, 1966.

[75] R.E. Jesse, P. Biloen, R. Prins, J.D.W. van Voorst and G.J. Hoijtink, Mol. Phys. 6, 633, 1963.

[76] E. de Boer, A.M. Grotens and J. Smid, to be published.

SUMMARY

Molecular orbital calculations on aromatic hydrocarbons with trigonal symmetry show that the first two antibonding π orbitals often have the same energy. As a consequence the corresponding mononegative ions which are prepared by alkali metal reduction in ethereal solvents like dimethoxyethane, tetrahydrofuran or polyglycolethers are orbitally degenerate. It has been found that this degeneracy affects several electronic properties of these radical ions in particular the g value and the spin-lattice relaxation time of the unpaired electron. Due to a mechanism which is not exactly known at present, but probably involves an enhanced spin-orbit interaction in the radical, the g value is raised and the spin-lattice relaxation time is shortened as compared to non-degenerate radicals.

In this thesis we have studied extensively the mononegative ions of triphenylene (Tp) and 1,3,5-triphenylbenzene (Tpb), which have according to MO calculations an orbitally degenerate groundstate. Whereas Tp^- showed again the above mentioned properties, Tpb^- did not; its g value and spin-lattice relaxation time proved to be comparable with those of non-degenerate systems. A tentative explanation for this extraordinary behaviour is presented.

Ion pairing studies revealed that Tp^- associates with the alkali ions in solvents with little solvating power like 2-methyl-tetrahydrofuran (MTHF) or tetrahydropyran (THP). Evidence for this association was obtained from the appearance of a sodium hyperfine splitting in the ESR spectrum of Tp^-.

It was also evident from the ESR measurements that ion pairing strongly influences the g value and the spin distribution in the anion. In the optical spectrum the perturbation of the cation manifested itself by a shift of the absorption peaks to shorter wave-lengths. Several ion pairing reactions have been studied quantitatively and thermodynamic quantities characterizing the equilibria have been determined.

From proton NMR experiments on Tpb^- the magnitude and sign of some proton coupling constants could be determined. Information about the proton spin relaxation mechanisms has been obtained from the NMR linewidths.

Further reduction of the mononegative ions resulted in the formation of paramagnetic dinegative ions. From the temperature dependence of the magnetic susceptibility followed that these ions have a triplet groundstate in solvents with good solvating properties like polyethers. The ESR spectra of the dianions of Tp, Tpb and 2,4,6-triphenyl-sym-triazine (Tpt) were characterized by only one zero-field splitting parameter (D) indicating that the dinegative ions have threefold symmetry. In poorly solvating solvents like 2-MTHF or THP the ESR spectra of $Tp^=$ and $Tpt^=$ must be described by two parameters D and E, the latter being a measure for the deviation from axial symmetry. It has been made plausible, both experimentally and theoretically, that this deviation is caused by the electrostatic perturbation of the cations, which are supposed to be located outside the trigonal axis. As a result the groundstate of $Tpt^=$ is even no longer a triplet state: the nearby singlet state has become lower in energy (about 0.015 eV).

Though drastic changes of the zero-field splitting parameter D of $Tpb^{=}$ occur when polyethers are added to MTHF solutions, no loss of symmetry has been observed. This means that the cations must be located on the trigonal axis.

Finally a brief account is given of experiments carried out on some other trigonal molecules.

SAMENVATTING

Uit molecular orbital berekeningen aan aromatische koolwaterstoffen met drietallige symmetrie blijkt dat de eerste twee antibindende π orbitalen vaak dezelfde energie hebben. Tengevolge daarvan zijn de overeenkomstige mononegatieve ionen, die worden bereid door reductie met alkalimetalen in etherische oplosmiddelen als dimethoxyethaan, tetrahydrofuraan of polyglycolethers, baanontaard. Men heeft ontdekt dat deze ontaarding verscheidene electronische eigenschappen van deze radicalen beinvloedt, in het bijzonder de g waarde en de spin-rooster relaxatietijd van het ongepaarde electron. Tengevolge van een mechanisme wat op het ogenblik nog niet precies bekend is, maar wat waarschijnlijk te maken heeft met een verhoogde spin-baaninteractie in het radicaal, is de g waarde groter en de spin-rooster relaxatietijd korter vergeleken met niet ontaarde systemen.

In dit proefschrift zijn uitvoerig de mononegatieve ionen bestudeerd van trifenyleen (Tp) en 1,3,5-trifenylbenzeen (Tpb), welke volgens MO berekeningen een baanontaarde grondtoestand hebben. Terwijl Tp^- weer de boven genoemde eigenschappen bleek te vertonen, was dit niet het geval met Tpb^-: de g waarde en spin-rooster relaxatietijd van laatstgenoemd radicaal bleken vergelijkbaar te zijn met die van niet ontaarde radicalen. Er wordt getracht een verklaring te geven voor dit merkwaardige verschijnsel.

In oplosmiddelen met gering solvaterend vermogen zoals 2-methyltetrahydrofuraan (MTHF) of tetrahydropyraan (THP) bleek Tp^- te associëren met de alkaliionen. Aanwijzigingen

voor deze associatie werden verkregen uit het optreden van een natriumhyperfijnsplitsing in het ESR-spectrum van Tp^-. Uit ESR-spectra bleek ook duidelijk dat de vorming van ionenparen sterk de g waarde en de verdeling van de ongepaarde spindichtheid in het anion beinvloedde. In het optische spectrum manifesteerde de storing van het kation zich in een verschuiving van de absorptielijnen naar kortere golflengten. Verscheidene reacties waarin ionenparen een rol spelen zijn kwantitatief bestudeerd en thermodynamische grootheden, die de evenwichten karakteriseren, zijn bepaald.

Uit experimenten met protonresonantie aan Tpb^- kon het teken en de absolute waarde van enkele protonkoppelingskonstanten worden bepaald. Informatie over de relaxatie-mechanismen van de protonspin is verkregen uit de NMR-lijnbreedten.

Verdere reductie van de mononegatieve ionen resulteerde in de vorming van paramagnetische dinegatieve ionen. Uit het temperatuurverloop van de magnetische susceptibiliteit volgde dat deze ionen een triplet grondtoestand hebben in oplosmiddelen met goede solvaterende eigenschappen zoals polyethers. De ESR-spectra van de dianionen van Tp, Tpb en 2.4.6-trifenyl-sym-triazine (Tpt) waren gekarakteriseerd door slechts één nulveldsplitsingsparameter (D) hetgeen erop wijst, dat deze dinegatieve ionen een drietallige symmetrie hebben. In slecht solvaterende oplosmiddelen als MTHF of THP moesten de ESR-spectra van $Tp^=$ en $Tpt^=$ worden beschreven door twee parameters, D en E, waarbij de laatste een maat is voor de afwijking van axiale symmetrie. Zowel experimenteel als theoretisch is aannemelijk gemaakt dat deze afwijking veroorzaakt wordt door de electrostatische storing van de kationen, waarvan wordt verondersteld dat ze zich buiten de trigonale as bevinden.

Dientengevolge is de grondtoestand van $Tpt^{=}$ zelfs niet langer meer een triplettoestand: de dichtbijgelegen singulettoestand heeft een lagere energie gekregen (ongeveer 0,015 eV).

Alhoewel er drastische veranderingen optreden in de nulveldsplitsingsparameter D van $Tpb^{=}$ als polyethers worden toegevoegd aan MTHF-oplossingen, is geen verlaging van de symmetrie waargenomen. Dit betekent dat de kationen gelocaliseerd moeten zijn op de trigonale as.

Tenslotte wordt een kort verslag gegeven van experimenten die zijn uitgevoerd aan enkele andere trigonale moleculen.

STELLINGEN

I

De conclusie die Ballhausen trekt uit de berekening van de g waarde van $Ni(H_2O)_6^{2+}$ is nietszeggend.

C.J. Ballhausen, Introduction to Ligand Field Theory, McGraw-Hill, 1962

II

De verklaring die door Bonati e.a. wordt gegeven voor het effect dat verschillende alkylgroepen hebben op de C-N stretchvibratie van dithiocarbamaten is onjuist.

F. Bonati, G. Minghetti and S. Cenini, Inorganica Chemica Acta, 2, 376 (1968)

III

Voor de discrepantie die bestaat tussen de spin-roosterrelaxatietijden van het anion van benzeen zoals die gemeten zijn door Wormington enerzijds en Kooser e.a. anderzijds is een andere verklaring mogelijk dan die, welke door eerstgenoemde auteur wordt gegeven.

P. Wormington, Thesis, Minnesota (1969)
R.G. Kooser, W.V. Volland and J.H. Freed
J. Chem. Phys., 12, 5243 (1969)

IV

Bij de berekening van de electrische veldgradient in bis (N,N-dialkyldithiocarbamato) ferri-halogeniden verwaarlozen Ake en Harris-Loew ten onrechte het covalente karakter van de bindingen met het centrale atoom.

R.L. Ake and C.A.M. Harris-Loew, J. Chem. Phys., 3, 1098 (1970)

V

De opmerking van Fischer en McDowell dat radicaal anionen met symmetrie $D_x h(x=3,6,8)$ een baanontaarde grondtoestand hebben is een onjuiste generalisatie.

P.H.H. Fischer and C.A.M. McDowell, Mol. Phys., 8, 361 (1964)

VI

De conclusie die Foster en Morris trekken uit de variatie van de complexatieconstante van pyridine en methylgesubstitueerde pyridine met trinitrobenzeen kan ook worden afgeleid uit het verloop van de chemical shift.

R. Foster and J.W. Morris,
J. Chem. Soc., B, 703 (1970)

VII

De argumenten die Müller e.a. gebruiken voor de toekenning van de structuren van de fotodimeren van o-distyrylbenzeen zijn onvoldoende en aan bedenkingen onderhevig.

E. Müller, H. Meier und M. Sauerbier,
Chem. Ber., 103, 1356-1363 (1970)

VIII

Het feit dat Mg^{2+} de ATPase optimaal stimuleert bij een Mg^{2+}/substraatverhouding van 1 is door Hekkelman en Herrmann-Erlee onvoldoende onderkend.

J.W. Hekkelman and M.P.M. Herrmann-Erlee,
Proceedings of the Third Parathyroid
Conference, Montreal, October 1967

IX

Bij de reactie tussen P_2S_5 en aromatische ketalen kunnen zowel ketonen als thioketonen worden gevormd. Bij de thioketonvorming treden waarschijnlijk dithiometafosfaatesters ($ROPS_2$) op als intermediair, bij de ketonvorming echter niet. Voor de reactie met orthoformiaten ligt de zaak juist omgekeerd.

X

Het idee om gastarbeiders aan te trekken voor de industrie heeft mogelijk inspirerend gewerkt voor de oplossing die men onlangs gevonden heeft om het tekort aan religieuzen in de katholieke kerk te ondervangen.

Nijmegen, 2 oktober 1970 J.A.M. van Broekhoven